Optimisation of a multi-subtype multiplex PCR to screen for key drug resistance mutations in HIV

by

Catherine Joanne James

A dissertation submitted to the Faculty of Science, University of the Witwatersrand, in fulfilment of the requirements for the degree

Master of Science

School of Molecular and Cell Biology
Faculty of Science
University of Witwatersrand

Centre for HIV and STIs
National Institute of Communicable Diseases

Johannesburg
2019

DECLARATION

I, Catherine Joanne James, am a student registered for the degree of MSc Molecular and Cell Biology in the academic year 2017 - 2018.

I hereby declare the following:

I am aware that plagiarism (the use of someone else's work without their permission and/or without acknowledging their original source) is wrong.

I confirm that the research proposal submitted is for assessment for the above degree and is my own unaided work except where explicitly indicated otherwise and acknowledged.

I have followed the required conventions in referencing the thoughts and ideas of others.

I understand that the University of the Witwatersrand may take disciplinary action against me if there is a belief that this is not my own unaided work or that I have failed to acknowledge the source of the ideas or words in my writing.

Signature: …… ……

Date: 01/08/2019

ACKNOWLEDGEMENTS

I would like to thank:

My supervisors for their valued insights and guidance.

The National Institute for Communicable Diseases Centre for HIV and STIs Virology Section for allowing me to conduct my research at their institute.

Everyone at the HIV Virology Section, who welcomed me and provided a friendly and supportive environment.

The HIV Drug Resistance team for accepting me as part of their team and providing their support, guidance and assistance as needed.

The Centers for Disease Control and Prevention for providing the RNV assay kits and allowing me the opportunity to validate the assay.

My family for their constant support, particularly my husband Willie.

The research for this dissertation was funded by:

National Health Laboratory Service Research Trust Grant: GRANT004 94666

Poliomyelitis Research Foundation Grant Number 17-31

This work was partially funded by the Centers for Disease Control and Prevention Innovation Fund (iFund)

OPTIMISATION OF A MULTIPLEX PCR TO SCREEN FOR KEY DRUG RESISTANCE MUTATIONS IN HIV

by

Catherine Joanne James

SUPERVISOR: Prof Yasien Sayed

CO-SUPERVISORS: Dr Gillian Hunt and Dr Muhklid Yousif

SCHOOL: Molecular and Cell Biology

DEGREE: MSc Molecular and Cell Biology

ABSTRACT

BACKGROUND: Sub-Saharan Africa hosts over two thirds of the global HIV-infected population. South Africa (SA), with the highest national incidence of HIV, also has the largest antiretroviral therapy programme globally. In an effort to reach the UNAIDS 90-90-90 targets, SA implemented a universal test-and-treat approach in 2016 and has committed to increasing the number of HIV-infected individuals on ART over the next few years. The first line regimen in SA includes an NRTI backbone of tenofovir and emtricitabine, combined with efavirenz as the NNRTI. Treatment failure as a result of the development of drug resistance mutations is the greatest risk to successful ART. The most prevalent drug resistance mutations in SA, K103N, M184V and K65R, confer broad high level resistance to NRTI and NNRTIs and may affect the efficacy of second-line regimens. HIV drug resistance testing is not recommended at treatment initiation or at first-line regimen failure, due to the high cost and limited laboratory capacity. The HIV Drug Resistance RNV (derived from K65**R**, K103**N**, and M184**V**) Multiplex Assay was designed by the CDC to simultaneously detect the K65R, K103N and M184V mutations in the presence of virological failure. The aim of this study is to optimise the assay in a South African setting, by comparing assay results to the current gold standard, namely nested PCR and sequencing using Sanger sequencing technologies.

METHODS: A total of 225 whole plasma specimens collected from patients infected with HIV-1 were selected for study, and include specimens with the K65R, K103N and M184V and wild-type genotypes as well as specimens with both low (<600 copies per ml) and high (≥600 copies/ml) viral load. Nucleic acids were extracted using the MagNA pure LC instrument and template was generated using PCR amplification of the entire *protease* gene and codons 1-250 of the *reverse transcriptase* gene. Detection of HIV variants harbouring these mutations was performed by determining the change in the cycle threshold (ΔCt) of the total copy and mutation detection components of the assay. Specimens with discrepancies between conventional genotype and RNV assay were re-sequenced using next generation sequencing.

RESULTS: Of the 225 specimens selected for this study, 47 specimens had a VL < 600 copies/ml, and 178 specimens had a VL ≥ 600 copies/ml. Of 171 specimens with known genotype, 105 specimens had a WT genotype and 66 specimens had one or more mutation present (the remaining 54 specimens were not genotyped due to low VL result). For the total copy component of the assay, which differentiates specimens by VL based on a cut-off of 600 copies/ml, 180 (84%) specimens had results concordant to the previous VL result and 45 (16%) specimens had discordant results. The sensitivity of this component was 91% and specificity 60%. For the mutation detection component of the assay, the 161 specimens that had a high VL using both the RNV assay and standard VL methodologies were screened. Of these 161 specimens, 130 (81%) were concordant with the known genotype, 28 (17%) were discordant and 3 (2%) had no amplification. The sensitivity of this component of the assay was 94%, and specificity 74%. Next generation sequencing detected low prevalence mutations in five specimens that were not present in the Sanger sequence, but were detected in the RNV assay. New thresholds were proposed to improve test statistics: for the total copy component, the recommended threshold was reduced from 25.00 to 21.78 cycles; this increased sensitivity to 95% and specificity to 85%. For the RNV component, a recommended change in cycle threshold value of 10.94 cycles decreased the number of discordant specimens to 25 (15%). This increased the sensitivity of the assay to 84%, and specificity to 86%.

CONCLUSIONS: The RNV multiplex assay was successful in amplifying the three key drug resistance mutations in South African Subtype C specimens. The success of the assay thus makes it a viable screening tool to detect the K65R, K103N and M184V drug resistance mutations at first-line therapy failure. However, our recommended cut-offs should be considered by the developers to improve the sensitivity and specificity of the assay

TABLE OF CONTENTS

LIST OF FIGURES

LIST OF TABLES

LIST OF ABBREVIATIONS

(-)	Minus
(+)	Plus
>	Greater than
<	Less than
≤	Less than or equal to
ΔCt	Change in (delta) cycle threshold
λ	Lambda
µl	Microlitre
µM	Micromolar
3TC	Lamivudine
ABC	Abacavir
ADR	Acquired drug resistance
AIDS	Acquired immune deficiency syndrome
APV	Amprenavir
ART	Antiretroviral therapy
ARV	Antiretroviral
AS-PCR	Allele-specific PCR
ATV	Atazanavir
AZT	Zidovudine
BIC	Bictegravir
Bp	Base pairs
C	Cytosine
CA	Capsid protein
CDC	Centers for Disease Control and Prevention
cDNA	Complementary deoxyribonucleic acid
CRF	Circulating recombinant form
Ct	Cycle threshold
CYP450	Cytochrome P450

d4T	Stavudine
DBS	Dried blood spot
ddC	Zalcitabine
ddI	Didanosine
DEL	Delavirdine
diH_2O	Distilled water
DNA	Deoxyribonucleic acid
dNTP	Deoxynucleotide triphosphate
DRC	Democratic Republic of the Congo
DRV	Darunavir
DTG	Dolutegravir
EDTA	Ethylenediaminetetracetic acid
EFV	Efavirenz
EIA	Enzyme immunoassay
Env	Envelope
EtOH	Ethanol
ETV	Etravirine
EVG	Elvitegravir
Ex	Excitation
FPV	Fosamprenavir
FTC	Emtricitabine
g	Gravitational force
GB	Gigabytes
H_2O	Water
HCl	Hydrogen Chloride or hydrochloric acid
HIV	Human immunodeficiency virus
HIVDB	Stanford HIV Drug Resistance Database
HREC	Human Research Ethics Committee
I	Isoleucine

IC_{50}	Half maximal inhibitory concentration
ID	Identifier
IDV	Indinavir
Ig	Immunoglobulin
IN	Integrase
InSTI	Integrase strand-transfer inhibitor(s)
K	Lysine
Kb	Kilo-base pair
KCl	Potassium chloride
kD	Kilo Dalton
Kg	Kilogram
LPV	Lopinavir
LPV/r	Ritonavir boosted lopinavir
M	Methionine
MA	Matrix protein
MgCl	Magnesium chloride
$MgSO_4$	Magnesium sulphate
Min(s)	Minute(s)
ml	Millilitre
mM	Millimolar
mRNA	Messenger RNA
NaOH	Sodium hydroxide
NC	Nucleocapsid protein
NFV	Nelfinavir
NGS	Next-generation sequencing
Nm	Nanometer
NNRTI	Non-nucleoside reverse transcriptase inhibitor(s)
nPCR	Nested polymerase chain reaction
NRTI	Nucleoside reverse transcriptase inhibitor(s)

NTC	No template control
NVP	Nevirapine
OH	Hydroxyl
OLA	Oligonucleotide ligation assay
PANDAA	Pan-degenerate amplification and adaptation
PCR	Polymerase chain reaction
PDR	Pre-treatment drug resistance
PEP	Post-exposure prophylaxis
PI	Protease inhibitor(s)
PIC	Pre-integration complex
PMTCT	Prevention of mother-to-child transmission
Pol	Polymerase
PR	Protease
PrEP	Pre-exposure prophylaxis
R	Arginine
RAL	Raltegravir
RNA	Ribonucleic acid
RNase H	Ribonuclease H
RNCV	RNV positive control
ROC	Receiver operating characteristic
Rpm	Revolutions per minute
RPV	Rilpivirine
RT	Reverse-transcriptase
RTV	Ritonavir
RT-PCR	Reverse transcriptase polymerase chain reaction
s	Seconds
SA	South Africa
SIV	Simian Immunodeficiency Virus
SP1	Spacer peptide 1

SP2	Spacer peptide 2
START	Strategic Timing of Antiretroviral Therapy
SQV	Saquinavir
ssRNA	Single-stranded RNA
TAF	Tenofovir alafenamide
TAM	Thymidine analogue mutation
TB	Tuberculosis
TC	Total Copy
TDF	Tenofovir disoproxil fumarate
TDR	Transmitted drug resistance
TE	Tris-EDTA
TFV	Tenofovir
Tm	Melting temperature
TPV	Tipranavir
Tris	2-amino-2-(hydroxymethyl)propane-1,3-diol
U	Units
UNAIDS	Joint United Nations Programme on HIV/AIDS
URF	Unique recombinant form
USA	United States of America
V	Valine
VL	Viral load
WHO	World Health Organization
WT	Wild-type

CHAPTER 1:

LITERATURE REVIEW

1.1 INTRODUCTION

1.1.1 Current Status of HIV Epidemic

Infection with the human immunodeficiency virus (HIV) remains a global public health priority with 36.9 million people living with HIV by the end of 2017 (Joint United Nations Programme on HIV/AIDS, 2018b). Eastern and Southern Africa are the worst affected regions hosting more than 50% of the global burden (Joint United Nations Programme on HIV/AIDS, 2018b). Early initiation of antiretroviral (ARV) therapy (ART) for treatment of HIV infection can significantly reduce HIV-related morbidity and mortality by suppressing HIV replication and reducing the risk of HIV transmission (TEMPRANO ANRS 12136 Study Group, 2015; The INSIGHT START Study Group, 2015). Current World Health Organization (WHO) ART guidelines recommend a "universal test and treat" approach where ART is initiated in HIV-infected individuals regardless of immune competency (World Health Organization, 2016b). In efforts to control the HIV epidemic, the Joint United Nations Programme on HIV/AIDS (UNAIDS) has called for countries to aim to achieve the "90-90-90" treatment targets by 2020 (Joint United Nations Programme on HIV/AIDS, 2014). These targets are defined as 90% of HIV-infected persons should know their HIV status, 90% of these HIV-infected individuals should be on ART and 90% of those receiving treatment should have sustainable viral suppression.

South Africa (SA) has the highest number of people living with HIV, with approximately 7.2 million by the end of 2017. The country is one contributor to new infections globally, with an estimated 270 000 new HIV infections in 2017 (Joint United Nations Programme on HIV/AIDS, 2018b). South Africa has the largest ART programme globally with almost 4.4 million HIV-infected individuals on ART as of 2017 (Joint United Nations Programme on HIV/AIDS, 2018b).

The development of HIV drug resistance (HIVDR) remains the biggest threat to successful treatment programs (Tang and Shafer, 2012). Of individuals in ART globally, it is estimated that 9.7% have acquired drug resistance mutations during therapy (World

Health Organization, 2017). Of the HIV-infected individuals on ART in SA, 87.5% were estimated to be virologically suppressed in 2017 based upon a viral load (VL) less than (<) 1000 HIV-1 RNA copies/ml (Human Sciences Research Council, 2018). Of those with an unsuppressed VL on an NNRTI-based regimen, the prevalence of drug resistance was between 89% and 96.1% (Hunt *et al.*, 2017; Steegen *et al.*, 2017).

Over the past decade, there has been an increase in the levels of HIVDR in patients initiating ART, notably to the non-nucleoside reverse transcriptase inhibitor (NNRTI) drug class, particularly in low- and middle-income countries (World Health Organization, 2016b, 2017). The levels of NNRTI drug resistance in low- and middle-income countries were estimated to be increasing by between 11% and 29% annually and the prevalence ranged from 7.2% to 15.5% in 2016, depending on the geographic region (World Health Organization, 2017).

1.2 VIRION AND GENOMIC STRUCTURE OF HIV

1.2.1 Biological Properties

Human immunodeficiency viruses are enveloped retroviruses approximately 100 to 120 nanometers (nm) in diameter (Freed and Martin, 2013). Within the virion is a cone shaped cylindrical core containing the dimeric HIV-1 RNA genome.

1.2.2 Genomics

The HIV-1 genome is a single-stranded ribonucleic acid (ssRNA) genome of 9719 nucleotides (nt) in length (Kaslow *et al.*, 2014). The genome has nine open reading frames which encode fifteen structural, regulatory and accessory proteins. The structural genes are *gag*, *pol* and *env*, the regulatory genes are *tat* and *rev*, and the accessory genes are *nef*, *vif*, *vpr* and *vpu* (Figure 1.1) (Watts *et al.*, 2009).

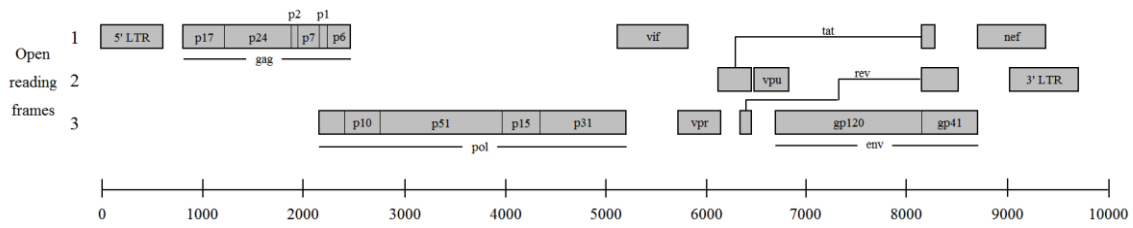

Figure 1.1: Genomic organisation of the HIV-1 genome. The structural genes are *gag*, *pol* and *env*, the regulatory genes are *tat* and *rev*, and the accessory genes are *nef*, *vif*, *vpr* and *vpu* (Freed and Martin, 2013; Kaslow *et al.*, 2014).

1.2.3 Gag Polyproteins

1.2.3.1 Gag Proteins

The p55 *gag* polyprotein precursor is cleaved by the protease (PR) enzyme to form the p17 matrix (MA) protein, the p24 capsid (CA) protein, the p7 nucleocapsid (NC) protein, the p6 protein and the two spacer proteins, SP1 and SP2 (Kaslow *et al.*, 2014). These proteins are involved in the formation and assembly of the structural elements of the virion and contribute to the reverse transcription process (Lu *et al.*, 2011; Freed and Martin, 2013).

1.2.3.2 Pol Proteins

The polymerase (*pol*) gene encodes for the enzymes involved in replication and viral integration. These include the p10 protease (PR) enzyme, the heterodimeric reverse transcriptase (RT), and the p31 viral integrase (IN) (Freed and Martin, 2013). The function of PR is to proteolytically cleave the Gag-Pol precursor molecule in order to release the functional Gag and Pol proteins (Freed and Martin, 2013). The HIV-1 IN enzyme is involved in the catalysation of the insertion of the viral double stranded deoxyribonucleic acid (dsDNA) produced by reverse transcription into the host chromosome as described in Section 1.3 below (Freed and Martin, 2013).

The HIV-1 RT is a heterodimeric enzyme consisting of the p66 and p51 subunits (Freed and Martin, 2013). Proteolytic cleavage of the C-terminal of the p66 subunit forms the p51 subunit, and the additional 15-kilo Dalton (kD) fragment that remains forms the ribonuclease H (RNase H) (Hansen *et al.*, 1988).

The function of HIV-1 RT is threefold: it is at times an RNA-dependant deoxyribonucleic acid (DNA) polymerase, a DNA-dependant DNA polymerase as well as an endonuclease (Herschhorn and Hizi, 2010). The major role of HIV-1 RT is during reverse transcription, where the viral ssRNA is converted into dsDNA, as described in Section 1.3 below.

The fidelity of RT enzymes in general is lower than that of cellular DNA polymerases, however, the RT of lentiviruses specifically have been shown to be even less accurate than other reverse transcriptase enzymes (Mansky and Temin, 1995). The lower fidelity of these enzymes can be attributed to their lack of 3’ to 5’ exonucleolytic proofreading activity (Herschhorn and Hizi, 2010; Menéndez-Arias *et al.*, 2017).

1.2.4 Env Glycoproteins

The gp120 and gp41 envelope glycoproteins are cleaved from the single chain gp160 polyprotein precursor by cellular proteases (Poignard *et al.*, 2001). During translation of the gp160 precursor, glycosylation occurs followed by proteolytic cleavage (Checkley *et al.*, 2011; Freed and Martin, 2013). These processes are vital as uncleaved gp160 is unable to be incorporated into virions and glycosylation is required for correct folding gp120 for $CD4^+$ binding (Li *et al.*, 1993; Welman *et al.*, 2007).

The cleaved gp120 and gp41 glycoprotein products form a complex via a weak, non-covalent association (Freed and Martin, 2013). The gp120-gp41 complex is transported to the plasma membrane, during which many of the oligosaccharide side chains are modified by the addition of complex carbohydrates, which obscures gp120 from immune recognition by the host (Freed and Martin, 2013). The gp120-gp41 complex form the glycoprotein spikes on the surface of virions which are responsible for $CD4^+$ binding during the infection of cells (Checkley *et al.*, 2011).

1.2.5 Regulatory and Accessory Proteins

There are two regulatory proteins, Tat and Rev, which are involved in the transcription of viral messenger RNA (mRNA) and its export out of the nucleus (Groom *et al.*, 2009; Debaisieux *et al.*, 2012). The accessory proteins Vif, Vpr, Vpu and Nef are involved in viral pathogenesis by enhancing the infectivity of virions and contributing to immunosuppression (Geyer *et al.*, 2001; Muthumani *et al.*, 2006; Nomaguchi *et al.*, 2008; Freed and Martin, 2013).

1.3 HIV LIFE CYCLE

The main cellular target of HIV-1 virions is $CD4^+$ T-lymphocytes, however, infection of dendritic cells and other $CD4^+$ macrophages also occurs (Freed and Martin, 2013; Kaslow *et al.*, 2014). Virus entry involves binding of gp120 on the viral cell surface to the $CD4^+$ receptor as well as either the CCR5 or CXCR4 chemokine receptors on the surface T-lymphocytes (Poignard *et al.*, 2001). This binding leads to conformational changes in gp120 and gp41 that results in delivery of the viral core into the host cell cytoplasm (Welman *et al.*, 2007; Checkley *et al.*, 2011).

Reverse transcription begins after the HIV-1 virus core enters the cell (Kaslow *et al.*, 2014). In this process, the HIV RT reverse transcribes the viral RNA template into

complementary dsDNA. Recombination can occur during this process when the RT transcribes DNA from segments of both of the HIV-1 RNA molecules present in the infected cell (Herschhorn and Hizi, 2010; Levin *et al.*, 2010). The genomic RNA template is then degraded by RNase H hydrolysation (Beilhartz and Götte, 2010).

The ds DNA product formed by reverse transcription is then integrated into the host genome by HIV IN (Delelis *et al.*, 2008). Integrase forms part of the pre-integration complex (PIC), which includes other viral and cellular components and catalyses the endonucleolyic cleavage of the host DNA and insertion of the viral DNA into the gap (Delelis *et al.*, 2008). Cellular enzymes repair the gap to produce a segment of integrated proviral DNA chromatin (Vandegraaff and Engelman, 2007).

The integrated viral genome is used as a template by cellular RNA polymerase II to transcribe viral mRNA (Freed and Martin, 2013). Viral mRNA are processed as cellular mRNA and are exported via Rev or host-mediated mechanisms (Wu, 2004; Freed and Martin, 2013). Expression of the viral mRNA is mediated by Tat, Rev and host regulatory elements (Liu *et al.*, 2011).

Viral RNA binds to p55 gag polyproteins and migrate to the plasma membrane for assembly (Scarlata and Carter, 2003; Freed and Martin, 2013). Maturation into virions occur when PR cleaves the Gag polyprotein, and the mature virions subsequently bud off of the host cell (Scarlata and Carter, 2003; Fujii *et al.*, 2009; Freed and Martin, 2013).

1.4 PATHOGENESIS OF HIV INFECTION

Within 72 hours of the initial infection, HIV establishes itself at the infection site and draining lymph nodes through infection of inactivated $CD4^+$ T lymphocytes, and within the first week disseminates to other lymph nodes to establish systemic infection (Freed and Martin, 2013; Kaslow *et al.*, 2014). During this phase of infection, inflammatory cytokines and chemokines are induced, which increases trafficking of T-lymphocytes to the lymph nodes, thereby enhancing virus replication and spread (Hunt, 2007; Levy, 2009; Maartens *et al.*, 2014). The earliest that virus is detectable in the blood is approximately 8 to 10 days after infection during the acute viraemic stage, where the VL can reach over one million copies per millilitre (copies/ml) (Figure 1.2) (Fiebig *et al.*, 2003; Kaslow *et al.*, 2014). The $CD4^+$ T-lymphocyte cells undergo a marked decline during this period, particularly in the gastrointestinal tract where the highest number of lymph nodes are located, from which the host does not fully recover (Levy, 2009; Kaslow

et al., 2014). Additionally, the HIV reservoirs are established during this acute phase, with the viral reservoir established by large numbers of viruses infecting follicular dendritic cells and the latent reservoir established by smaller numbers of virues integrating into resting $CD4^+$ T-lymphocytes (Kaslow *et al.*, 2014).

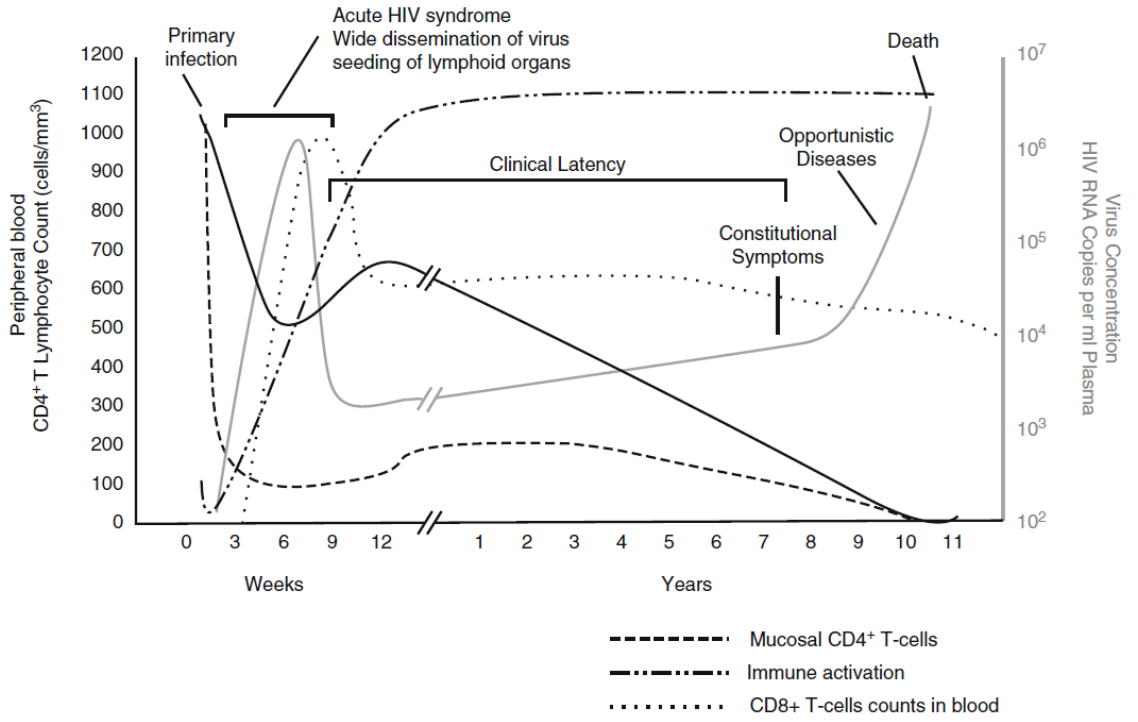

Figure 1.2: Course of HIV infection and host response (Kaslow *et al.*, 2014). The progression of HIV RNA concentration (grey), host peripheral $CD4^+$T-lymphocye count (solid black) host mucosal $CD4^+$T-lymphocyte count (dashed black), host $CD8^+$ T-cell count (dotted black) and host immune activation (broken black) responses following infection with HIV.

Following the acute phase, the viral load declines to a set point due to $CD8^+$ T-lymphocyte destruction of HIV-infected cells (Kaslow *et al.*, 2014; Maartens *et al.*, 2014) This also allows the $CD4^+$ T-lymphocyte counts to partially recover from the profound HIV- and $CD8^+$ T-lymphocyte-mediated destruction observed in early infection. The entire HIV population within an infected individual, called the HIV quasispecies, encompasses the entire viral population and develops from several rounds of replication, the high HIV replication rate and the error-prone RT (Tang and Shafer, 2012;). This results in a highly variable population of HIV-1 virions. Escape mutants develop in response to these $CD8^+$ T-lymphocyte and antibody responses, which develop after approximately three months post-infection, leading to immune escape (Frahm and Brander, 2007; Tang and Shafer, 2012; Maartens *et al.*, 2014). The host immune system does not manage to control viral replication thus allowing the HIV VL to increase at low levels, and during this latency

period the $CD4^+$ T-lymphocyte counts continue to decline (Levy, 2009; Kaslow *et al.*, 2014).

While direct destruction of infected $CD4^+$ T-lymphocytes by $CD8^+$ T-lymphocytes does contribute to the overall decline in $CD4^+$ T-lymphocytes observed in HIV infections, it alone is not responsible for the depletion of these cells (Hunt, 2007). The main contributing mechanism thought to contribute to this is the activation, apoptosis and autophagy of bystander $CD4^+$ T-lymphocytes in the blood and lymphoid tissues, among other factors (Hunt, 2007; Levy, 2009). The eventual failure of the immune system ensues resulting in the development of acquired immune-deficiency disease (AIDS) and death (Kaslow *et al.*, 2014).

1.5 CLINICAL MANIFESTATIONS OF HIV INFECTION

The symptoms experienced during the acute seroconversion stage of HIV infection are generally non-specific, with more serious symptoms occurring rarely (Soogoor and Daar, 2005; Melhuish and Lewthwaite, 2018). Chronic infection follows acute seroconversion and the only symptom generally observed is mild lymphadenopathy (O'Cofaigh and Lewthwaite, 2013; Melhuish and Lewthwaite, 2018). There may be systemic manifestations of HIV infection or other early signs of progression to advanced disease (Kuritzkes and Koup, 2013).

As the $CD4^+$ T-lymphocyte cell count declines, conditions such as unexplained weight loss, skin disorders, gastrointestinal symptoms, and pathogenic infections such as *Mycobacterium tuberculosis*, candiasis and varicella zoster may appear (Kuritzkes and Koup, 2013; Melhuish and Lewthwaite, 2018). Certain AIDS-defining infections such as *Pneumocyctis jirovecii*, cerebral toxoplasmosis, *Cryptosporidium* and *Microsporidium* are associated with a further decline in the $CD4^+$ T-lymphocyte cell count (Melhuish and Lewthwaite, 2018). Malignancies related to HIV may also develop at this stage of the infection (O'Cofaigh and Lewthwaite, 2013).

At end-stage disease, disseminated AIDS-defining infections become more common and include *Mycobacterium avium*, *Cryptococcus neoformans*, and cytomegalovirus reactivation (Melhuish and Lewthwaite, 2018). Malignancies, particularly viral-associated malignancies, are more common with non-Hodgkin's lymphoma and Kaposi's

sarcoma being the most observed (Kuritzkes and Koup, 2013; Melhuish and Lewthwaite, 2018).

1.6 DIAGNOSTIC AND MONITORING ASSAYS

Diagnosis of HIV is performed based upon the presence of certain HIV markers such as host antibodies, specific HIV component such as proteins, the p24 antigen or the HIV nucleic acid, or the whole virus itself (Iweala, 2004). Typical specimen types used for diagnostic purposes include venous whole blood in the form of capillary whole blood and dried blood spots (DBS), , serum, plasma, and oral fluid (World Health Organization, 2015a).

Serological assays involving enzyme immunoassays (EIA) are the most commonly used assay for HIV diagnosis (World Health Organization, 2015a). There are four different EIAs used for HIV diagnosis, differing based upon the antibody or antigen detected (World Health Organization, 2015a; Daskalakis, 2016). Typically, immunoglobulin (Ig) G is the target of EIAs as the concentration of IgM is usually not high to produce a sensitive assay (Iweala, 2004).

Rapid diagnostic tests most commonly use HIV antigens affixed to filter paper or membranes to detect HIV antibodies (Greenwald *et al.*, 2006; Daskalakis, 2016). The antibodies present in the specimen, either oral fluid, whole blood, plasma or serum, bind to the HIV antigens and result in a colour change, through one of many mechanisms, that is visibly detectable as positive (Iweala, 2004; Greenwald *et al.*, 2006; Daskalakis, 2016). Rapid diagnostic tests have numerous advantages, including that they are simple and fast, generally do not require laboratory equipment or instrumentation and are relative cheap costing approximately US$ 1 - 2 (Kosack *et al.*, 2017).

Nucleic acid testing detects the HIV RNA genome through polymerase chain reaction (PCR) assays (Iweala, 2004; Fearon, 2005). HIV RNA is extracted from virions in the infected person’s plasma.followed by a reverse-transcriptase PCR (RT-PCR) in order to convert the RNA to DNA and increase the number of DNA copies, after which it is detected either by agarose gel electrophoresis or enzyme-linked quantification (Iweala, 2004; Newman *et al.*, 2014). Nucleic acid tests are the standard for diagnosing HIV in infants younger than 15 months as serological testing may be compromised by the

presence of maternal HIV antibodies in the patient (Iweala, 2004; Fearon, 2005; Kuritzkes and Koup, 2013).

Viral load monitoring, performed by quantitative PCR is generally used to monitor patients following HIV diagnosis and response to ART (Fearon, 2005; Kaslow *et al.*, 2014; Mossoro-Kpinde *et al.*, 2016). The PCR is real-time based and more sensitive clinical assays are able to detect as few as 20 copies of viral RNA per millilitre (ml) plasma (Kaslow *et al.*, 2014; Mossoro-Kpinde *et al.*, 2016).

The $CD4^+$ T-lymphocyte cell count is used to determine the immunological status andstage of disease (Kaslow *et al.*, 2014). The $CD4^+$ T-lymphocytes are measured by flow cytometry, which counts cells bound to chemiluminescent-tagged antibodies (Glencross *et al.*, 2008; Kaslow *et al.*, 2014). There are also portable $CD4^+$ T-lymphocyte analysers that can determine the $CD4^+$ T-lymphocyte cell count at the point of care (Glencross *et al.*, 2012).

1.7 EPIDEMIOLOGY OF HIV

1.7.1 Global Epidemiology of HIV

Recent data published by the UNAIDS estimates that 36.9 million people world-wide are living with HIV in 2017 (Joint United Nations Programme on HIV/AIDS, 2018b). The region that has the highest number of people living with HIV is Eastern and Southern Africa, with more that 50% of the HIV infected population found in this region that accounts for only 6.2% of the global population (Joint United Nations Programme on HIV/AIDS, 2016b). Among the countries in this region, South Africa, Mozambique and, Tanzania contribute to over 50% of the infections in this region (Kharsany and Karim, 2016).

It is further estimated that approximately 21.7 million HIV-infected individuals are accessing ART globally (Joint United Nations Programme on HIV/AIDS, 2018b). Within Eastern and Southern Africa, 12.9 million people living with HIV are receiving ART, making up 66% of the HIV-infected population of that region (Joint United Nations Programme on HIV/AIDS, 2018a, 2018b).

In 2014, UNAIDS stated that they sought to end the AIDS epidemic by 2030, and set the "90-90-90" targets. These targets state that 90% of all people living with HIV should

know their status, 90% of those diagnosed with HIV should be on sustainable ART and 90% of those on ART should be virally suppressed (Joint United Nations Programme on HIV/AIDS, 2014). This translates to 90% of the HIV population knowing their status, 81% of all people living with HIV accessing ART and 73% all infected persons to be virally suppressed (Joint United Nations Programme on HIV/AIDS, 2014, 2016b). As of data collected by 2017, the global progress towards these goals is that 75% of the HIV population know their status, 59% of people living with HIV are on ART and 47% of people living with HIV and on ART are virally suppressed (Joint United Nations Programme on HIV/AIDS, 2018a). The progress towards these goals differ vastly by country and region. The greatest progress was observed in the Western and Central Europe region with 85%, 76% and 65% progress, and the least progress was observed in Northern Africa and the Middle East region with 50%, 29% and 22% progress towards the 90-90-90 goals, respectively (Joint United Nations Programme on HIV/AIDS, 2018b).

1.7.2 Origin and Spread of HIV

Acquired Immune Deficiency Syndrome was first noticed in homosexual men in the United States of America (USA) in 1981 (Sharp and Hahn, 2011), with the causative agent later identified as a retrovirus in 1983 (Barré-Sinoussi *et al.*, 1983). The origins of HIV, however, have been traced to approximately 1920 in Central Africa, where they emerged from cross-species transmission of simian immunodeficiency virus (SIV) from chimpanzees and sooty mangabeys to humans, most likely through exposure of the mucous membranes to infected blood or body fluids (Sharp and Hahn, 2011; Faria *et al.*, 2014).

The four lineages of HIV-1, Groups M, N, O and P, resulted independently cross-species transmission of SIV to humans (Faria *et al.*, 2014). Group M, the pandemic form of HIV-1 and the first lineage discovered, resulted from cross-species transmission of SIV from the *Pan troglodytes troglodytes* chimpanzees found in the South-eastern corner of Cameroon (Sharp and Hahn, 2011). Group O HIV remained non-pandemic with infections of this group being rare and typically constrained to West Africa, particularly Cameroon and Gabon (Sharp and Hahn, 2011; Faria *et al.*, 2014). Group N, which is even rarer than Group O, is only found in Cameroon, and has been traced to *P. t. troglodytes* chimpanzees in South-central Cameroon (Sharp and Hahn, 2011). Group P, which has been detected

in two persons to date, has been traced back to SIVs from gorillas in the West-central Africa region (Sharp and Hahn, 2011).

The transmission event of SIV to humans that resulted in Group M HIV-1 has been modelled back to approximately 1910 to 1930 (Sharp and Hahn, 2011; Faria *et al.*, 2014). Following the transmission event of Group M HIV-1 to humans, presumably via bloodborne transmission from ape blood to human hunters, the virus spread along the Congo river to Kinshasa in the Democratic Republic of the Congo (DRC), where the earliest strains of HIV-1 were discovered (Sharp and Hahn, 2011). The virus then spread and diversified in that region for approximately 50 to 70 years before it was recognised (Sharp and Hahn, 2011; Faria *et al.*, 2014).

The origins of HIV-2, first identified in 1986, was traced to a cross-species transmission event of SIV from sooty mangabeys in West Africa (Sharp and Hahn, 2011). The HIV-2 epidemic is mainly limited to West Africa, with Guinea-Bissau and Senegal having the highest prevalence (Sharp and Hahn, 2011). Compared to HIV-1, HIV-2 has lower VLs, making the virus less transmissible; and results in a slower progression to AIDS (Sharp and Hahn, 2011; Kaslow *et al.*, 2014). These factors are resulting in reduced prevalence rates of HIV-2 and the gradual replacement of HIV-2 with HIV-1 in most countries in that region (Sharp and Hahn, 2011).

1.7.3 Geographical Distribution and Subtypes

It is hypothesised that most, if not all, of the evolution of HIV-1 Group M into the nine subtypes occurred in the area around Kinshasa following its introduction in the beginning of the twentieth century (Hemelaar *et al.*, 2011; Sharp and Hahn, 2011). This is supported by the fact that the genetic diversity of HIV-1 Group M was much greater and more complex in the DRC by the end of the 1980s compared to the rest of the world, and that all subtypes have been identified there (Sharp and Hahn, 2011; Faria *et al.*, 2014).

The classification of subtypes or clades within HIV-1 Group M was originally based on the envelope (*env*) sequences, with a variation of 20 to 35% observed between viruses of different clades, and only 8 to 20% variation observed between viruses belonging to the same clade (Hemelaar *et al.*, 2011). The nine clades (A-D, F-H, J and K) may also recombine in dual-subtype infected individuals to form circulating recombinant forms (CRFs), found in three or more epidemiologically unlinked individuals, or unique

recombinant forms (URFs), found in fewer than three individuals (Kijak and McCutchan, 2005; Taylor *et al.*, 2008). To date, there have been over 96 CRFs identified (Recordon-Pinson *et al.*, 2018). The most prevalent subtypes are A, B, C, D CRF01_AE and CRF02_AG, which combined account for approximately 85% of global infections (Hemelaar *et al.*, 2011).

Due to being the origin of HIV, it is logical that the greatest subtype diversity is found in Central Africa, where all subtypes and many CRFs and URFs co-circulate (Kijak and McCutchan, 2005; Hemelaar *et al.*, 2011).. In Southern Africa, the dominant subtype is almost exclusively subtype C, from where it spread to also dominate the epidemic in Ethiopia and India and circulate in other surrounding countries (Hemelaar *et al.*, 2011; Sharp and Hahn, 2011). Subtype C is the most prevalent subtype globally (approximately 48% of infections) and has been responsible for major epicentres of the HIV pandemic by spreading through countries in Southern Africa and Southern and Central Asia (Hemelaar *et al.*, 2011). The global distribution of HIV-1 subtypes is illustrated in Figure 1.3 below.

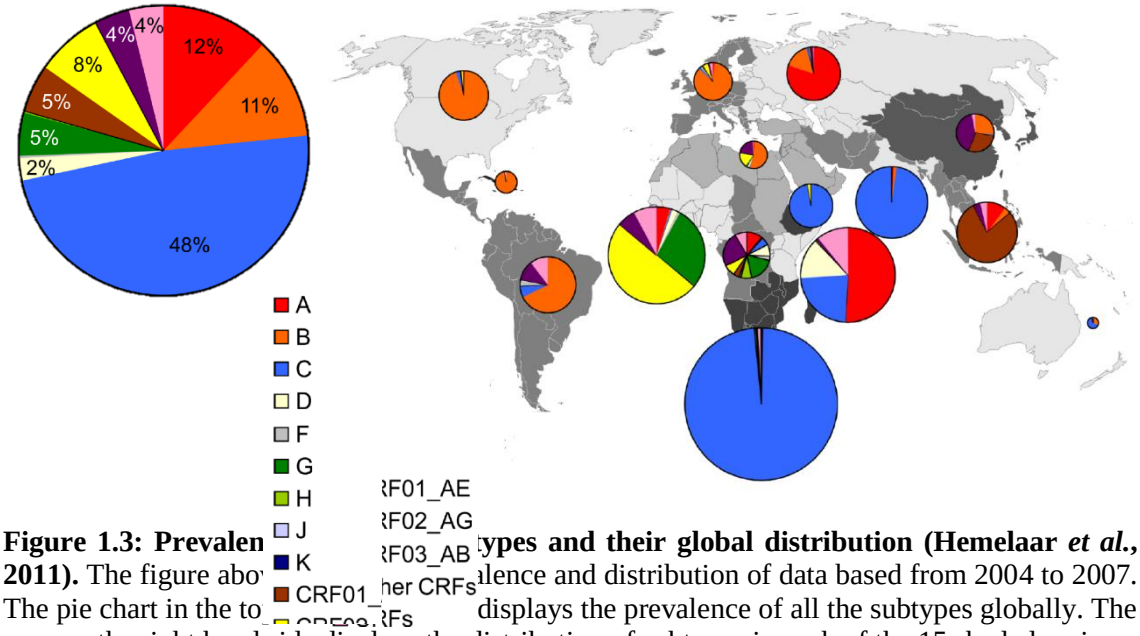

Figure 1.3: Prevalen ypes and their global distribution (Hemelaar *et al.*, 2011). The figure abo alence and distribution of data based from 2004 to 2007. The pie chart in the to displays the prevalence of all the subtypes globally. The map on the right hand side displays the distribution of subtypes in each of the 15 shaded regions.

1.7.4 Transmission

Transmission of HIV-1 occurs via exposure to blood or other biological fluids at mucosal surfaces or percutaneously (Shaw and Hunter, 2012; Kaslow *et al.*, 2014). The major routes which HIV-1 is transmitted includes through anal or vaginal, sharing of needles or

other injection devices with an infected person and through perinatal exposures which include transplacental, intrapartum and postpartum exposures (Kaslow *et al.*, 2014). Mother-to-child transmission carries the highest risk of HIV-1 transmission, either through intrauterine, intrapartum or transmission via breastmilk (Shaw and Hunter, 2012).

The global epidemic is primarily driven by sexual transmission, the majority of these being heterosexual transmissions, despite having the lowest transmission probabilities (Shaw and Hunter, 2012; Kaslow *et al.*, 2014; Cohen *et al.*, 2016). The greatest contributing factor to the risk of transmission for sexual exposures is the VL, with an approximate 2.5-fold increased risk of transmission for every ten-fold increase in the VL (Shaw and Hunter, 2012; Maartens *et al.*, 2014). As a corollary, acute phase infections are also associated with an increased risk of transmission as the plasma VL is high during this phase (Maartens *et al.*, 2014). In addition to the high VL, the lack of neutralising antibodies and the clonal expansion of viruses highly capable of initiating productive infections are thought to play a role in the increased risk of transmission during acute phase infections (Shaw and Hunter, 2012). The presence of genital ulcer disease, particularly ones that result in inflammation and ulceration increase the risk of transmission by approximately 2 to 11-fold (Gray *et al.*, 2001; Shaw and Hunter, 2012).

1.7.5 Key Populations

The World Health Organization identifies five key populations who are disproportionately affected by the HIV epidemic, namely men who have sex with men (MSM), transgender people, people who inject drugs, sex workers and people in prisons and other closed settings (World Health Organization, 2016a). These population groups make up almost 50% of the global HIV-infected population (Joint United Nations Programme on HIV/AIDS, 2018b).

While the incidence does differ by region, outside of Western, Central, Eastern and Southern Africa the proportion of new HIV infections attributed to key populations and their sexual partners was as high as 96% in some regions in according to UNAIDS data from 2014 (Joint United Nations Programme on HIV/AIDS, 2016a).

1.7.1 Epidemiology of HIV in South Africa

Approximately 33% of infections in Eastern and Southern Africa are from SA, and it has one of the highest prevalence rates of HIV globally, with an estimated 7.2 million people living with HIV (Joint United Nations Programme on HIV/AIDS, 2018b). With an estimated 4.4 million people accessing ART, SA has the largest ART programme worldwide (Joint United Nations Programme on HIV/AIDS, 2016a, 2018b). With regards to the 90-90-90 targets, as of the end of 2017 84.9% of the HIV-infected population know their status, 70.6% of HIV-infected persons are accessing ART, and 87.5% of people with HIV are virally suppressed (Human Sciences Research Council, 2018).

1.8 ANTIRETROVIRAL THERAPY

Chemotherapeutic treatment of HIV is achieved through ART, which can be administered as combination ART for the management of HIV infection, or to prevent infection either through pre-exposure prophylaxis (PrEP or post-exposure prophylaxis (PEP). The first ARV, the NRTI zidovudine (AZT), was identified in 1985 and approved for management of HIV infection in 1987 (Cihlar and Ray, 2010; Cihlar and Fordyce, 2016). Over the years, more ARV drugs became available, including more NRTI, protease inhibitors (PI), entry inhibitors, fusion inhibitors and integrase strand-transfer inhibitors (InSTI) (Broder, 2010).

The current HIV treatment paradigm consists of triple therapy, however, initial ART regimens consisted of a single ARV. While viral suppression on monotherapy was achieved, it was not sustained, and the survival benefit attributed to such regimens was only a six to eighteen-month increase in lifespan (Hammer *et al*., 1994; de Béthune, 2010). Additionally, the other benefits of ART were also short-lived, primarily due to the development of drug resistance (Hammer *et al*., 1994). The efficacy of triple therapy, proven to be the most effective form of ART in 1997, is due to the prevention of drug resistance, which occurs early during monotherapy (Gulick *et al.*, 1997; Hammer *et al.*, 1994). The rapid development of drug resistance during monotherapy is due to the presence of drug-resistant variants present at low levels prior to ART initiation. The selection pressure of the drug combined with the inability of a single agent to completely halt the replication of the entire HIV quasispecies, results in low-level of these drug reseistance variant and a resulting increase in their prevalence (Coffin, 1995; Clutter *et*

al., 2016). The triple therapy ART approach currently used consists of a backbone of two NRTI with an additional ARV from another class (Martinez-Cajas and Wainberg, 2008).

1.8.1 Reverse Transcriptase Inhibitors

1.8.1.1 Nucleoside Reverse Transcriptase Inhibitors (NRTI)

The NRTI class of ARV agents are analogues of endogenous nucleosides and nucleotides that lack a 3'-hydroxyl group (Cihlar and Ray, 2010; Sherman, 2015), resulting in DNA chain termination during the elongation phase of reverse-transcription (El Safadi *et al.*, 2007; Sherman, 2015).

The NRTI are formulated as prodrugs that require phosphorylation to form active deoxynucleoside triphosphate (dNTP) analogues (Cihlar and Ray, 2010). Despite having a lower intracellular concentrations, these dNTP analogues are incorporated at similar rates and with similar efficiency as endogenous dNTPs (El Safadi *et al.*, 2007). Thus, the dNTP analogues compete with endogenous dNTPs for incorporation into by the HIV RT (Cihlar and Ray, 2010).

The NRTI include zidovudine (AZT), didanosine (ddI), zalcitabine (ddC), stavudine (d4T), lamivudine (3TC), abacavir (ABC), emtricitabine (FTC) and tenofovir (TFV). A number have fallen out of use, due to higher levels of toxicity, avoidance of thymidine analogues to reduce the accumulation of thymidine analogue mutations (TAMs), or cost implications (Martinez-Cajas and Wainberg, 2008; Venter, 2017). Currently, AZT, TFV, ABC, 3TC and FTC remain in use.

Despite being classified as an NRTI, TFV is an acyclic nucleotide analogue which only requires di-phosphorylation (Vivet-Boudou *et al.*, 2006; Cihlar and Ray, 2010). In addition to this, TFV has been formulated as the prodrug TFV disoproxil fumarate (TDF) in order to enhance oral bioavailability (Lyseng-Williamson *et al.*, 2005).

The NRTI have a significantly high intracellular persistence after phosphorylation compared to the plasma half-life, which has been suggested to be the reason behind the efficacy of certain NRTI regimens (Cihlar and Ray, 2010). The adverse effects observed when using NRTI include peripheral neuropathy, pancreatitis, lipoatrophy and fatal liver toxicity, many of which may be as a result of mitochondrial damage (El Safadi *et al.*, 2007; Sherman, 2015). There are few drug interactions associated with most of the NRTI,

however, concomitant use of two analogues deriving from the same nucleoside is contraindicated (Sherman, 2015).

1.8.1.2 Non-Nucleoside Reverse Transcriptase Inhibitors (NNRTI)

The NNRTI are non-competitive allosteric inhibitors of the RT enzyme (Safrin, 2015; Sherman, 2015; Valuev-Elliston and Kochetkov, 2017). They bind to a hydrophobic site adjacent to the active site inducing a conformational change that displaces the catalytic aspartate residues and results in a reduced nucleotide incorporation rate (Vivet-Boudou *et al.*, 2006).

The first-generation NNRTI include nevirapine (NVP), delavirdine (DEL) and efavirenz (EFV) (Deeks, 2018; Gu *et al.*, 2018). These NNRTI, however, proved to have a low generic barrier to resistance and could be rendered inactive by a single drug-resistance mutation (de Béthune, 2010; Gu *et al.*, 2018). The second-generation NNRTI, doravirine (DOR), etravirine (ETV) and rilpivirine (RPV), were formulated to be active against HIV-1 viruses with resistance mutations to the first-generation NNRTI (Valuev-Elliston and Kochetkov, 2017).

The relative safety and favourable toxicity profile combined with their effective inhibition of wild-type (WT) HIV-1 viruses has made NNRTI, specifically EFV, the preferred third drug used in first-line ART for the last several years (de Béthune, 2010; Venter, 2017). Due to the high specificity with which NNRTI inhibit HIV-1 RT, these drugs are inactive in other retroviruses including HIV-2 (de Béthune, 2010).

1.8.2 Protease Inhibitors (PI)

Protease inhibitors (PI) function by reversibly inhibiting the HIV protease enzyme thus preventing cleavage of the viral polyproteins into their component enzymes, ultimately preventing the formation of mature, infectious virus particles (Sherman, 2015). The PI were formulated to mimic the transition state intermediate formed during proteolytic cleavage, replacing the scissile bond with a hydroxyethylene group (Adamson, 2012), except in tipranavir which has a sulphonamide-containing dihydropyrone ring (Orman and Perry, 2008). The PI bind HIV PR with high affinity, but are not cleaved as PR cannot hydrolyse the hydroxyethylene group (Wensing *et al.*, 2010).

The first generation of PI approved for clinical use were saquinavir (SQV), ritonavir (RTV), indinavir (IDV) and nelfinavir (NFV). Due to the issues of low bioavailability,

high pill burden, multiple daily dosing and the associated adherence issues and suboptimal drug concentrations, the first-generation PIs have fallen out of use (Adamson, 2012; Venter, 2017).

The second-generation of PI were formulated to improve on the issues associated with the first-generation of PI. These include a reduced pill burden, better tolerability due to fewer adverse effects, and greater drug potency which can be further enhanced with RTV boosting (Adamson, 2012).The second-generation PI include amprenavir (APV) (and the prodrug fosamprenavir [FPV]), lopinavir (LPV), atazanavir (ATV), tipranavir (TPV) and darunavir (DRV) (Wensing *et al.*, 2010). In addition to the abovementioned improvements, these second-generation PI have a higher genetic barrier to resistance and develop a different pattern of mutations compared to the first-generation PI (Adamson, 2012).

The discovery that RTV inhibits cytochrome P450 (CYP450) enzymes has resulted in it being used to "boost" PI regimens by co-administering it in low doses with a PI (Larson *et al.*, 2014). This boosting results in substantially improved bioavailability, half-life and potency of the boosted PI (Adamson, 2012).

1.8.3 Integrase Strand Transfer Inhibitors (InSTI)

The integrase strand-transfer inhibitors (InSTI) are competitive inhibitors of HIV replication by binding IN in the active site, chelating the two metal cations required for enzyme function, and preventing the proviral DNA from binding (McColl and Chen, 2010). This chelation activity makes InSTI unsuitable to be taken together with antacid medications (Sherman, 2015). The adverse effects of InSTI use include nausea, diarrhoea, headaches and nervous disorders (Safrin, 2015; Sherman, 2015).

The first-generation InSTI include raltegravir (RAL) and elvitegravir (EVG). Both of these have proven to be potent ARVs for both initial and salvage regimens (Karmon and Markowitz, 2013). The second-generation InSTI were formulated to have a higher genetic barrier to resistance, and to be active in patients who have accumulated drug resistance mutations to RAL and EVG (Dow and Bartlett, 2014). The second generation InSTI include dolutegravir (DTG) and bictegravir (BIC), and unlike EVG, do not require pharmacokinetic boosting with cobicistat (Larson *et al.*, 2014; Badowski *et al.*, 2016; Markham, 2018).

In general, InSTI have proven to have a few adverse effects and drug interactions, making them relatively well tolerated (Mesplède and Wainberg, 2013). This tolerability makes InSTI a popular option as the third agent in ART regimens in wealthier countries (Venter, 2017). Due to the high genetic barrier of DTG and the ability to manufacture generic formulations, the WHO has recommended a DTG-based alternative first-line regimen (Venter, 2017; World Health Organization, 2018).

1.8.4 Entry Inhibitors

The use of entry inhibitors is generally reserved for patients who have accumulated multiple drug resistance mutations and require a drug targeting a novel site of action for salvage therapy (Adamson, 2012). Maraviroc binds directly to CCR5 in order to prevent its association with gp120 and thus block viral entry. This means it is only active against R5 viruses and not X4 viruses, which enter the host cell using CXCR4 (Checkley *et al.*, 2011). Therefore, it is important that patients undergo tropism testing prior to maraviroc initiation to ensure the drug will be effective (Tilton and Doms, 2010).

Enfuvirtide (T-20) blocks gp41 from coming into close proximity with the host cell membrane in order to form a fusion pore Unlike with maraviroc, viral tropism does not play a role in the treatment response to enfuvirtide (Matthews *et al.*, 2004). The use of enfuvirtide is limited compared to maraviroc as it is associated with significant toxicities (Venter, 2017).

1.8.5 Treatment of HIV

As with the treatment of any other medical condition, the goal of ART is to prolong the length and improve the quality of life of persons infected with HIV. This is done by suppressing viral replication to prevent the infection of new cells (Moyle *et al.*, 1998). Following ART initiation, there is a rapid decrease in the viral load, with an approximate 0.5 log reduction by four weeks and a one log reduction by eight weeks after initiation (Samuel *et al.*, (2006). In addition to the survival benefits, successful ART also reduces transmission, as higher viral loads are associated with a greater probability of sexual transmission of the virus (Cihlar and Fordyce, 2016; Cohen *et al.*, 2016).

The current treatment paradigm used to treat HIV is combination therapy and consists of two NRTI making up the “backbone” of the regimen, and an additional ARV from a second class (an NNRTI, PI or InSTI) (Cihlar and Fordyce, 2016). Triple therapy

regimens were proven clinically superior to their NRTI dual-therapy counterparts in two clinical trials ending in 1997 (Gulick *et al.*, 1997; Hammer *et al.*, 1997). At the time of these studies it was already established that dual-therapy was superior to monotherapy, and the results of these trials showed that triple-therapy was superior to dual-therapy in terms of virological suppression, HIV-1 RNA and CD4 cell responses and disease progression to AIDS or death.

Prior to 2016, ART initiation was deferred until the $CD4^+$ cell count was below a certain threshold, if there were symptoms of advanced HIV disease, if there was tuberculosis or hepatitis B co-infection, if the patient was pregnant or breastfeeding or if the patient had an HIV-negative partner (World Health Organization, 2013; National Department of Health, 2015). The Strategic Timing of Antiretroviral Therapy (START), the Strategies for Management of Antiretroviral Therapy (SMART) and TEMPRANO trials investigated the outcomes of patients starting ART earlier than recommended (The Strategies for Management of Antiretroviral Therapy (SMART) Study Group, 2008; TEMPRANO ANRS 12136 Study Group, 2015; The INSIGHT START Study Group, 2015). The results of these trials, all of which indicated reduced adverse events when initiating therapy earlier, prompted the WHO to update their guidelines on when to initiate ART (World Health Organization, 2015b). Following this, South Africa implemented the universal test-and-treat approach in September 2016 (National Department of Health, 2016).

The South African National Consolidated Guidelines for the prevention of mother-to-child transmission of HIV and the management of HIV in children, adolescents and adults is based upon the WHO 2016 treatment guidelines (National Department of Health, 2015; World Health Organization, 2016b). The first-line regimen prescribed for adults includes pregnant and breastfeeding women and should be prescribed as a fixed-dose combination. In the private sector, the regimen choice is the same, however, DTG is available in the place of EFV (Meintjes *et al.*, 2017).

Table 1.1: Preferred first-line ART regimen in South Africa for all age groups.

Population Group	Preferred First-line ART Regimen
Adults and adolescents older than 15 years and greater than 40 kilograms (kg)	TDF + 3TC/FTC + EFV
Children and adolescents 3 to 15 years and greater than 10 kg	ABC + 3TC + EFV
Children younger than 3 years and less than 10 kg	ABC + 3TC + LPV/r

While on ART, certain clinical and laboratory assessments are performed, including $CD4^+$ T-lymphocyte cell counts, VL monitoring, drug toxicity testing, screening for infection with *Mycobacterium tuberculosis* and determination of the WHO clinical stage (National Department of Health, 2015). Virological failure which is defined as at least two VL measurements > 1000 copies/ml two months apart despite good ART adherence, results in a regimen switch to second-line ART which consists of AZT, 3TC and ritonavir boosted lopinavir (LPV/r) (National Department of Health, 2015). Alternatives to these drugs for second-line ART include ABC, TDF and ATV/r. Failure of second-line ART requires referral to a specialist, however, the regimen will generally consist of an InSTI such as RAL, a second-generation PI such as DRV and / or a second-generation NNRTI such as ETR (National Department of Health, 2015).

1.9 HIV DRUG RESISTANCE

1.9.1 Resistance to NRTI

Drug resistance mutations targeted against NRTI arise using one of two mechanisms to confer resistance, the discrimination mechanism or the primer unblocking excision mechanism (Vivet-Boudou *et al.*, 2006; El Safadi *et al.*, 2007; Nikolenko *et al.*, 2011). The two NRTI resistance pathways, with the exception of the M184V mutation, are opposing pathways and therefore, the mutation pattern observed is either one primer unblocking mutations or multiple discriminatory mutations (Tang and Shafer, 2012). The discrimination mechanism allows the HIV RT to distinguish between endogenous dNTPs and chain terminating dideoxy-NRTI (Tang and Shafer, 2012), and is dependent on the competition between the endogenous dNTPs and the NRTI analogues as well as the rate of NRTI incorporation into DNA (Vivet-Boudou *et al.*, 2006; El Safadi *et al.*, 2007). These mutations occur close to or within the dNTP binding site and include the K65R, K70E/G/Q, L74V/I, F77L, M184V/I and the Q151M complex mutations (Vivet-Boudou *et al.*, 2006; El Safadi *et al.*, 2007; Cihlar and Ray, 2010; Nikolenko *et al.*, 2011; Tang and Shafer, 2012).

The excision mechanism of drug resistance uses adenosine triphosphate-lysis to excise the chain terminating NRTI analogue (El Safadi *et al.*, 2007; Cihlar and Ray, 2010; Nikolenko *et al.*, 2011; Tang and Shafer, 2012; Clutter *et al.*, 2016). These mutations are distant from the dNTP binding site and are generally termed TAMs as they first originated following the use of the thymidine analogues AZT and d4T (Nikolenko *et al.*, 2011; Clutter *et al.*, 2016). The TAMs include the M41L, D67N, K70R, L210W, T215F/Y and K219Q/E/N/R (El Safadi *et al.*, 2007; Cihlar and Ray, 2010; Nikolenko *et al.*, 2011; Tang and Shafer, 2012). The TAMs are generally found in one of two overlapping patterns, Type I (M41L, L210W and T215Y) or Type II (D67N, K70R, T215F and K219Q/E) (Tang and Shafer, 2012). While these mutations were originally associated with thymidine analogues, they are multidrug and also confer resistance to TDF, ABC and ddI (Cihlar and Ray, 2010; Tang and Shafer, 2012).

1.9.1.1 M184V

The Substitution of the methionine (M) with valine (V) or isoleucine (I) at position 184 of the RT (the M184V mutation) is the most common NRTI-resistance mutation in approximately 53% of failing regimens in resource limited settings (Hosseinipour *et al.*, 2013). It is typically the first drug resistance mutation to appear, often with NNRTI-associated resistance mutations, in cases where NNRTI are co-administered (Miller *et al.*, 2002). The mutation is selected for by 3TC, FTC, ABC, ddI and ddC, and confers resistance to all of these, particularly 3TC and FTC, where there is a 100 to 1000-fold increase in the half maximal inhibitory concentration (IC_{50}) (Miller *et al.*, 2002; Wainberg, 2004; Vivet-Boudou *et al.*, 2006; El Safadi *et al.*, 2007; Clutter *et al.*, 2016). The presence of M184V also increases the virus susceptibility to AZT and TVF (Wainberg, 2004; Tang and Shafer, 2012; Clutter *et al.*, 2016). Despite the high level of resistance to 3TC and FTC, these drug retain some residual activity in the presence of M184V (Miller *et al.*, 2002; Wainberg, 2004).

The M184 amino acid is located within the highly conserved YMDD catalytic motif of the HIV-1 RT, which is highly conserved and interacts with the 3' end of the primer, incoming dNTPs and metal ion cofactors (Miller *et al.*, 2002; Vivet-Boudou *et al.*, 2006). Substitution of the M184 with V or I results in steric hindrance with 3TC and FTC in particular as the sulphur atom in the oxathiolane ring of these NRTI project further than the standard ribose ring present in endogenous dNTPs (Gao *et al.*, 2000; Vivet-Boudou *et al.*, 2006). The M184I mutation typically precedes M184V, however, due to the low

enzymatic efficiency of M184I, it is outcompeted by M184V (Gao *et al.*, 2000; Miller *et al.*, 2002; Vivet-Boudou *et al.*, 2006; Clutter *et al.*, 2016).

There is an increased fidelity associated with the M184V mutation, however, it is not as high as that observed by some other drug resistance mutations such as K65R or M184I (Miller *et al.*, 2002; Wainberg, 2004; Vivet-Boudou *et al.*, 2006). The increased fidelity results in reduced fitness, which not only reduces the HIV-1 processivity and replicative capacity, but may also result in reduced HIV-1 RNA levels of approximately 1.5 log compared to WT viruses (Miller *et al.*, 2002; Wainberg, 2004; Vivet-Boudou *et al.*, 2006; Tang and Shafer, 2012; Clutter *et al.*, 2016). The reduced fitness is also conveyed in the fact that viruses rapidly revert to WT at the M184 amino acid site following 3TC or FTC discontinuation (Miller *et al.*, 2002; Vivet-Boudou *et al.*, 2006; Wilson *et al.*, 2015).

The presence of M184V is antagonistic and suppressive to the generation of TAMs, resulting in their emergence being limited or delayed (Miller *et al.*, 2002; Wainberg, 2004). The combination of M184V and certain TAMs in one virus results in an additive inhibition of RT to an enhanced degree than would be observed by either alone (Wainberg, 2004).

1.9.1.2 K65R

Substitution of lysine (K) with arginine (R) at position 65 (the K65R mutation) is commonly detected in patients failing TFV-based regimens, and is more commonly observed in HIV-1 Subtype C (Brenner *et al.*, 2006; Das *et al.*, 2009). The lysine at position 65 forms part of the RT binding pocket and contributes to the correct binding and relative positioning of the incoming dNTP (Das *et al.*, 2009). Mutation of this amino acid to R increases the fidelity of the HIV-1 RT and decreases the rate of dNTP incorporation by almost 3-fold (White *et al.*, 2005; Das *et al.*, 2009). The increased fidelity leads to even lower efficiency of dideoxy-NRTI incorporation due to the structural differences existing between them and endogenous dNTPs (White *et al.*, 2005; Vivet-Boudou *et al.*, 2006; Das *et al.*, 2009). The increased fidelity also results in a reduction in viral fitness as the virus is less able to adapt to changes in the host (Das *et al.*, 2009).

The K65R drug resistance mutation is primarily selected for by TFV use, but also by d4T, ABC, ddI and ddC use, and confers resistance to these drugs as well as to 3TC and FTC (White *et al.*, 2005; Vivet-Boudou *et al.*, 2006; El Safadi *et al.*, 2007; Tang and Shafer,

2012). It is not selected for in AZT use and provides increased susceptibility to the drug (Vivet-Boudou *et al.*, 2006; Garforth *et al.*, 2014).

The K65R and M184V mutations in conjunction with each other reduce susceptibility to ddI, ABC, 3TC and FTC and increase susceptibility to TFV, d4T and AZT compared to each mutation alone (Das *et al.*, 2009). In addition, viruses with both of these mutations have a greater reduction in fitness due to an even lower incorporation on dNTPs (Vivet-Boudou *et al.*, 2006). There is antagonism between the K65R and TAM drug resistance mutations, and the two of these present in one virus results in increased susceptibility to TFV (Vivet-Boudou *et al.*, 2006; Das *et al.*, 2009).

1.9.2 Resistance to NNRTI

Mutations conferring resistance to NNRTI generally occur within the vicinity of or within the NNRTI binding pocket and result in the RT having reduced affinity for NNRTI (Nikolenko *et al.*, 2011; Tang and Shafer, 2012). The mutations, which appear either single or as part of a complex, confer resistance to at least two or more NNRTI (Nikolenko *et al.*, 2011; Tang and Shafer, 2012). The most common NNRTI drug resistance mutations include L100I, K101E/P, K103N/S, V106A/M, E138K, Y181C/I/V, Y188C/H/L, G190A/S/E and M230L (El Safadi *et al.*, 2007; Nikolenko *et al.*, 2011; Tang and Shafer, 2012).

1.9.2.1 K103N

The K103N drug resistance mutation is the most common NNRTI drug resistance mutation and second most common drug resistance observed in resource-limited settings (Hosseinipour *et al.*, 2013). It confers broad, high-level NNRTI resistance to NVP, DEL and EFV, and is selected by these drugs (El Safadi *et al.*, 2007; Nikolenko *et al.*, 2011; Massarotti and Coluccia, 2016).

The mechanism in which K103N reduces NNRTI susceptibility is by stabilising the structure of the NNRTI binding pocket in a closed conformation (Hsiou *et al.*, 2001; Ren and Stammers, 2008; Massarotti and Coluccia, 2016). This is supported by the fact that direct interaction between the K103 amino acid side chains and incoming NNRTI has only been observed with DEL (Hsiou *et al.*, 2001; Ren and Stammers, 2008; Massarotti and Coluccia, 2016). The newer NNRTI such as ETV, have a less rigid structure and thus are able “wiggle” into the closed binding pocket, as represented by the minimal resistance

effect of K103N mutants on ETV efficacy (Tang and Shafer, 2012; Massarotti and Coluccia, 2016). There are other amino acid mutations that occur at the K103 amino acid site of RT, including K103S which results in a 9.5-fold reduction in susceptibility to EFV and even greater reduction to DEL and NVP susceptibility (Harrigan *et al.*, 2005).

1.9.3 Development of Drug Resistance

The development of drug resistance is due to the selective pressure exerted by ART agents on the replicating HIV-1 virus. Drug resistance is also specific to the drug or drug class from which it developed, and cross-resistance between classes generally does not occur, even between NRTI and NNRTI drug resistance mutations (Tang and Shafer, 2012). The genetic barrier to resistance of an ARV is defined as the number of mutations required to confer resistance to that drug and Figure 1.4 describes the genetic barrier of several common ARVs as a function of their potency (Tang and Shafer, 2012).

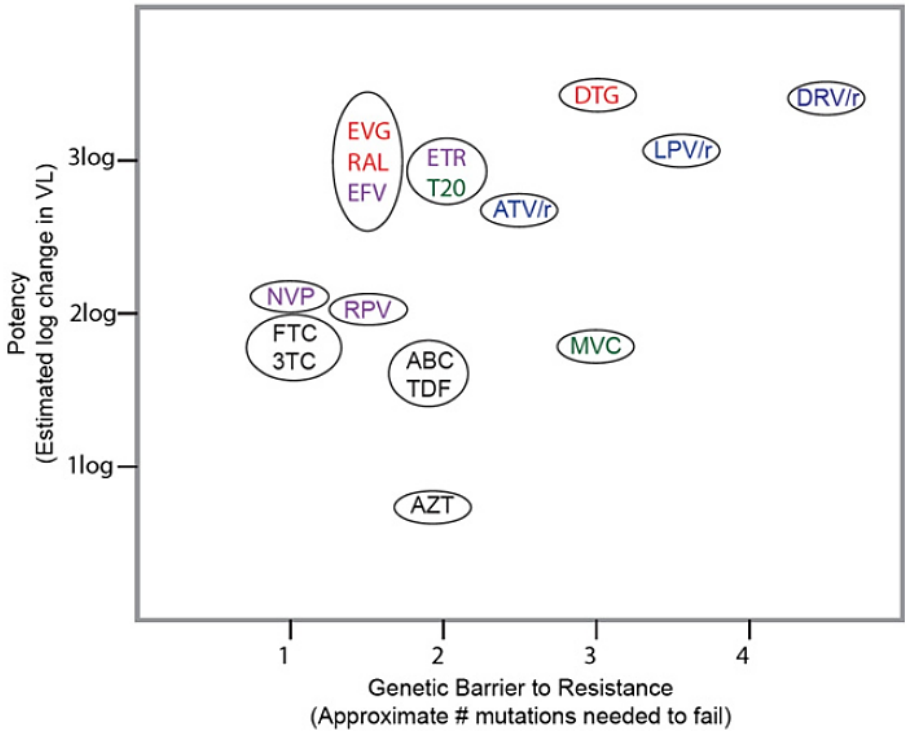

Figure 1.4: Genetic barrier to resistance of commonly used antiretrovirals as a function of their potency (Tang and Shafer, 2012). The potency compared to genetic barrier of commonly used ARVs. Drug classes are as follows: NRTI in black font, NNRTI in purple font, PI in blue font, InSTI in red font and entry inhibitors in green font. Antiretrovirals within the same ellipse are considered to have similar potencies and genetic barriers to resistance.

The genetic barrier of the drug classes reserved for second- and third-line ART, namely the PI, InSTI and second-generation NNRTI have a higher genetic barrier to resistance

than the NRTI and NNRTI commonly used in first-line ART regimens (National Department of Health, 2015; World Health Organization, 2016b). This is due to the fact that cross-class drug resistance is rare, and thus provides a new drug class to which the patient is fully susceptible (Tang and Shafer, 2012). These drugs also have a higher potency, defined as the extent to which the ARV lowers plasma HIV-1 levels, and thus are more ideal in situation where the NRTI backbone may be compromised (Tang and Shafer, 2012; Clutter *et al.*, 2016).

The development of drug resistance mutations is facilitated by the high replication rate in conjunction with the low fidelity of the viral RT resulting in a high mutation rate (Daar and Richman, 2005; Tang and Shafer, 2012). Suboptimal ART levels allows for continued HIV replication and due to the selection pressure of the drug, minor-variant drug-resistant strains present within the HIV population increase in prevalence and result in replicating drug-resistant viruses (El-Khatib *et al.*, 2010; Clutter *et al.*, 2016). While non-adherence is a common cause of suboptimal ART levels, other virus and host factors play a role as well including poor drug absorption and suboptimal therapeutic drug levels resulting in continued HIV replication (Rong *et al.*, 2007; Clutter *et al.*, 2016). It is estimated that approximately 5% of patients develop genotypic resistance after one year on combination ART, 10% after two years and within six years almost 30% experience virological failure with a minimum of one major drug resistance mutation (Wilson *et al.*, 2015). It should however be noted that as most drug resistant variants are less fit, they are frequently out-competed by the more fit circulating WT variants in the absence of drug pressure (Clutter *et al.*, 2016).

The above describes how acquired drug resistance (ADR) is developed, however, drug resistant viruses may also be transmitted from person-to-person (Clutter *et al.*, 2016). Infection with a resistant virus, termed transmitted drug resistance (TDR), carries an increased risk of virological failure and possible development of additional drug resistance mutations (Tang and Shafer, 2012). Detection of TDR is limited by the fact that drug resistance mutations may not be present without the selective pressure of the ART after a certain amount of time as the mutant variant may be archived in the viral reservoirs (Hanna and D'Aquila, 2001). Screening of TDR is often performed by analysing pre-treatment drug resistance (PDR), which is also subject to previous ART exposure (Tang and Shafer, 2012).

1.9.4 Review of HIVDR trends

A systematic literature review of rates of PDR including studies performed between 2001 and 2016 was reported in the 2017 WHO HIV Drug Resistance Report (World Health Organization, 2017), where in rates of PDR have increased annually by 29% in Eastern Africa and 23% in Southern Africa, and between 11 and 17% in other regions. A sequence data meta-analysis similarly showed increases in odds of NNRTI TDR in most regions, including a 1.09-fold increase in sub-Saharan Africa (Rhee *et al.*, 2015). Figure 1.5 below shows the results of the meta-analysis of NNRTI and NRTI drug resistance in Southern Africa (World Health Organization, 2017).

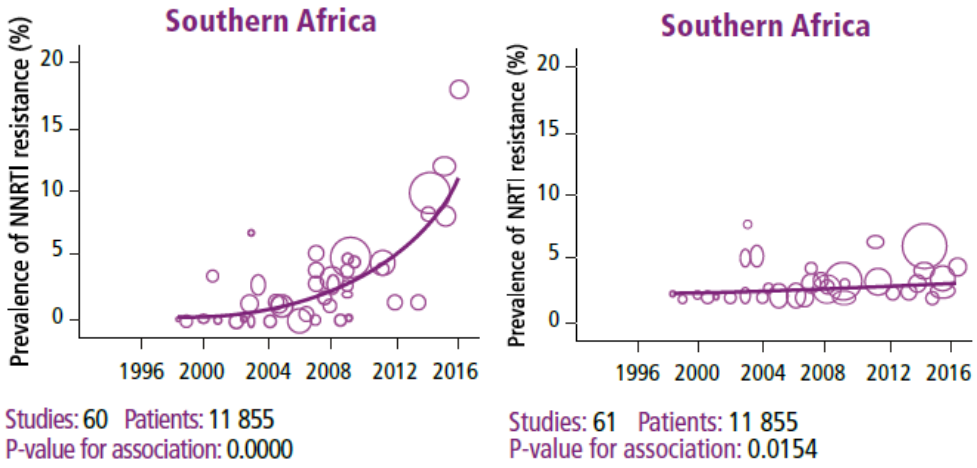

Figure 1.5: Pre-treatment drug resistance in Southern Africa (World Health Organization, 2017). Then approximate levels of non-nucleoside reverse transcriptase inhibitor resistance (left) and nucleoside reverse transcriptase inhibitor resistance (right) in Southern Africa.

The paediatric PDR prevalence was estimated to be 31.3% by the WHO Drug Resistance Report (World Health Organization, 2017). A meta-analysis performed by Boerma *et al.* (2016) determined the level of PDR in children in sub-Saharan Africa based upon exposure to for prevention of mother-to-child transmission (PMTCT). This study found a PDR prevalence of 42.7% for prevention of mother-to-child transmission (PMTCT)-exposed and 12.7% for those unexposed children. There was also found to be higher levels of dug resistance in children aged less than (<) 3 years (40.9%) compared to children 3 years or older (17.6%) (Boerma *et al.*, 2016). This higher level of PDR children < 3 years in sub-Saharan Africa is concordant with the results of a multi-country analysis performed in five sub-Saharan African countries where the overall PDR was found to be 54.1% in newly-diagnosed infants < 18 months of age (Jordan *et al.*, 2017).

The WHO 2017 HIV Drug Resistance Report further reported trends in ADR, with a global prevalence of 70.7% among adults failing ART (World Health Organization, 2017). Figure 1.6 below summarises the drug resistance mutations detected by ARV class and major mutation (World Health Organization, 2017). Within Southern Africa, the prevalence of drug resistance in adults failing ART was estimated to be approximately 87.3% (World Health Organization, 2017).

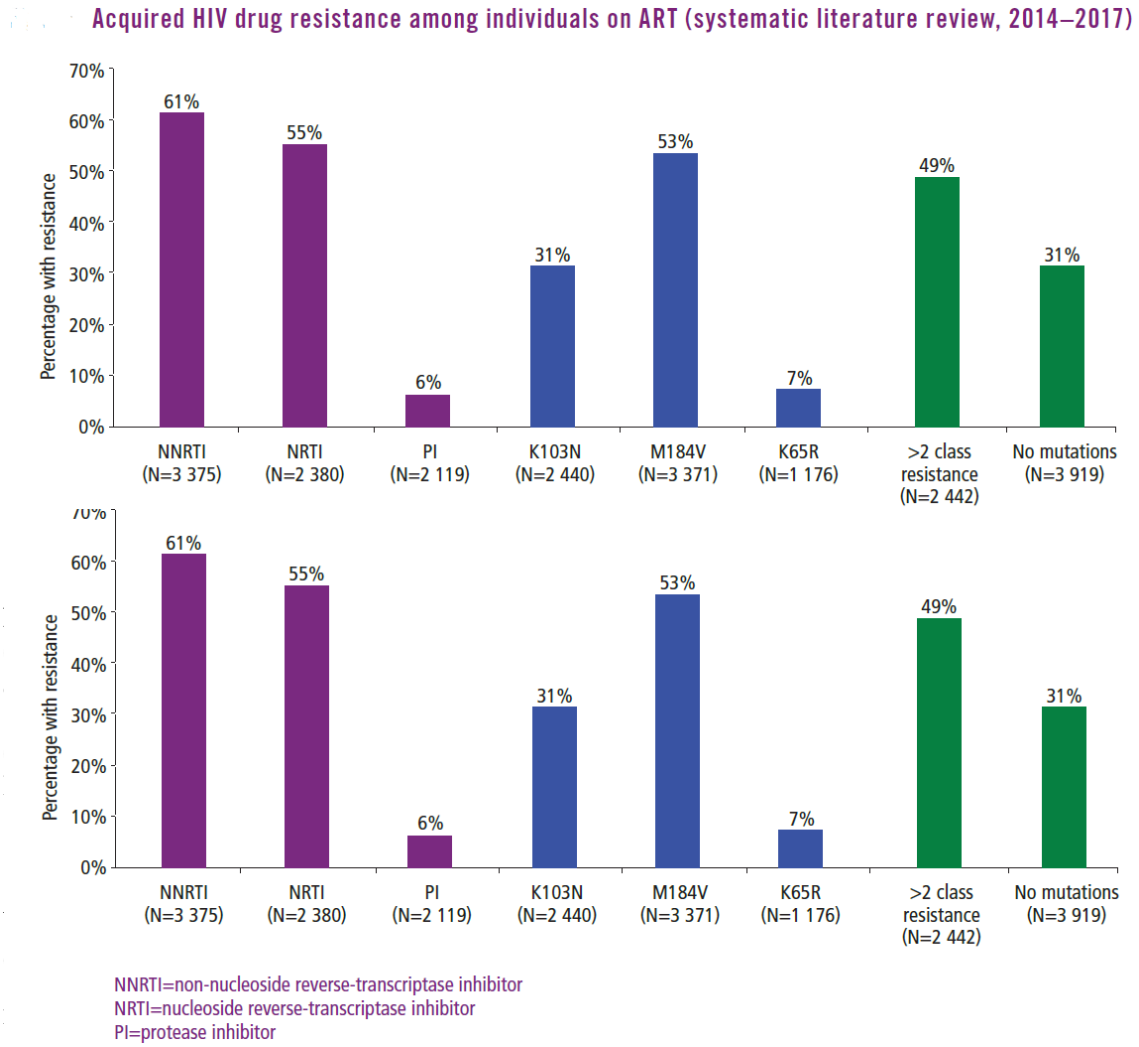

prevalence of NNRTI PDR was found to be 24.0% and 56.8%, and NRTI PDR was 10.7% and 14.8%, respectively, according to whether PMTCT-naïve or –exposed (Kuhn *et al.*, 2014).

There have been multiple studies in SA assessing the levels of ADR at first-line treatment failure (El-Khatib *et al.*, 2010; Wallis *et al.*, 2010; Sigaloff *et al.*, 2011; van Zyl *et al.*, 2011; Steegen *et al.*, 2014, 2017; Skhosana *et al.*, 2015; Hunt *et al.*, 2017). The most prevalent mutation detected in SA is M184V/I, and has been detected in high numbers since 2007, ranging from 60.4% to 91.3%. Mutations that confer resistance to NNRTI are

also prevalent, with K103N being the most common with a prevalence ranging from 35.3% to 53.0%. As with M184V, there is also a general increase in the prevalence.

The K65R NRTI-resistance mutation has dramatically increased in prevalence since 2007, with an increase from between 1.1% to 8.8% prior to 2010 to 44.7% to 53.8% in TFV-based regimens after 2010 (El-Khatib *et al.*, 2010; Wallis *et al.*, 2010; Sigaloff *et al.*, 2011; van Zyl *et al.*, 2011; Steegen *et al.*, 2014, 2017; Skhosana *et al.*, 2015; Hunt *et al.*, 2017). The substantial increase in the prevalence of this mutation is due to the change in first-line ART guidelines in 2010 recommending a TDF-based regimen, which selects K65R, in the place of a d4T-based regimen, which selects TAMs (Martinez-Cajas and Wainberg, 2008; National Department of Health, 2015; Steegen *et al.*, 2017).

1.9.5 Resistance Detection Assays

Phenotypic drug resistance assays measure the *in vitro* susceptibility of a viral inoculum to increasing ARV concentrations (Tang and Shafer, 2012). The susceptibility is based upon the ratio of the ARV concentration that inhibits 50% (IC_{50}) of the virus being tested relative to the IC_{50} of the wild-type (WT) reference, measured as a fold change in susceptibility (Cohen *et al.*, 2002; Tang and Shafer, 2012). Phenotypic drug resistance assays are generally not performed for clinical management due to high costs and turnaround time (Clutter *et al.*, 2016).

Genotypic drug resistance testing relies on the detection of drug resistance mutations at the sequence level, usually performed using PCR and dideoxynucleotide Sanger sequencing (Clutter *et al.*, 2016). The sequencing reaction is performed on the PCR amplification product of the PR, RT or IN gene (Tang and Shafer, 2012). The resulting electropherogram can then be analysed using software tools that provide consistency with regards to the identification of nucleotide mixtures (Clutter *et al.*, 2016). While Sanger sequencing can detect variation in the HIV population, the limit of detection is approximately 20% of the mutant in a WT background (Tang and Shafer, 2012; Parikh *et al.*, 2017). Interpretation of the detected mutations to determine the effect each has on drug resistance can be performed using multiple algorithms such as the Stanford HIV Drug Resistance Database (HIVDB) (Clutter *et al.*, 2016).

Other genotypic assays have sought to improve upon the sensitivity of Sanger sequencing and include next-generation sequencing (NGS), real-time allele-specific PCR (AS-PCR),

oligonucleotide ligation assays (OLAs), pan-degenerate amplification and adaptation (PANDAA) assays and ligation on RNA assays (Hunt *et al.*, 2011; Tang and Shafer, 2012; Inzaule *et al.*, 2016; Natoli *et al.*, 2017; Panpradist *et al.*, 2017; Parikh *et al.*, 2017). These assays are capable of reliably detecting mutations present at levels as low as 0.01 to 5% of the HIV-1 population (Parikh *et al.*, 2017). Table 1.2 below compares Sanger sequencing, NGS, and point mutation assays in general in terms of their advantages and disadvantages (Hanna and D'Aquila, 2001; Tang and Shafer, 2012; Inzaule *et al.*, 2016). The improved sensitivity of these assays, with a focus on AS-PCR, has been used to detect minority drug resistance mutations undetectable by Sanger sequencing (Johnson *et al.*, 2008; Pillay *et al.*, 2008; Coovadia *et al.*, 2009; Rowley *et al.*, 2010; Hunt *et al.*, 2011; Li *et al.*, 2011; Hoffman *et al.*, 2013). It is important to note that point mutation assays, while having the potential to be multiplexed, are designed to detect mutations present at a single codon and therefore will not detectedother mutations present in the amplicon (Inzuale *et al.*, 2016).

Table 1.2: Comparison of the advantages and disadvantages of drug resistance assays (Hanna and D'Aquila, 2001; Tang and Shafer, 2012; Inzaule *et al.*, 2016)

Drug Resistance Assay	Advantages	Disadvantages
Phenotypic drug susceptibility assays	• Reproducible • Available in a kit	• Labour intensive and time consuming • In vitro selection of drug resistance mutations • Lack of consensus on clinically significant fold change values • Insensitive to antagonistic mutations
Sanger sequencing	• Widely validated • Available in a kit • Broad subtype • Commonly available • Can be used with DBS	• Labour intensive • Limited automation potential • High initial capital cost • Low sensitivity to variants below 20% • Ill-suited for parallel testing
Next-generation sequencing	• Specimens can be pooled and run in parallel to save costs • High sensitivity • Can be used with validated primers • Can be used with DBS	• Labour intensive • Complex workflow • Can be subject to PCR errors • Complex and costly data analysis • Requires wide validation • High initial capital cost • Possible read problems or uneven sequence coverage
Point mutation assays	• High sensitivity • Potential for use with validated primers • Potential for point-of-care implementation	• Limited multiplex capability • Not commercially available • Requires extensive validation

1.9.5.1 The HIV Drug Resistance RNV Multiplex Assay

The HIV Drug Resistance RNV (named for its detection of the K65**R**, K103**N**, and M184**V** mutations) Multiplex Assay was developed by the Centers for Disease Control and Prevention (CDC) for the purpose of detecting HIV-1 expression and screening for three key drug resistance mutations associated with resistance to reverse transcriptase inhibitors. Detection of unsuppressed HIV replication and the three key drug resistance mutations, namely K65R, K103N and M184V occurs simultaneously. This allele-specific assay uses a real-time platform with the SYBR-green intercalating fluorescent dye for the quantitative detection of the amplification levels (Wei *et al.*, 2015).

The RNV assay consists of two PCR reactions, the total copy (TC) PCR component and the RNV PCR component, which are performed simultaneously. The TC PCR component is the VL component of the assay and qualitatively differentiates between a high (≥600 copies/ml) and a low (<600 copies/ml) VL. Specimens classified as having a high VL are further analysed using the RNV PCR component. The RNV component is a multiplex reaction that simultaneously detects the K65R, K103N and M184V mutations, Mutation detection is performed by estimating the approximate mutant virus in the HIV population for that specimen by using the change in the cycle threshold (ΔCt) value of the RNV curve compared to the TC curve of that specimen. As both the viral load and mutation detection component are qualitative, this assay serves as a screening method for the identification of patients experiencing virological failure or harbouring drug-resistant HIV.

There is no differentiation of the RNV PCR component amplification products as the RNV assay uses an intercalating dye, however, agarose gel electrophoresis of the RNV PCR products allows for identification of specific mutations in specimens with mutations detected. The expected product sizes are 118 bp for the K65R product, 129 bp for the K103N product and 190 bp for the M184V product.

The value of this assay is that while it is not quantitative, it can be implemented for routine viral load monitoring as it can detect virological failure. The mutation detection component of this assay also allows for screening of patients that require further drug resistance testing or better adherence counselling, thus reducing the number of unnecessary drug resistance tests performed. The approximate percentage of mutant virus in the HIV population of a specific specimen can be estimated by using the change in the

cycle threshold (ΔCt) value of the RNV curve compared to the total copy (viral load) curve of that specimen.

This RNV assay is a relatively simple assay to set up and can be used on most real-time platforms, making it feasible to implement in the majority of laboratories in SA and sub-Saharan Africa. It is also cost effective, and will reduce not only the number of drug resistance tests performed, but the number of patients switched to second-line regimens, both of which have significant cost implications (Inzaule *et al.*, 2016).

1.10 AIM

The aim of this study was to validate and optimise the HIV Drug Resistance RNV Multiplex Assay in a South African setting.

1.11 OBJECTIVES

The primary objective of this study is:

1. To validate the HIV Drug Resistance RNV Multiplex Assay using specimens collected from South African HIV-1 patients failing first-line ART.

2. To compare the results of the assay to previously determined VL and genotype data.

The secondary objectives of the study include:

1. To analyse discrepant specimens using NGS to assess if the RNV assay is more sensitive.

2. To explore polymorphic changes in discrepant specimens that may be contributing to assay failure. To analyse the nucleotides in the primer binding region using the previously generated Sanger sequences in any specimen where the allele-specific multiplex PCR did not detect a mutation present in the Sanger sequence data.

3. To optimise the assay by recommending alternative TC and RNV thresholds based on the pervious VL and Sanger sequence data.

CHAPTER 2:

MATERIALS AND METHODS

2.1 SPECIMEN SELECTION

A total of 225 remnant plasma specimens were selected for this study, with known VL and genotype (if the VL was > 1,000 copies/ml). These specimens were obtained through previous drug resistance surveillance studies where participants were receiving ART (University of the Witwatersrand Human Research Ethics Committee [HREC] number M150740 and M131021). Of these, 47 specimens had a VL < 600 copies/ml, and 178 specimens had a VL ≥ 600 copies/ml. Of those with known genotype, 105 specimens had a WT genotype at the 65, 103 and 184 amino acid sites, and 66 specimens had one or more of the K65R, K103N and/or M184V mutations detected by conventional Sanger sequencing technologies. The remaining 54 specimens were not previously genotyped due to low VL. All specimens were delinked by the primary study principal investigators and given a unique study identifier (ID).

2.2 SPECIMEN PROCESSING AND TEMPLATE GENERATION

Whole blood specimens were originally collected in ethylenediaminetetraacetic acid (EDTA) vacutainer tubes. Specimens were shipped from the sample collection site within 96 hours. The plasma was separated by centrifugation at 4°C for 10 min at 440 g, and the plasma was transferred to a new tube and stored at -80°C.

2.2.1 Nucleic Acid Extraction

Total nucleic acid (TNA) extraction of viral RNA was performed on 200 µl of plasma using the automated MagNAPure LC instrument (Roche Diagnostics) using the MagNA Pure LC Total Nucleic Acid Isolation Kit (Roche Diagnostics) according to the manufacturer's instructions. The procedure involves lysis, in which the lysis buffer and proteinase K disrupted and digested the proteins and enzymes present. The magnetic glass particles used consist of a silica surface with a magnetic core. The magnetic glass particles and wash buffer I (containing isopropanol and guanidium chloride) were added to the lysed mixture, allowing the nucleic acids present to bind to the silica surface of the beads while the wash buffer removed the proteins and other contaminating molecules. The magnetic glass particles were isolated from the digested cellular material and debris by

applying the magnet, and washing performed using wash buffers II and III. The isolated nucleic acids were released from the magnetic glass particles into the elution buffer by applying heat and low-salt conditions (Roche Diagnostics GmbH, 2008).

The nucleic acids were eluted into 50 µl of the provided elution buffer and stored at -80°C until use. The instrument has capacity for 30 specimens to be processed in a single batch. Each batch included a HIV-positive and a HIV-negative control.

2.2.2 Reverse-Transcriptase PCR

An RT-PCR was initially performed to generate template for the RNV assay, using conditions described by Zhou *et al.*, 2011. In this assay, complementary DNA (cDNA) synthesis and RT-PCR was combined into a single reaction step using the SuperScript® III One-Step RT-PCR System (Invitrogen, Carlsbad, CA, USA), and performed on the Applied Biosystems 2720 Thermal Cycler (Applied Biosystems, Foster City, CA, USA). Included in every batch of RT-PCR were positive and no-template controls. The RT-PCR primers RT-R1 and PrtM-F1, which is an equimolar mixture of PrtM-F1a and PrtM-F1b (Table 2.1), generate a first-round template that is 1.3 kilo-bp (kb) in length (nucleotide position 2057 to 3370). The reaction conditions were: 1X Reaction Mixture which contained 0.2 millimolar (mM) of dNTP and 1.2 mM magnesium sulphate ($MgSO_4$), 1 microlitre (µl) of the SuperScript® III RT Enzyme Mix (Invitrogen) and 0.4 micromolar (µM) of each primer, to a final volume of 40 µl. To each reaction, 10 µl of extracted TNA was added.

Table 2.1: Primers used for cDNA synthesis and initial amplification of the *pol* gene (Zhou *et al.*, 2011).

Primer	Sequence (5' to 3')	Position (nt)	Orientation	Tm (°C)
PrtM-F1a	TGA ARG AIT GYA CTG ARA GRC AGG CTA AT	2057 to 2085	Forward	56
PrtM-F1b	ACT GAR AGR CAG GCT AAT TTT TTA G	2068 to 2092	Forward	51
RT-R1	ACT CCT GCA TAA ATC TGA CTT GC	3370 to 3348	Reverse	54

The PCR cycling conditions were: 50°C for 45 minutes (min) for cDNA synthesis, 94°C for 2 min (initial denaturation) followed by 40 cycles consisting of 94°C for 15 seconds (s), 50°C for 20 s and 72°C for 2 min; ending with 72°C for 10 min for final

product extension and cooling to 4°C. The RT-PCR products were stored at -20°C until further use.

Product verification of RT-PCR products was performed via agarose gel electrophoresis using a 2% agarose gel, made with UltraPure™ Agarose (Invitrogen) stained with ethidium bromide (5 µg/ml) (Bio-Rad Laboratories, Hercules, CA, USA) and the PCR products were visualised under UV light using the Bio-Rad ChemiDoc™ MP Imaging System (Bio-Rad Laboratories).

2.3 THE HIV-1 DRUG RESISTANCE RNV MULTIPLEX ASSAY

2.3.1 Kit components and purpose

The HIV-1 Drug Resistance Multiplex Assay was designed by the Division of HIV/AIDS Prevention, Centres for Disease Control (CDC), Atlanta, GA as a simple and affordable assay to simultaneously detect HIV viraemia levels and three key drug resistance mutations (K65R, K103N and M184V) using an intercalating fluorescent dye and real-time PCR platforms (Wei *et al.*, 2015). Specifically, the kit quantifies the relative amplification level of a HIV-1 total copy (TC) PCR to which the mutation specific (RNV) PCR is compared. The TC PCR component acts as a qualitative measure of circulating virus levels using a lower detection limit of 600 copies/ml as a basis for qualitative categorisation.

The kit provides vials of lyophilised TC and RNV reaction mixture that are reconstituted to the required concentration immediately prior to use using distilled water. In addition, included in each kit are two control plasmids, the RNCV control plasmid, which contains each of the K65R, K103N and M184V control plasmids, and a WT control plasmid that function as internal controls and measure the ability of the assay to distinguish mutant from WT. The assay requires generation of amplified RT-PCR template of the HIV polymerase gene as input for the assay, and is intended to be adaptable to any template product method, and any real-time PCR platform.

2.3.2 Assay protocol

The lyophilised TC and RNV reaction mixes were reconstituted with 1150 µl diH_2O, whereas the plasmid controls were reconstituted with 200 µl diH_2O.

For all reactions, the final reaction mixture included 23 µl of the relevant reconstituted TC or RNV enzyme mixture and 2 µl of the RT-PCR template product or plasmid control. Each specimen or control was added to each of two wells, one containing the TC enzyme mixture and the other the RNV enzyme mixture. Figure 2.1 illustrates the typical plate layout used for the RNV assay. A maximum of 45 specimens could be included in each run.

	1	2	3	4	5	6	7	8	9	10	11	12
A	TC + S1	RNV + S1	TC + S9	RNV + S9	TC + S17	RNV + S17	TC + S25	RNV + S25	TC + S32	RNV + S32	TC + S39	RNV + S39
B	TC + S2	RNV + S2	TC + S10	RNV + S10	TC + S18	RNV + S18	TC + S26	RNV + S26	TC + S33	RNV + S33	TC + S40	RNV + S40
C	TC + S3	RNV + S3	TC + S11	RNV + S11	TC + S19	RNV + S19	TC + S27	RNV + S27	TC + S34	RNV + S34	TC + S41	RNV + S41
D	TC + S4	RNV + S4	TC + S12	RNV + S12	TC + S20	RNV + S20	TC + S28	RNV + S28	TC + S35	RNV + S35	TC + S42	RNV + S42
E	TC + S5	RNV + S5	TC + S13	RNV + S13	TC + S21	RNV + S21	TC + S29	RNV + S29	TC + S36	RNV + S36	TC + S43	RNV + S43
F	TC + S6	RNV + S6	TC + S14	RNV + S14	TC + S22	RNV + S22	TC + S30	RNV + S30	TC + S37	RNV + S37	TC + S44	RNV + S44
G	TC + S7	RNV + S7	TC + S15	RNV + S15	TC + S23	RNV + S23	TC + S31	RNV + S31	TC + S38	RNV + S38	TC + S45	RNV + S45
H	TC + S8	RNV + S8	TC + S16	RNV + S16	TC + S24	RNV + S24	TC + RNCV	RNV + RNCV	TC + WT	RNV + WT	TC + NTC	RNV + NTC

Figure 2.1: Typical plate layout of the RNV assay. Layout of a typical RNV PCR assay plate. Grey shading represents tubes with the TC enzyme mixture while white shading indicates tubes with the RNV enzyme mixture. The specimens are represented by S1 to S45.

The real-time PCR reaction was performed using the LightCycler 480 instrument (Roche Diagnostics, Mannheim, Germany) under the following conditions: 95°C for 10 mins followed by 35 cycles of 95°C for 30 s, 50°C for 15 s and 59°C for 30 s. Fluorescence was collected after the annealing step at the SYBR Green acquisition wavelengths of excitation at 465 nm to emission at 510 nm.

2.3.3 Real-time PCR data analysis methods

The amplification curves were analysed using two absolute quantification methods, namely the second derivative maximum and the fit point methods, to determine the cycle threshold (Ct, also known as crossing point) values. The second derivative maximum Ct value was calculated by the Light Cycler instrument (Roche Diagnostics) by determining the equation of the amplification curve and the exact point where the second derivative of this was at a maximum, such as described by Tichopad *et al.*, (2003). This was done

automatically by the instrument after selecting the method for analysis. The crossing point / cycle threshold in relation to the second derivative and amplification curves is shown in Figure 2.2 below.

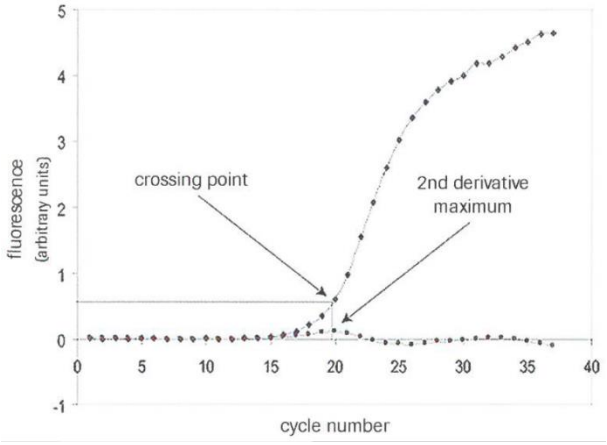

Figure 2.2: The crossing point (Ct) of an amplification curve in relation to the second derivative values. The crossing point (Ct) value illustrated in relation to the amplification curve at the point where the second derivative is at a maximum.

The fit point method requires the user to select a threshold which eliminates background noise and the Ct values are determined as the point where the amplification curve crosses this user-defined threshold. The threshold is selected at the beginning of the exponential phase of the RNCV and WT control amplification curves. Figure 2.3 illustrates the noise band position and the points fit to curves after eliminating the noise below the threshold. Calculation of the Ct value following placement of the threshold or noise band is determined by the Light Cycler instrument software.

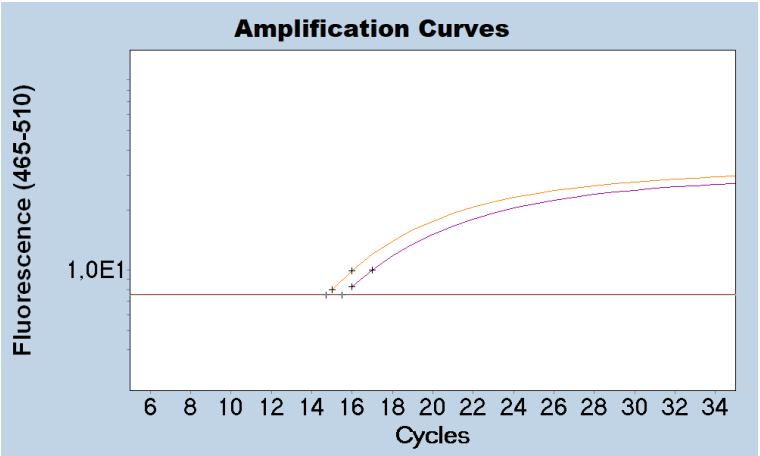

Figure 2.3: Determination of the Ct using the fit points method. The RNCV (orange), WT (purple) and H_2O (grey) RNV control amplification curves and the noise band (red) following

removal of the noise beneath the threshold. The point fit to curve (black cross) were used to calculate the Ct value.
Using either data analysis method to determine the Ct values, the change in ΔCt value was calculated for each control by subtracting the TC Ct value from the RNV Ct value. This was performed using Microsoft Excel 2016 (Microsoft Corporation, WA, USA)

2.3.4 Preparation and validation of assay control plasmids

The control plasmids provided in the kit are used to verify and validate the functionality of the assay on the instrument, as well as to verify and validate each run. In addition to the WT control plasmid, was the 65R, 103N and 184V control plasmids. All control plasmids are reconstituted in 200 µl diH_2O.

An initial validation run was performed using the plasmid 65R, 103N, and 184V diluted in the WT control to specified values to ensure that the sensitivity of the diluted positive controls were within the specified range. Dilutions of the 65R, 103N and 184V control plasmids were created by mixing 5 µl of the reconstituted mutant plasmid control with 20 µl of the WT plasmid to create a 20% mutant:WT mixture. This 20% control mixture was further diluted in the same way to produce the 4% control, and further diluted to create the 0.8% control. Each dilution preparation was processed on the RNV assay in triplicate. The initial validation run included the WT and a no template control (NTC).

2.3.5 Specimen processing using the Allele-specific RNV PCR Assay

All 225 RT-PCR templates were processed on the RNV Multiplex Assay as described in Sections 2.3.2 and 2.3.3. Each specimen was processed and analysed in triplicate by performing three separate RNV PCR reactions using the same RT-PCR template. The RNCV and WT controls were included in all runs to act as an internal run validation control.

Prior to analysing the TC Ct values, the amplification curves of each specimen were analysed and qualitatively classified as being either amplification positive or negative based on the sigmoidal shape of the amplification curve. Specimens that had visible amplification were subsequently analysed to determine the Ct value while TC specimens with no amplification were assumed to have a VL < 600 copies/ml. The RNV amplification curves were analysed and classified in the same way.

For all triplicate values, the mean TC, RNV and ΔCt, values for each specimen were calculated. If any of the individual results differed from mean by > 3.0 cycles, then that run was considered discrepant and the data was not used. In such cases, the RNV assay, including the TC PCR and RNV PCR, was repeated on that specimen.

2.3.6 Assay validation criteria

The following criteria apply to the assay:

- For successful validation, the mean ΔCt of each mutant plasmid preparation was expected to be ≤ 11.0 cycles and the mean ΔCt of the WT plasmid was expected to be > 12.0 cycles. This criteria applies to the 100%, 20% and 4% mutant:WT dilutions of the 65R, 103N and 184V plasmids prepared.
- The RNCV control ΔCt must fall within 4.5 ± 1.0 PCR cycles.
- The WT control ΔCt must be ≥ 12.0 PCR cycles.
- The Ct value for the specimen TC reaction of should fall within 10 to 25 cycles. If the RT-PCR product is too concentrated (TC < 10 cycles, the template should be diluted 1:20 or further in diH2O to fall within this range and the assay performed again.
- ΔCt cutoff for positive detection of mutation in specimens is ≤ 11.0 PCR cycles.
- The limit of detection of the assay is defined as a TC Ct value of ≤ 25.0 cycles, equivalent to a HIV VL of 600 copies/ml. All specimens with a TC Ct value of > 25.0 are therefore considered as having a VL of < 600 copies/ml and are not analysed further.
- Mutations are determined to be present if the difference between TC and RNV Ct values (ΔCt) are ≤ 11.0 cycles.
- Agarose gel electrophoresis of the RNV PCR reaction product is subsequently performed to determine which mutation(s) are present on specimens that are RNV positive (ΔCt ≤ 11.0) only.

2.3.7 Agarose Gel Electrophoresis of RNV Assay Products

Specimens that had were positive for mutations using the RNV component of the assay underwent agarose gel electrophoresis to determine which of the mutations were detected by the RNV assay. The RNV assay PCR product was loaded onto a 4% agarose gel (Invitrogen) stained with ethidium bromide (10 mg/ml) (BioRad Laboratories). The agarose gel was viewed using the Bio-Rad ChemiDoc™ MP Imaging System (Bio-Rad

Laboratories). The K65R, K103N and M184V amplification products were at 118 bp, 129 bp and 190 bp, respectively.

2.4 NEXT-GENERATION SEQUENCING (NGS)

2.4.1 Nested PCR

The nested PCR (nPCR) reaction was performed on the RT-PCR products that was used as template for the RNV assay. This was performed on all specimens selected to undergo NGS, which included the specimens discrepant between the RNV assay and Sanger sequencing as well as specimens with additional mutations present in the agarose gel electrophoresis analysis of the RNV amplification products that were not present in the Sanger sequence data. The PCR was done as described by Zhou *et al.*, (2011). The nested primers Prt-F2 and RT-R2 primers (Table 2.3) generate a product of 1,084 kb in length (nucleotide position 2243 to 3326). Included in every batch of nPCR was the positive and negative control described in Section 2.2.1.

Table 2.2: Primers used for nPCR for amplification of the *pol* gene (Zhou *et al.*, 2011).

Primer	Sequence (5' to 3')	Location (based on HXB2)	Orientation	Tm (°C)
Prt-F2	CTT TAR CTT CCC TCA RAT CAC TCT	2243 to 2266	Forward	56
RT-R2	CTT CTC TAT GTC ATT GAC AGT CC	3326 to 3304	Reverse	55

The reaction mixture consisted of 1X GeneAmp® 10X Gold Buffer (Applied Biosystems), 2 mM magnesium chloride ($MgCl_2$) (Applied Biosystems), 0.2 mM PCR Nucleotide Mix (Roche Diagnostics), 0.2 µM of each of the forward and reverse primer, and 5 units (U) of the AmpliTaq Gold® DNA Polymerase (Applied Biosystems). The 1X GeneAmp® 10X Gold Buffer (Applied Biosystems) contained 15 mM 2-amino-2-(hydroxymethyl)propane-1,3-diol (Tris) hydrogen chloride (HCl) and 0.05 mM potassium chloride (KCl).

Four µl of the RT-PCR was added to the 46 µl of the reaction mixture. The reaction conditions were as follows: 94°C for 4 min, followed by 40 cycles of 94°C for 15 s, 55°C for 20 s, and 72°C for 2 min; ending with 72°C for 10 min and cooling to 4°C. The nested PCR (nPCR) products were stored at -20°C until use.

Product verification was performed via agarose gel electrophoresis. A 1% agarose gel (Invitrogen) stained with ethidium bromide (5 μg/ml) (BioRad Laboratories) was used for electrophoresis and the PCR product was visualised under a UV light using the Bio-Rad ChemiDoc™ MP Imaging System (Bio-Rad Laboratories). Any specimen that had a visible band was further processed for NGS.

2.4.2 PCR Product Purification

Purification of the nPCR products was done by size exclusion bead purification using Agencourt AMPure XP (Beckman Coulter Life Sciences, Indianapolis, IN, USA) magnetic beads in order to remove the excess primers, salts, enzymes and dNTPs. Each PCR products was topped up with 1X Tris-EDTA (TE) buffer (Invitrogen) to a final volume of 50 μl. The AMPure XP magnetic beads were added to the specimens in a ratio of 0.75:1 and mixed by pipetting. The mixture was then incubated at room temperature for 5 min then placed on a DynaMag™-96 Side Magnetic Stand (Invitrogen) for separation. Once the supernatant became clear, it was discarded by pipetting, and the beads were washed twice with 70% ethanol (EtOH). This was done by adding 200 μl of 70% EtOH to the magnetic beads while on the magnetic stand, leaving for 1 min, and removing the supernatant. Following the wash step, the magnetic beads were dried for 5 min, and then removed from the magnetic stand. The magnetic beads were then resuspended in 60 μl 1X TE buffer, (or 30 μl for specimens with a faint band on the agarose gel. Once the supernatant was clear, it was removed and placed into a new microcentrifuge tube, and stored at -20°C until further use.

2.4.3 Quantification

Purified nPCR products were quantified using the Quant-It PicoGreen dsDNA Assay Kit (Invitrogen) according to the manufacturer's instructions. A 50X dilution of the lambda (λ) DNA standard (100 μg/ml; Invitrogen) was prepared using TE buffer (Invitrogen) and further diluted in TE buffer to generate a dilution series consisting of 200 ng/ml, 100 ng/ml, 50 ng/ml, 25 ng/ml, 12.5 ng/ml, 6.25 ng/ml and 3.12 ng/ml. A TE blank consisting of 100 μl of TE buffer was included in the dilution series. One μl of each purified nPCR product to be quantified was added to a separate well in the fluorometer plate, to which 99 μl of TE buffer was added. The λ dilution series was added to the final column of the fluorometer plate in descending order.

A 200X dilution of the PicoGreen reagent was prepared and 100 µl of this was added to each well containing either. The plate was incubated for 10 min out of the light, following which the fluorescence was read. The fluorescence was measured using the Glomax Multi Detection System (Promega, Madison, MI, USA) using the blue optical kit (excitation: 490 nm, emission: 510-570 nm). The measured fluorescence of the λ dilution series was used to create a standard curve, which was used to calculate the concentration of the purified PCR products.

2.4.4 MiSeq Illumina

NGS was performed on purified nPCR products (Section 2.4.1) on the MiSeq System (Illumina, San Diego, CA, USA). All NGS processing was performed by a centralised sequencing core facility. Prior to proceeding with the NGS protocol, fluorometric quantification of each specimen was performed again using the Qubit dsDNA BR Assay system (Thermo Fisher Scientific, Waltham, MA, USA).

Library preparation was performed using the Nextera XT Library Preparation Kit (Nextera). This involved tagmentation, where each specimen is fragmented and tagged with an adapter sequence; amplification, clean-up and normalisation of the libraries and pooling of the libraries. Tagmentation was performed by adding 1 ng of specimen DNA to 10 µl of the Tagment DNA Buffer (Nextera). To this, 5 µl of Amplicon Tagment Mix (Nextera) was added. This was followed by centrifugation at 280 g at 20°C for 1 min, heating in a thermal cycler for 5 min at 55°C, followed by cooling to 10°C. Immediately following this, 5 µl of Neutralize Tagment Buffer (Nextera) was added and each specimen. This was followed by centrifugation at 280 g at 20°C for 1 min, and incubation at room temperature (22°C) for 5 min.

Library amplification was performed by adding 15 µl of Nextera PCR Master Mix (Nextera) to the tagmented specimens, followed by centrifugation at 280 g at 20°C for 1 min. The reaction conditions were as follows: 72°C for 3 min, 95°C for 30 s, followed by 12 cycles of 95°C for 10 s, 55°C for 30 s and 72°C for 30 s, ending with 72°C for 5 min. Following amplification, library clean-up was performed as described in Section 2.4.2.

Library normalisation was performed to ensure equal library representation once the specimens had been pooled. Normalisation was performed by adding 200 µl of Library Normalisation master mix (Nextera) to each specimen. The Library Normalisation master

mix (Nextera) consisted a 4:23 mixture of Library Normalisation Additives (Nextera) and Library Normalisation Beads (Nextera). Following this, specimens were shaken at 1800 revolutions per minute (rpm) for 30 min, then placed on a magnetic stand for separation, and the supernatant was discarded. This was followed by two was steps involving the addition of 45 µl of Library Normalisation Wash (Nextera), shaking at 1800 rpm for 5 min, separation on a magnetic stand and removal of the supernatant. Subsequent to washing, 30 µl of 0.1 normal (N) sodium hydroxide (NaOH) was added followed by shaking at 1800 rpm for 5 min to resuspend the specimens. Separation on a magnetic stand was followed by the transfer of 30 µl of the supernatant to a new tube containing 30 µl of Library Normalisation Storage Buffer (Nextera).

Libraries were subsequently pooled. This was performed by diluting each specimen and combining to the starting concentration of 6 pM. The libraries were spiked with 0.1 nM PhiX (10nM) (Illumina) as a sequencing control. The libraries were loaded onto the MiSeq System (Illumina) using the MiSeq Reagent Kit v3 600 cycle (Illumina). The cluster densities using this were in the range of 1200 to 1400 k/mm^2 and the maximum number of reads reaching up to 25 million. The generated FastQ files were a maximum of 15 gigabytes (GB) and were analysed using DeepChek® (Advanced Biological Laboratories, Luxembourg, Luxembourg) using a 1% threshold.

2.5 STATISTICAL ANALYSIS

2.5.1 Validation of the RNV Assay

Using the thresholds for TC and ΔCt described in Section 2.3, the sensitivity (Equation 1), specificity (Equation 2) and area under receiver operating characteristic (ROC) curve (Equation 3) (DeLong *et al.*, 1988) were calculated by comparing the RNV assay to standard VL and genotyping methodologies.

$$Sensitivity = \frac{True\ positives}{True\ positives + False\ negatives} \quad \textbf{1}$$

$$Specificity = \frac{True\ negatives}{True\ negatives + False\ positives} \quad \textbf{2}$$

$$Area\ under\ ROC\ curve = \int_{\infty}^{-\infty} True\ positive\ rate(T) \times False\ positive\ rate'(T) \times dT \quad \textbf{3}$$

Statistical analyses were all performed using MedCalc Version 14.8.1 (MedCalc Software bvba, 2014). Comparison of the TC component of the RNV assay to standard VL quantification was performed on all 225 specimens, while comparison of the ΔCt to standard genotyping was only performed on those specimens with a positive TC and a VL ≥ 600 copies/ml.

Further optimisation of the RNV assay used ROC curve analysis and the Youden J index (Equation 4). The sensitivity, specificity and area under the ROC curve were calculated for the optimised thresholds and cut-off for comparison.

$$Youden\ Index\ J = Sensitivity + (Specificity - 1) \quad \textbf{4}$$

2.6 ETHICAL REVIEWS

This study was granted ethical approval by the University of the Witwatersrand HREC as a sub-study under the protocol number M180295.

CHAPTER 3:

RESULTS

The objective of this project was to validate the HIV Drug Resistance RNV Multiplex assay in a South African context. A total of 225 remnant plasma specimens were selected for this study, with known VL and drug resistance genotype. Of these, 47 specimens had a VL < 600 copies/ml, and 178 specimens had a VL ≥ 600 copies/ml. Of 171 specimens with known genotype, 105 specimens had a WT genotype and 66 specimens had one or more mutation present.

3.1 SPECIMEN PROCESSING

3.1.1 Nucleic acid extraction and RT-PCR

All 225 specimens were extracted using the MagNaPure TNA kit (Roche Diagnostics) with the MagNAPure LC instrument (Roche Diagnostics) as described in Section 2.2.1 and amplified by RT-PCR as described in Section 2.2.2. Gel visualisation of the 1.3kb RT-PCR template was only performed on the nucleic acid extraction positive and negative controls and the RT-PCR positive and NTC (Figure 3.1). This was done to remain blinded as to whether the specimen had a high or low VL.

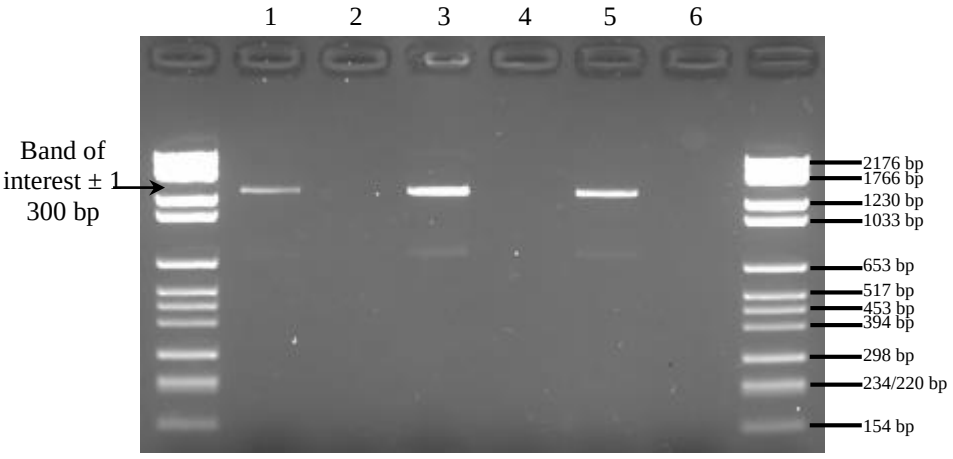

Figure 3.1: Image of an agarose gel following electrophoresis for band separation of RT-PCR controls. The image above shows the agarose gel of the controls included in an RT-PCR. The amplified product is approximately 1.3 kb in size. Lane 1 and 3 contain extraction positive controls, lane 2 and 4 contain extraction negative controls, lane 5 contains a PCR positive control and lane 6 contains the NTC.

3.2 VALIDATION OF ASSAY USING THE SERIAL MUTANT:WT DILUTIONS OF THE 65R, 103N AND 184V CONTROL PLASMIDS

Control plasmids were prepared as described in Section 2.3.4, wherein reconstituted mutant plasmids were mixed with WT plasmids to generate a 0.8%, 4%, 20%, and 100% mutant control dilution series. All controls were run on the same 96-well plate, and processed in triplicate. The amplification curves obtained from processing the control plasmids using the RNV assay are illustrated in Figure 3.2 below.

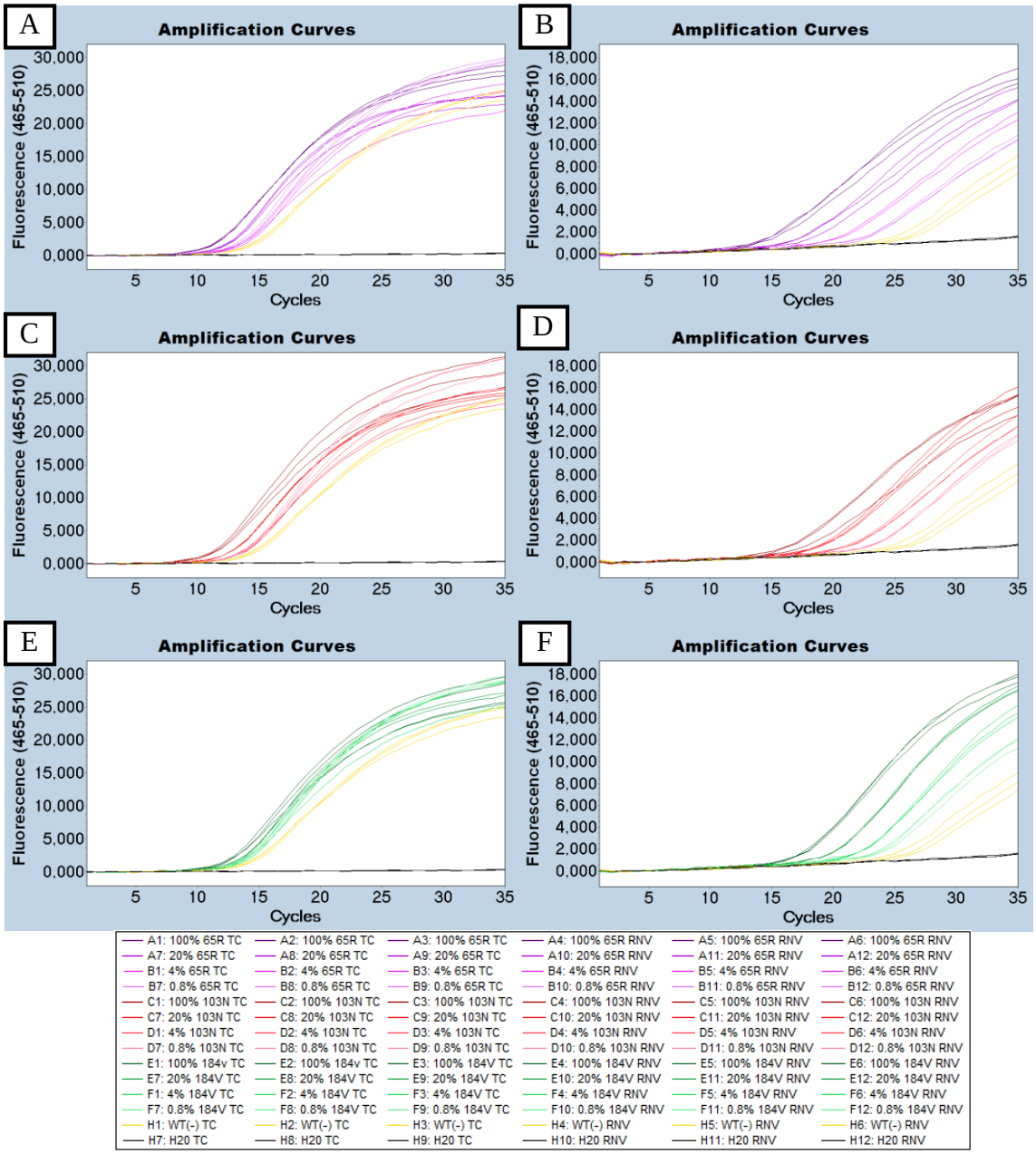

Figure 3.2: RNV validation run amplification curves. The amplification curves for the TC component (A, C and E) and the RNV component (B, D and F) of the RNV validation run are shown for the K65R (A and B), K103N (C and D) and M184V (E and F) controls with the wild type (yellow) and H_2O (black) controls represented in each.

3.2.1 Amplification Curve Analysis Using the Fit Points Method

Analysis of the amplification curves was first performed using the fit point data analysis method. This method allows for user-based manipulation of the noise band, and the Ct value is subsequently determined by the cycle at which the specimen amplification curve crosses the noise band. The noise band was set above the NTC and at the beginning of the exponential phase as illustrated in Figure 3.3 below. While only the M184V control is shown in the figure below, all the controls used the same noise band.

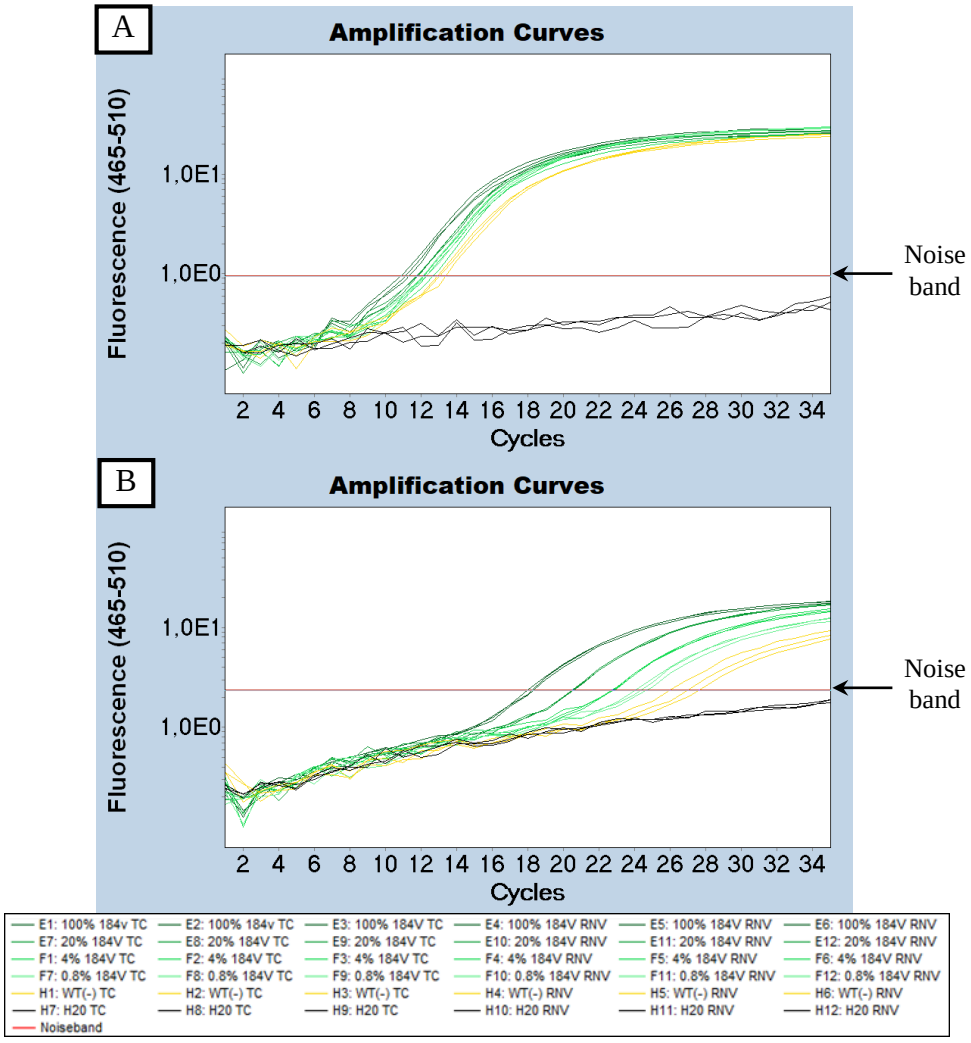

Figure 3.3: Noise band amplification curves for the RNV Validation run. The noise band (red) for the TC component (A) and RNV component (B) of the M184V controls of the RNV validation run.

The results of the validation are summarised in Table 3.1 below. The ΔCt values for 100%, 20% and 4% mutant were all ≤ 11.0 cycles for each mutant, whereas the ΔCt values at 0.8% mutant concentration were > 11.0 cycles. The WT control had a ΔCt value of > 12.0 cycles.

Table 3.1: Mean ΔCt values and outcome of the RNV validation run analysed using the fit point method.

Percent Mutant	K65R		K103N		M184V		Wild-Type	
	Mean ΔCt	Outcome	Mean ΔCt	Outcome	Mean ΔCt	Outcome	Mean ΔCt	Outcome
100%	5.46 (5.18 to 5.74)	Pass	7.81 (6.81 to 8.82)	Pass	6.73 (6.47 to 6.99)	Pass	13.71 (12.90 to 14.52)	Pass
20%	7.24 (6.48 to 8.01)	Pass	8.49 (8.32 to 8.65)	Pass	8.69 (8.61 to 8.77)	Pass		
4%	9.12 (8.73 to 9.51)	Pass	10.03 (9.68 to 10.37)	Pass	10.34 (9.96 to 10.71)	Pass		
0.8%	11.65 (11.36 to 11.94)	Fail	11.66 (11.47 to 11.85)	Fail	12.08 (11.58 to 12.58)	Fail		

Calculated mean ΔCt values for all controls were plotted against the mutant concentration as shown in Figure 3.4 below. The correlation coefficients are 0.9926, 0.9704 and 0.9987 for the K65R, K103N and M184V controls, respectively. The WT control value was ≥12.0 cycles. As the validation requirements are not required for the 0.8% mutant control for successful validation of the control, the validation of diluted plasmids was considered successful.

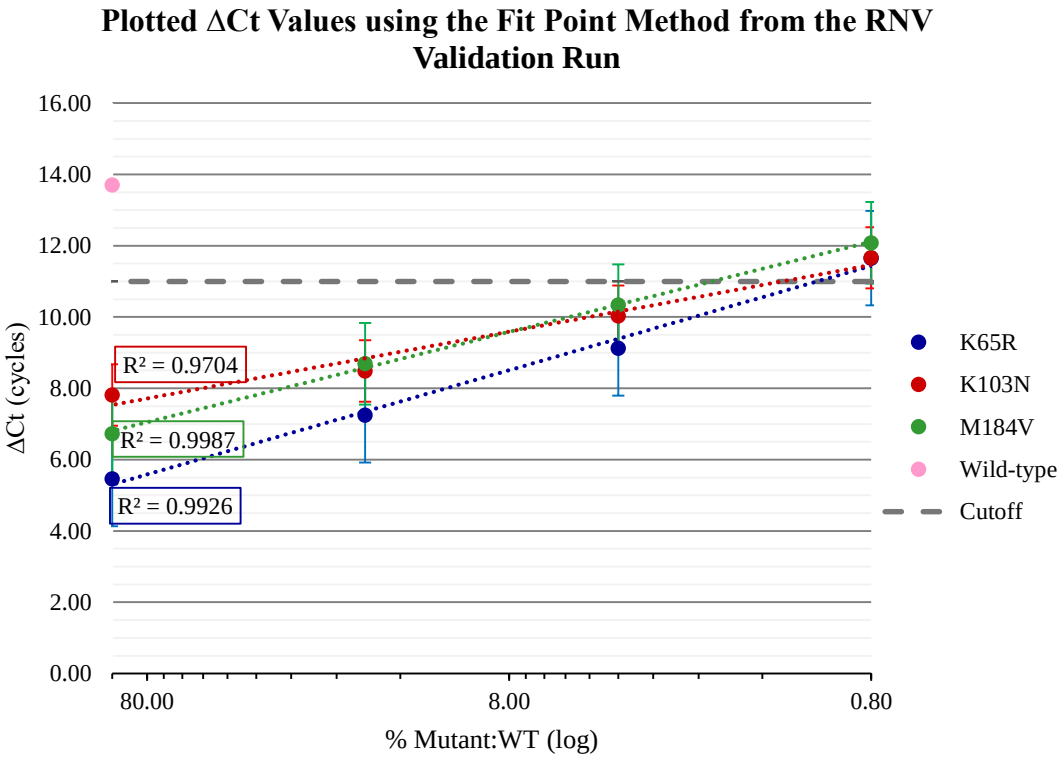

Figure 3.4: Line graph displaying the mean ΔCt values of the controls using the fit point method of analysis. A line graph with a logarithmic x-axis displaying the mean ΔCt value of each mutant control as a function of the dilution. The K65R (blue), K103N (red) and M184V (green) control ΔCt values should increase linearly and the correlation coefficients (R^2) values for each trendline (dotted line) is shown in the boxes to left of each. The wild-type control (pink) was not diluted and thus only has one value at the 100% dilution. The cut-off (grey dotted line) represents the line below which the mutant positive controls at the 100%, 20% and 4% should fall below and the wild-type should fall above.

The K65R and M184V correlation coefficients were both >0.99, with the K103N mutation at >0.97, indicating consistency in the detection of all three mutations. The 4% mutations were all above the ΔCt cut-off of 11.0 cycles, indicating that mutations can be reliably detected at this level using the fit points method of analysis.

3.2.2 Amplification Curve Analysis Using the Second Derivative Maximum Method

Control plasmid Ct values were calculated using the second derivative maximum analysis method. Using this approach, the Ct value was calculated by the Light Cycler instrument (Roche Diagnostics) by determining the equation of the amplification curve and the exact point where the second derivative of this was at a maximum. The ΔCt values for 100%, 20%, 4% and 0.8% mutant were all ≤ 11.0 cycles for each mutant. The WT control had a ΔCt value of > 11.6 cycles.

Table 3.2: Mean ΔCt values and outcome of the RNV validation run analysed using the second derivative maximum method.

Percent Mutant	K65R		K103N		M184V		Wild-Type	
	Mean ΔCt	Outcome	Mean ΔCt	Outcome	Mean ΔCt	Outcome	Mean ΔCt	Outcome
100%	3.25 (2.97 to 3.53)	Pass	5.74 (5.09 to 6.39)	Pass	5.18 (5.10 to 5.27)	Pass	11.63 (11.09 to 12.18)	Fail
20%	5.26 (4.55 to 5.97)	Pass	7.09 (6.90 to 7.29)	Pass	7.12 (6.97 to 7.26)	Pass		
4%	7.33 (7.28 to 7.38)	Pass	8.45 (8.29 to 8.61)	Pass	8.77 (8.63 to 8.91)	Pass		
0.8%	9.25 (9.12 to 9.37)	Pass	9.88 (9.60 to 10.16)	Pass	10.13 (9.74 to 10.51)	Pass		

Calculated mean ΔCt values for all controls were plotted against the mutant concentration as shown in Figure 3.5 below. The correlation coefficients for the K65R, K103N and M184V controls were 0.9998, 0.9939 and 0.9998, respectively. Using this method, all controls passed validation criteria; however, the WT plasmid had a ΔCt slightly below the required cutoff of ≥12.0 cycles.

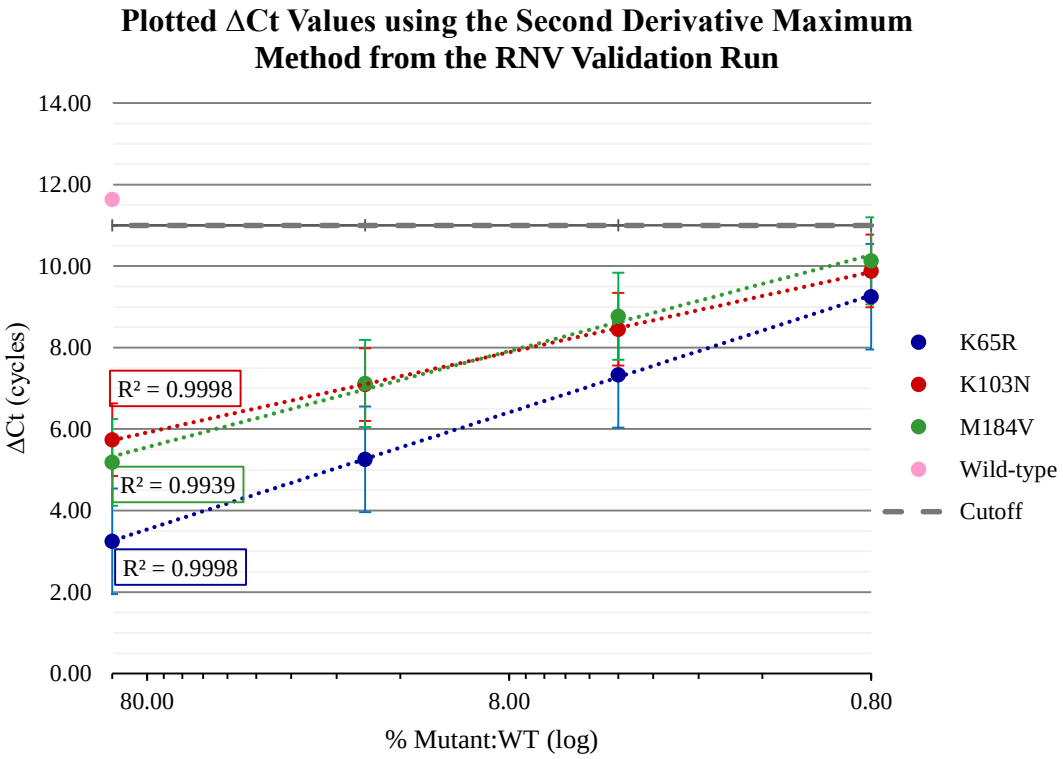

Figure 3.5: Line graph displaying the mean ΔCt values of the controls using the second derivative maximum of analysis. A line graph with a logarithmic x-axis displaying the mean ΔCt value of each mutant control as a function of the dilution. The K65R (blue), K103N (red) and M184V (green) control ΔCt values increased linearly and the correlation (R^2) values for each trendline (dotted line) is shown in the boxes to left of each. The wild-type control (pink) was not diluted and thus only has one value at the 100% dilution. The cut-off (grey dotted line) represents the line below which the mutant positive controls at the 100%, 20% and 8% should fall below and the wild-type should fall above.

The K65R, K103N and M184V correlation coefficients were all >0.99, indicating consistency in the detection of all three mutations. The 0.8% mutations were all above the ΔCt cut-off of 11.0 cycles, indicating that mutations can be reliably detected at this level using the second derivative maximum method of analysis. Both the correlation coefficients and mutation limit of detection were better than observed with the fit point method of analysis.

3.3 PROCESSING OF SPECIMENS USING THE RNV MULTIPLEX ASSAY

The RNV assay was subsequently performed in triplicate on all 225 specimens, as described in Section 2.3. An example of the amplification curves generated by the TC component of the assay is shown in Figure 3.6. Specimens that had a TC Ct value of ≤ 10 cycles (Figure 3.6A) were diluted 1:20 to 1:160000 and RNV assay repeated. Specimens that showed amplification and had a TC Ct value of ≥ 10 cycles (Figure 3.6B) were analysed for mutations using the RNV Ct value to calculate the ΔCt value. Specimens

that showed no evidence of amplification by either the TC and/or RNV component of the assay (Figure 3.7C) were reported as no-amplification and described as having a VL < 600 copies/ml.

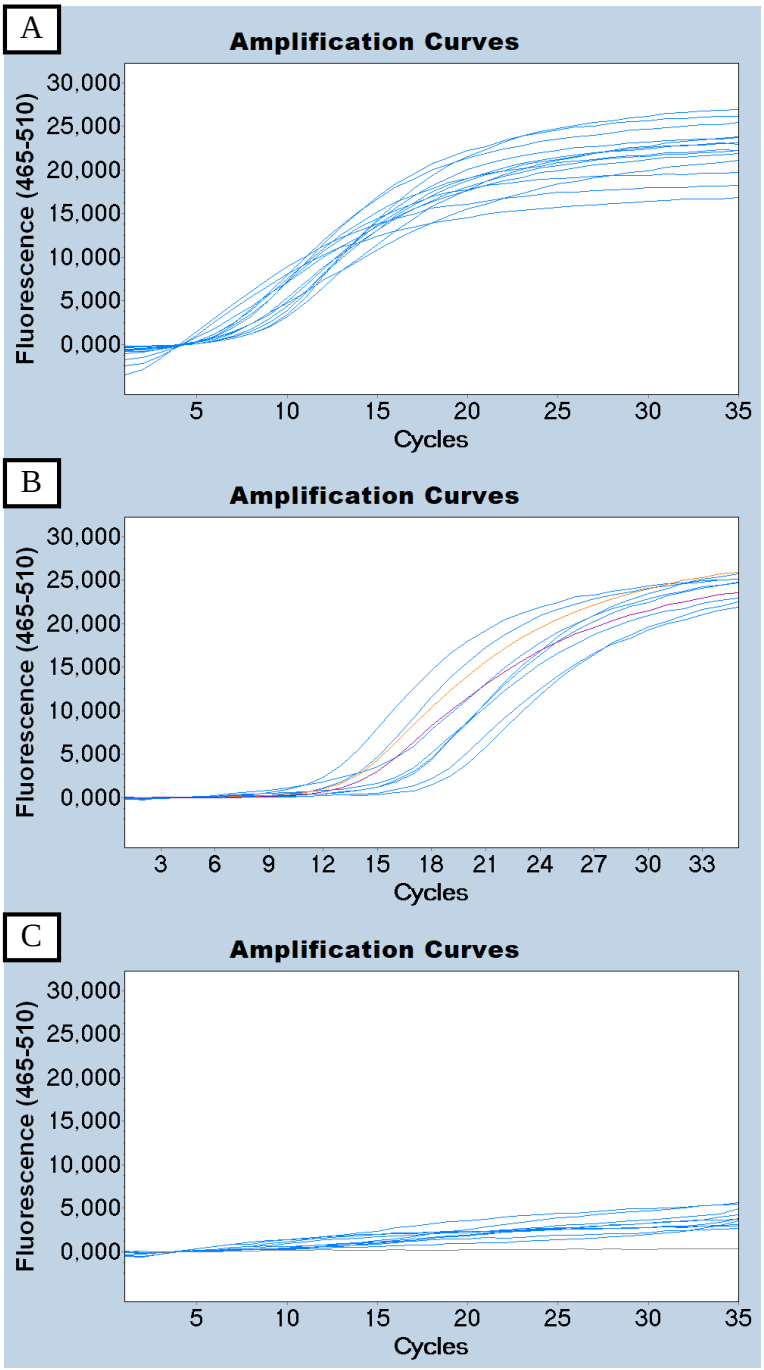

Figure 3.6: RNV Assay TC amplification curves. Amplification curves representing the TC component of an RNV Assay reaction. All the amplifications curves shown above are from a single run, however, they are separated into specimens with early amplification that required dilution (A), amplification positive specimens (B) and specimens that showed no amplification (C). Specimens are represented by blue, the RNCV control by orange, the WT control by purple and the NTC control by grey.

3.3.1 Analysis of the TC Component of the Assay Using the Fit Point Method

Of the 225 specimens analysed using the fit point method, 180 specimens had a mean TC Ct value between the positive range of 10.0 to 25.0 cycles and 45 were considered as TC negative, defined as either a TC Ct > 25.0 cycles or no amplification observed. Twenty-four of these had no amplification observed and were assumed to have a VL < 600 copies/ml.

Of these 180 TC positive specimens, 161 had VL ≥ 600 copies/ml (as previously determined using standard VL assays) while 19 specimens had VL < 600 copies/ml (Figure 3.7, Appendix A). Of the 45 specimens that were TC negative, 28 specimens had VL < 600 copies/ml whilst 17 specimens had a VL ≥ 600 copies/ml. In total, 189 (84.0%) specimens had RNV TC results concordant to the prior VL quantification and 36 (16.0%) specimens had discordant results. In each run, the RNCV control was between 3.5 and 5.5 cycles and the WT control was >12.0 cycles.

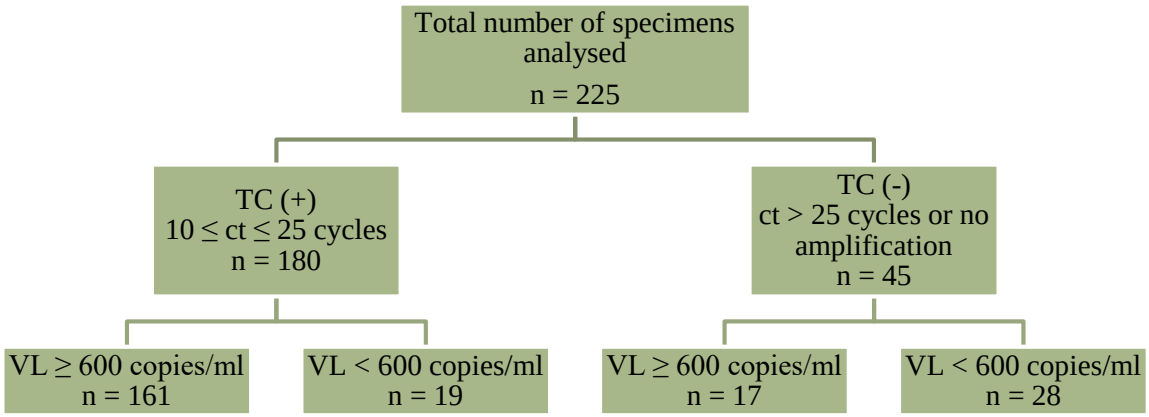

Figure 3.7: Comparison of the results of the RNV assay TC component using the fit point method of analysis to standard viral load methodology using the original cut-off. The results of the mean TC Ct value analysed using the fit point method for all 225 specimens compared to the VL data available for each specimen.

3.3.2 Analysis of the TC Component of the Assay Using Second Derivative Maximum

When applying the second derivative maximum method, only 3 of the 43 RNV PCR assay runs with RNCV and WT control Ct values fell within the expected ranges of 3.5 to 5.5 cycles and >12.0 cycles, respectively. Analysis of the RNV assay was therefore not performed any further using second derivative maximum analysis method.

3.3.3 Analysis of the RNV Component of the RNV Assay Using the Fit Point Method

A total of 180 specimens that had a TC Ct ≤ 25 cycles were further analysed for mutations. Of these, 19 specimens did not have a genotype results for comparison, due to non-amplification or non-testing as Sanger genotyping is usually performed on specimens with VL > 1000 copies/ml only. Of note, five of these were RNV positive for mutations (three had VL < 1000 copies/ml), 10 were negative, and 4 had no amplification.

The mean ΔCt was calculated for the remaining 161 specimens and compared to the qualitative result for the combined genotype at the K65, K103 and M184 amino acid sites obtained from Sanger sequencing. Figure 3.8 summarises the results of this comparison.

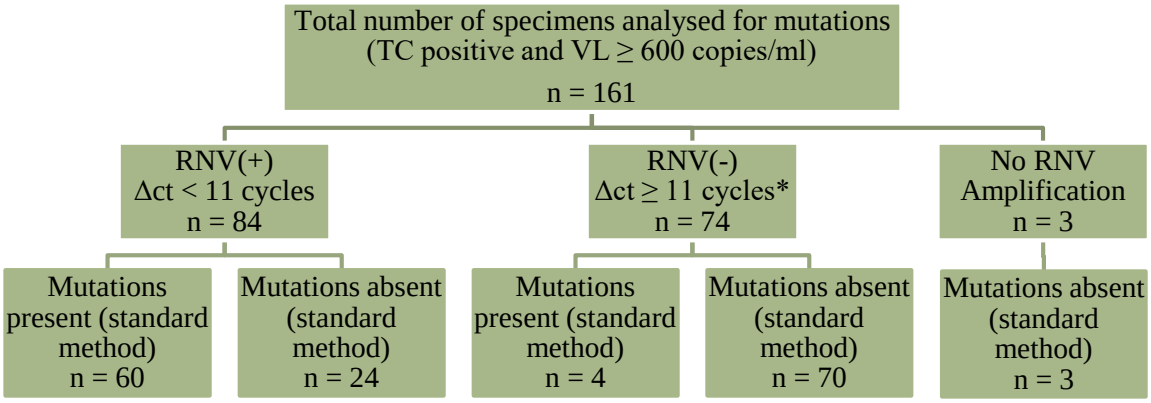

Figure 3.8: Comparison of the results of the RNV component using the fit point method of analysis to standard genotyping methodology using the original cut-off. The results of the mean ΔCt value analysed using the fit point method for all specimens with a positive TC and VL greater than 600 copies/ml compared to the genotype data available for each specimen. Three specimens that showed no amplification in the RNV amplification curves were assumed RNV negative.

Of the 161 specimens analysed for mutations and compared to Sanger sequencing results, 84 specimens had a positive RNV defined by a ΔCt of ≤ 11.0 cycles, 74 specimens had a negative RNV defined by a ΔCt of > 11.0 cycles and three specimens had no RNV amplification observed. Of the 84 RNV positive specimens, 60 had mutations present in the Sanger sequence, whereas 24 had no mutations detected. The 74 RNV negative specimens had 70 WT Sanger sequence genotypes whereas 4 specimens had mutations identified by Sanger sequencing. The three specimens (AMP077, AMP136 and AMP183, Appendix A) that had no amplification observed were all WT according to the Sanger sequence. Of the 161 specimens, 130 (80.7%) were concordant between the RNV assay and Sanger sequencing and 28 (17.4%) were discordant.

3.3.4 TC and RNV Assay Test Statistics

Using the fit point method to analyse the amplification curves, the TC component of the assay has a sensitivity of 90.5% and specificity of 59.6% (Table 3.3). The accuracy of the TC determination compared to the VL was fair (area under the ROC curve = 0.75).

The RNV component of the assay has a sensitivity of 93.8% and specificity of 74.5%. The accuracy of the RNV determination compared to the genotype results was considered good (area under ROC curve = 0.84).

Table 3.3: Test statistics for comparison of the TC and RNV components of the assay.

Test Statistic	TC (95% CI)	RNV (95% CI)
Sensitivity	90.45% (85.15% – 94.34%)	93.75% (84.76% to 98.27%)
Specificity	59.57% (44.27% - 73.73%)	74.47% (64.43% to 82.91%)
Area under ROC curve	0.750 (0.688 to 0.805)	0.841 (0.775 to 0.894)

3.3.5 Agarose Gel Electrophoresis

Agarose gel electrophoresis was performed on the RNV component of the RNV assay PCR product of each specimen that had mutations detected in the RNV assay (Figure 3.9). The consensus of the agarose gel electrophoresis results are listed in Appendix A. Bands that were observed but were faint were indicated in brackets. Comparing the consensus of the agarose gel results to Sanger sequencing genotype in RNV positive specimens, 14 specimens had additional mutations observed in the agarose gel band analysis.

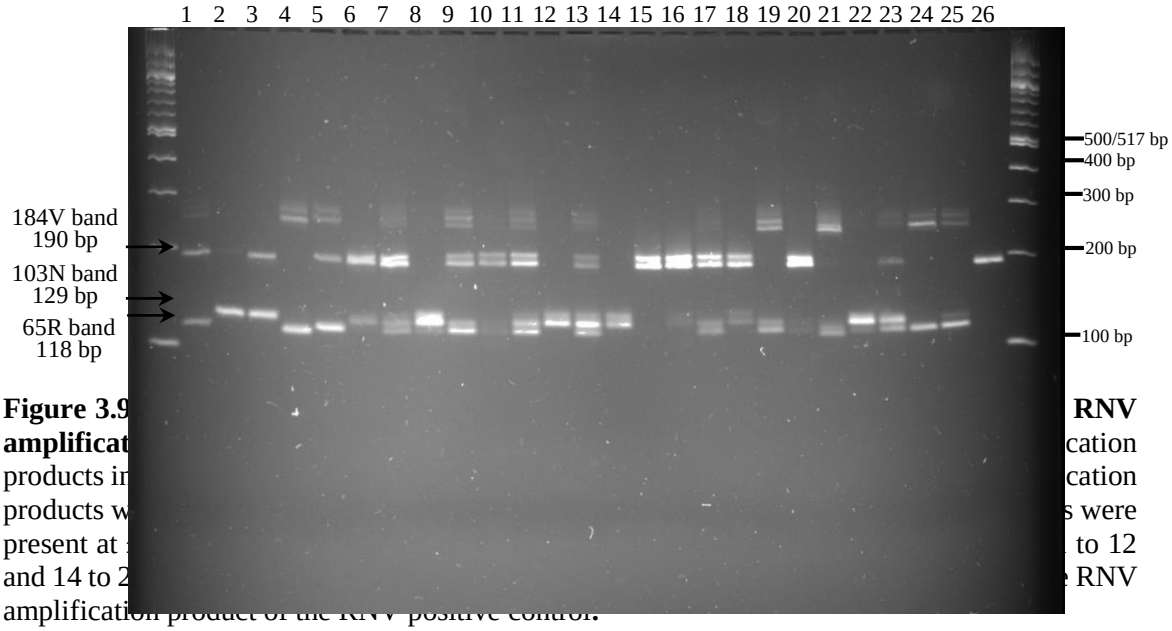

Figure 3.9 RNV amplificat cation products in cation products w s were present at to 12 and 14 to 2 RNV amplification product of the RNV positive control.

The impact of the approximately 270 bp non-specific amplification products observed in the agarose gel have not been determined. The lack of primer sequences to compare product sizes to has made it difficult to determine whether this product is due to primer binding in non-targeted areas or PCR products combining to form larger than expected product sizes due to the multiplexing.

3.4 NEXT-GENERATION SEQUENCING

3.4.1 Next-Generation Sequence Analysis

Specimens selected to undergo NGS underwent nPCR as described in Section 2.4 using the RT-PCR product as described in Section 2.2 as a template. Following purification, the specimens were quantified on the Glomax Multi Detection System (Promega) and submitted for sequencing using the MiSeq System (Illumina) platform.

Of the 24 specimens with mutations detected by the RNV assay but not by Sanger sequencing, 20 underwent NGS. Four specimens were not sequenced using NGS due to insufficient material (AMP012, AMP023, AMP046 and AMP147). The results of the NGS performed on the 20 specimens is summarised in Table 3.4 below. Five specimens had minor variants detected by NGS (AMP043, AMP088, AMP110, AMP152 and AMP155), with prevalence percentages of 1.7%, 3.3%, 3.6%, 1.2% and 1.3%, respectively. The minor variants present in these five specimens therefore confirm the result of the RNV assay. The remaining 15 specimens had a confirmed WT genotype by NGS, and thus were classified as true discrepant specimens and RNV false positives. One specimen (AMP158) had a ΔCt value near the mutation detection cut-off of 11.0 cycles (10.99), however, the remaining 14 specimens (AMP005, AMP027, AMP047, AMP061, AMP082, AMP089, AMP098, AMP101, AMP103, AMP127, AMP158, AMP167, AMP210, AMP261 and AMP273) had ΔCt values that ranged between 5.5 and 9.9 cycles.

Table 3.4: NGS results of the 20 specimens discrepant between the RNV assay and Sanger sequencing.

Specimen ID	ΔCt	Agarose Gel Bands	Sanger Sequence Mutations	NGS Mutations	Prevalence	Outcome
AMP005	8.77	M184V	None	None		RNV discrepant
AMP027	9.93	K65R, M184V	None	None		RNV discrepant
AMP043	7.68	K65R, M184V	None	K65R	1.7%	Minor variant (K65R)

Table 3.4: Continued.

Specimen ID	ΔCt	Agarose Gel Bands	Sanger Sequence Mutations	NGS Mutations	Prevalence	Outcome
AMP047	8.21	K65R, K103N, M184V	None	None		RNV discrepant
AMP061	5.51	M184V	None	None		RNV discrepant
AMP082	9.60	K65R, K103N, M184V	None	None		RNV discrepant
AMP088	9.09	K65R, K103N, M184V	None	K65R	3.3%	Minor variant (K65R)
AMP089	7.54	K103N, M184V	None	None		RNV discrepant
AMP098	6.59	K65R, M184V	None	None		RNV discrepant
AMP101	6.61	K65R, K103N, M184V	None	None		RNV discrepant
AMP103	9.24	K65R, M184V	None	None		RNV discrepant
AMP110	7.61	K65R, K103N, M184V	None	K65R	3.6%	Minor variant (K65R)
AMP127	9.83	K65R, M184V	None	None		RNV discrepant
AMP152	4.82	M184V	None	M184V	1.2%	Minor variant (-
AMP155	9.59	K65R, K103N, M184V	None	K65R	1.3%	Minor variant (K65R)
AMP158	10.99	K65R, M184V	None	None		RNV discrepant
AMP167	7.67	M184V	None	None		RNV discrepant
AMP210	9.94	K65R, M184V	None	None		RNV discrepant
AMP261	8.83	M184V	None	None		RNV discrepant
AMP273	6.85	M184V	None	None		RNV discrepant

Four specimens had no mutations detected by the RNV assay (RNV negative, $\Delta Ct > 11.0$ cycles) yet had mutations present in the Sanger sequence. Two of these four discrepant specimens underwent NGS (Table 3.5), whereas no more specimen was available for the third and fourth. These two specimens (AMP252 and AMP291) were true false RNV negatives as the same mutations detected by Sanger sequencing were detected by NGS.

Table 3.5: NGS results of the three specimens with mutations detected by Sanger sequencing but not the RNV assay.

Specimen ID	RNV Assay ΔCt	Sanger Sequence Mutations Detected	NGS Mutations Detected	Prevalence	Outcome
AMP252	13.33	K103N	K103N	99.4%	RNV discrepant
AMP291	11.70	K103N, K103S	K103N, K103S, M184V	19.7% 48.5% 42.8%	RNV discrepant

Fourteen specimens had mutations detected by both the RNV assay and Sanger sequencing but had additional mutations detected in the agarose gel of the RNV assay product; these were also repeat sequenced using NGS to confirm the presence of these mutations using a different sequencing platform. These 14 specimens are described in Table 3.6 below. Twelve of these specimens (AMP001, AMP051, AMP100, AMP104, AMP125, AMP132, AMP177, AMP217, 236, AMP245, AMP293 and AMP315) had identical genotypes outcomes at the K65, K103 and M184 amino acid sites in the NGS and Sanger sequence data, and thus the additional mutations detected in the agarose gel of the RNV amplification products were confirmed as false positives.

Table 3.6: NGS results of the 14 specimens with additional mutations detected by agarose gel electrophoresis.

Specimen ID	ΔCt	Agarose Gel Bands	Sanger Sequence Mutations	NGS Mutations	Prevalence	Outcome
AMP001	10.16	K65R, K103N, M184V	K103N	K103N	78.4%	K65R and M184V not confirmed
AMP051	6.44	K103N, M184V	K103N	K103N	99.0%	M184V not confirmed
AMP100	8.93	K65R, K103N, M184V	K103N	K103N	98.6%	K65R and M184V not confirmed
AMP104	8.16	K103N, M184V	K103N	K103N	39.6%	M184V not confirmed
AMP125	9.85	K65R, K103N, M184V	K103N, M184V	K103N, M184V	99.1%, 99.3%	K65R not confirmed

Table 3.6 Continued.

Specimen ID	ΔCt	Agarose Gel Bands	Sanger Sequence Mutations	NGS Mutations	Prevalence	Outcome
AMP132	9.79	K103N, M184V	K103S, M184V	K103S, M184V	98.7%, 99.1%	Detected K103S as K103N
AMP150	10.75	K65R, K103N	M184V	K103N, M184V	7.1%, 99.0%	Minor Variant (K103N), K65R not confirmed
AMP177	7.38	K103N, M184V	K103N	K103N	58.3%	M184V not confirmed
AMP217	9.05	K103N, M184V	K103S, M184V	K103S, M184V	98.9%, 49.9%	Detected K103S as K103N
AMP236	10.94	K65R, M184V	M184V	M184V	99.1%, 99.2%	K65R not confirmed
AMP245	8.10	K65R, K103N	K103N	K103N	99.0%	K65R not confirmed
AMP293	5.04	K103N, M184V	K103N	K103N	99.0%	M184V not confirmed
AMP297	9.45	K103N, M184V	M184V	K65R, M184V	5.6%, 98.0%	K103N not confirmed
AMP315	8.13	K65R, M184V	K103N, M184V	K103N, M184V	98.5%, 99.3%	K65R not confirmed

Two of these 14 specimens had additional minor variant mutations detected using NGS. Specimen AMP150 had M184V detected using Sanger sequencing and NGS yet this band was not present on the agarose gel. The K103N mutation was present in the NGS sequence at a prevalence of 7.1%). However, the K65R gel band was not present in the Sanger or NGS sequence. Specimen AMP297 had the K65R mutation detected at a prevalence of 5.6%; however, this band was not visible on the agarose gel. The K103N gel band was not present in the Sanger or NGS sequence. Specimens AMP132 and AMP217 had a K103S mutation present in the Saner and NGS sequence; these corresponding bands were present on the agarose gel. Three specimens (AMP031, AMP055 and AMP236) that also had the K103S mutation in the Sanger sequence but did not have a K103N band on the agarose gel.

Phylogenetic analysis of the 36 Sanger and NGS 20% consensus sequences was performed to ensure sequence similarity (Figure 3.10). The branch lengths between the

NGS 20% consensus and the corresponding Sanger sequences were all short indicating minimal sequence divergence. In addition to relatedness, the phylogenetic tree also separated specimens according to subtype. The three specimens most closely related to the HXB2 reference genome, namely AMP249, AMP263 and AMP272, were subtype B, while the rest were all subtype C.

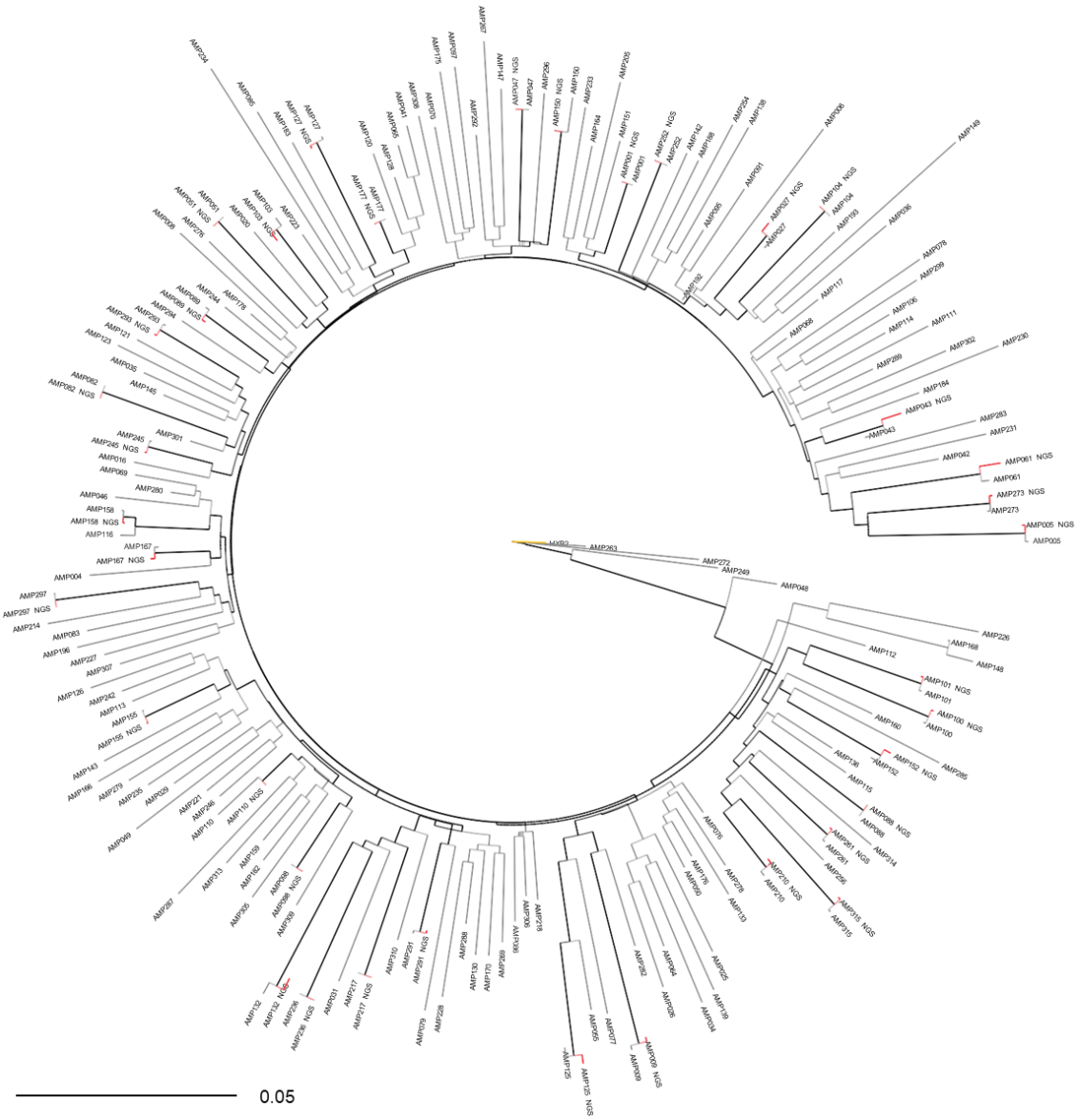

Figure 3.10: Neighbour-joining phylogenetic tree for comparison of previous sequences to new sequences. Neighbour-joining phylogenetic tree generated using the Kimura 2-parameter distance model. The HXB2 outgroup is shown in yellow, the NGS sequences are indicated in red and the previously performed sequencing in grey.

3.5 SEQUENCE ANALYSIS OF MUTATIONS NOT DETECTED BY THE RNV ASSAY

Analysis of the three specimens which had mutations present in both the Sanger and NGS data but not detected by the RNV assay is detailed below. There were no K65R or M184V

mutations that were not detected by RNV assay. Comparison of the AY77269 subtype C reference sequence from SA to those of the three specimens that had the K103N mutation is found in Table 3.7 below. The K103N nucleotides, AAA, are in the centre with the 12 nucleotides upstream and downstream on the left and right, respectively.

Table 3.7: Comparison of the sequence surrounding the K103 amino acid of HXB2 genome and the specimens that did not amplify using the RNV assay.

Nucleotide Position	**295**	**296**	**297**	**298**	**299**	**300**	**301**	**302**	**303**	**304**	**305**	**306**	**307**	**308**	**309**	**310**	**311**	**312**	**313**	**314**	**315**	**316**	**317**	**318**	**319**	**320**	**321**
Amino Acid Position	**G99**			**L100**			**K101**			**K102**			**K103**			**K104**			**S105**			**V106**			**T107**		
AY772699	G	G	G	T	T	A	A	A	A	A	A	G	A	A	A	A	A	A	T	C	A	G	T	G	A	C	A
AMP196	•	•	•	•	•	•	•	•	•	•	•	•	•	•	S	•	•	•	•	•	•	•	•	•	•	•	•
AMP252	•	•	•	•	•	•	•	•	•	C	•	•	•	•	C	•	•	G	•	•	•	•	•	A	•	•	•
AMP291	•	•	•	•	•	•	•	•	•	•	•	•	•	•	W	•	•	•	•	•	•	•	•	•	•	•	•

*S: G or C; W: A or T.

The mean ΔCt values of the specimens were 11.43, 13.33 and 11.70, respectively for AMP196, AMP252 and AMP291. Two of the three specimen runs used to calculate the ΔCt value for AMP196 had a mean ΔCt value of ≤ 11 cycles, however the third triplicate ΔCt value was > 13 cycles and therefore resulted in the mean ΔCt being calculated as >11 cycles. The three runs used to calculate the mean ΔCt for AMP252 and AMP291 were all > 11 cycles.

Two of the specimens analysed, AMP196 and AMP291, had no differences compared to the AY772699 reference sequence other than the mutation at the 3' end of codon 103. The three nucleotides detected in AMP252 that were not present in the reference sequence were analysed in all other sequences they were present to determine if they affected RNV primer binding. The transversion from A to C at nucleotide position 304 was present in five other sequences, AMP047, AMP110, AMP150, AMP170 and AMP192. None of these other sequences had the K103N mutation, thus the effect on primer binding could not be ascertained. The transition from A to G at nucleotide position 312 was present in nine other sequences, AMP033, AMP047, AMP048, AMP068, AMP091, AMP143, AMP177, AMP227 and AMP296. This mutation was also present in AMP143 and AMP177, both of which had only the K103N mutation present and thus did not influence the K103N primers from binding. The transition from G to A at nucleotide position 318 was present in 30 other sequences, six of which had the K103N mutation. Only one of these, AMP177, had only the K103N mutation alone, and did not affect primer binding.

3.6 EXPLORATORY ANALYSIS FOR RECOMMENDATION OF DIFFERENT ASSAY THRESHOLDS

The raw data was further analysed statistically to provide alternative recommended cut-off values for the TC and RNV components of the assay, using both fit-point and second derivative maximum methods for determining Ct values. For this analysis, the 24 specimens that did not amplify by TC component were excluded.

3.6.1 Optimised Thresholds and cut-offs for TC component, using fit-point method

Mean TC Ct values were compared to known VL values using categorisations of above and below 50, 100, 200, 400 and 600 copies/ml. For each analysis, sensitivity, specificity, a ROC curve was generated.

Table 3.8: Test statistics for the mean TC component compared to different VL thresholds using 200 specimens with detectable TC values.

Statistic	≥ 50 copies/ml	≥ 100 copies/ml	≥ 200 copies/ml	≥ 400 copies/ml	≥ 600 copies/ml
Number of specimens	189	185	180	171	166
Sensitivity	91.15	92.02	94.48	92.28	83.13
Specificity	88.89	76.92	85.00	66.67	74.29
Area under ROC curve	0.924	0.851	0.913	0.841	0.842
Youden J index	0.8003	0.6894	0.7948	0.5965	0.5742
Associated TC Ct	≤24.03	≤24.03	≤21.78	≤19.18	≤15.86

Table 3.8 indicates the test statistics obtained for the VL thresholds of ≥ 50, 100, 200, 400 and 600 copies/ml. The greatest length of the Youden J index was observed with a VL of ≥ 50 copies/ml, as well as highest specificity and Area under curve. However, the associated CT value of 24 cycles may compromise the RNV component of the assay, as >11 cycles are required to classify a specimen as WT. The test statistics for the VL ≥ 200 copies/ml produced a Youden index of 0.7948, with a specificity of 94.48 and specificity of 85.00.

These figures predicted that a cycle threshold cut-off of ≤21.78, equivalent to 200 copies/ml provides alternative recommended values for the TC component of the assay

Figure 3.11 below shows the ROC curve comparing the mean TC Ct values to standard VL methodologies using a VL threshold of ≥ 200 copies/ml.

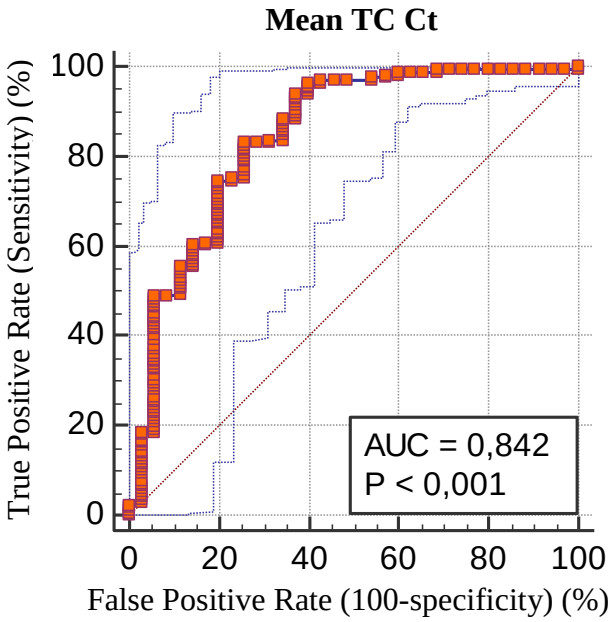

Figure 3.11: Receiver operating characteristic curve for mean TC Ct values analysed using the fit point method compared to a viral load greater or equal to 200 copies/ml. Receiver operating characteristic curve displaying the change in sensitivity and false positive rate (100-specificity) for mean TC Ct values (red squares) classified based according to the VL being ≥ 200 copies/ml. The diagonal line represents where the sensitivity equals 100-specificity.

Figure 3.12 summarises the results of the comparison of the RNV assay to standard VL methodologies using a TC Ct cut-off of ≤ 21.78 cycles for determination of a VL ≥ 200 copies/ml. With these thresholds, there were 188 (93.5%) specimens that were concordant and 13 (6.5%) specimens discordant between the RNV assay and standard VL assays.

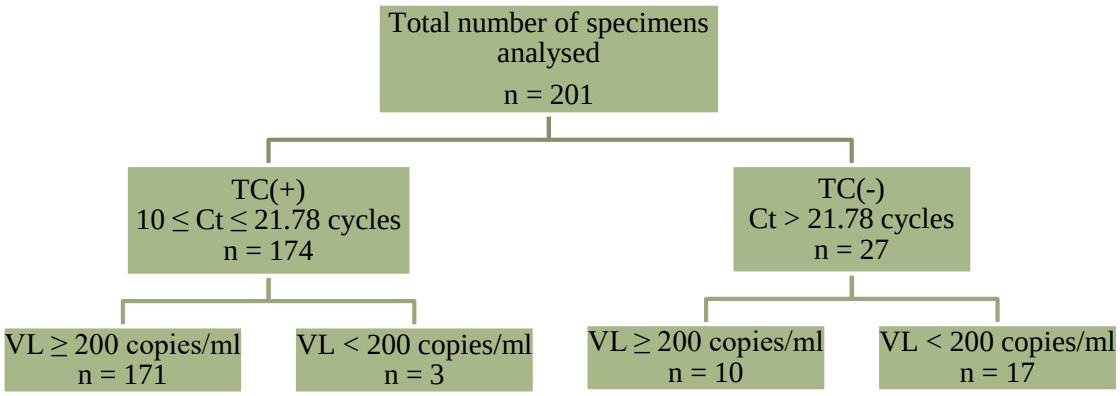

Figure 3.12: Comparison of the results of the RNV assay TC component to standard viral load methodology using the optimised cut-off for the fit point method of analysis. The results of the mean TC Ct value analysed using the fit point method for al specimens compared to the VL data available for each specimen.

Based on the above thresholds described for the TC component, the optimal ΔCt cut-off for mutation detection was determined. The 171 that had a positive TC and a VL ≥ 200 copies/ml were compared to standard genotyping methods with the exception of 13

specimens which had no available genotyping data and three specimens that did not amplify on the RNV component of the assay. The comparison performed on the 155 is shown in the ROC curve in Figure 3.13 below.

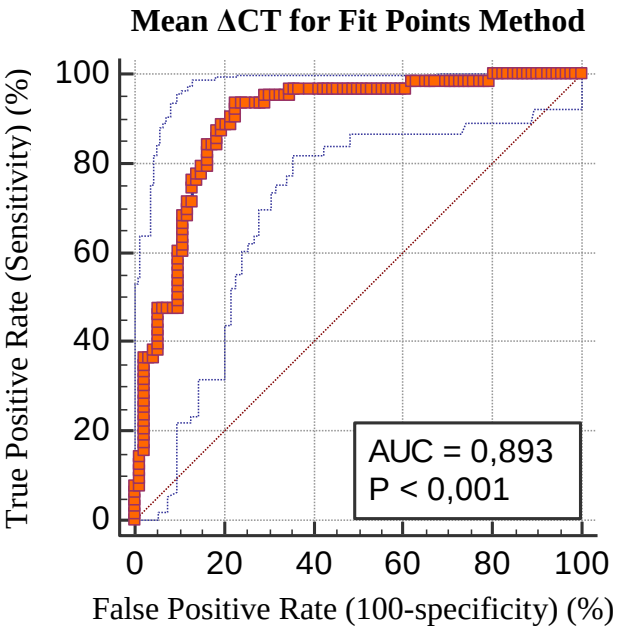

Figure 3.13: Receiver operating characteristic curve for mean ΔCt values analysed using the fit point method compared to standard genotyping. Receiver operating characteristic curve displaying the change in sensitivity and false positive rate (100-specificity) for mean ΔCt values (red squares) classified based according to the Sanger sequencing genotype. The diagonal line represents where the sensitivity equals 100-specificity.

The Youden J index J of 0.7082 was associated with a ΔCt value of ≤ 10.94 cycles. The sensitivity, specificity and area under the ROC curve compared to standard genotyping methods were 93.65%, 77.17% and 0.893. Figure 3.14 summarises the comparison of the results of the RNV assay mutation detection component to standard genotyping methodologies.

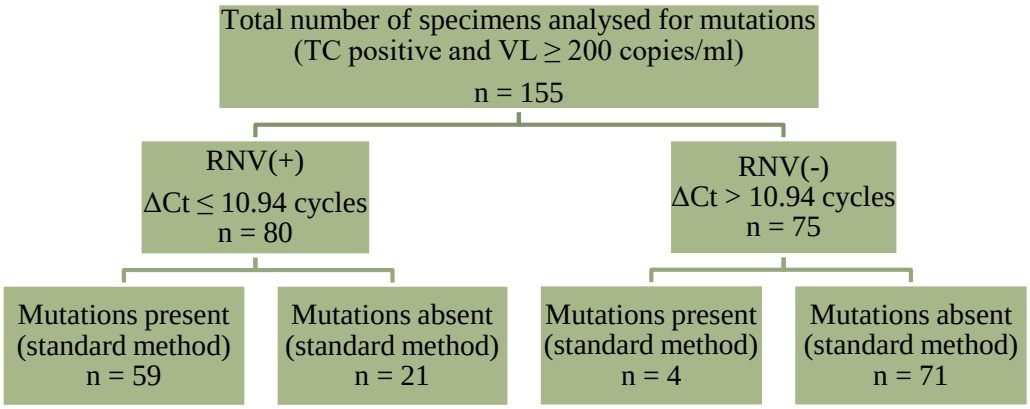

Figure 3.14: Comparison of the results of the RNV assay RNV component using the fit point method of analysis to standard genotyping methodology using the optimised cut-off. The results of the mean ΔCt value analysed using the second derivative method for all specimens with a positive TC and VL greater than 200 copies/ml compared to the genotype data available for each specimen.

3.6.2 Optimised Second Derivative Maximum Thresholds and Cut-offs

To determine values for the RNCV control and the WT control, the median with 95% CI of the raw data values were calculated after exclusion of outlier values. The 95% confidence intervals were calculated to be at 1.99 and 3.65 cycles. The proposed cut-off values for the RNCV control are: 2.82 ± 0.83 cycles. Any runs with a RNCV control value outside of this range were considered invalid and the run data was not included in the analysis.

As a range is not required for the WT control, but rather a cut-off value, the lower 95% confidence interval was calculated to be at 9.70 cycles. Any runs with a WT control value < 9.70 were considered to be invalid and the data from that run was not included in the analysis.

The mean TC RNV and ΔCt values were calculated for each specimen based on the first three RNV assay results. Test statistics were determined using VLs ≥ 50, 100, 200, 400 and 600 copies/ml (Table 3.9).

Table 3.9: Test statistics for the mean TC cycle values cycles compared to different VL limits of detection using 201 specimens. The 24 specimens that did not amplify by TC component of the assay were excluded.

Statistic	≥ 50 copies/ml	≥ 100 copies/ml	≥ 200 copies/ml	≥ 400 copies/ml	≥ 600 copies/ml
Sensitivity	91.15	92.02	94.48	95.32	96.39
Specificity	88.89	76.92	85.00	63.33	60.00
Area under curve	0.928	0.836	0.900	0.823	0.830
Youden J index	0.8003	0.6894	0.7948	0.5865	0.5639
Associated Ct value	≤ 23.75	≤ 23.75	≤ 21.51	≤ 21.51	≤ 21.51

The test statistics showed using a VL ≥ 50 copies/ml or ≥ 200 copies/ml and associated with Ct values of 23.75 and 21.51, respectively, were most optimal. However, the 200 copies/ml criteria is therefore recommended as this value is unlikely to compromise the RNV component of the assay. Figure 3.15 below shows the ROC curve comparing the mean TC Ct values to standard VL methodologies using a VL threshold of ≥ 200 copies/ml.

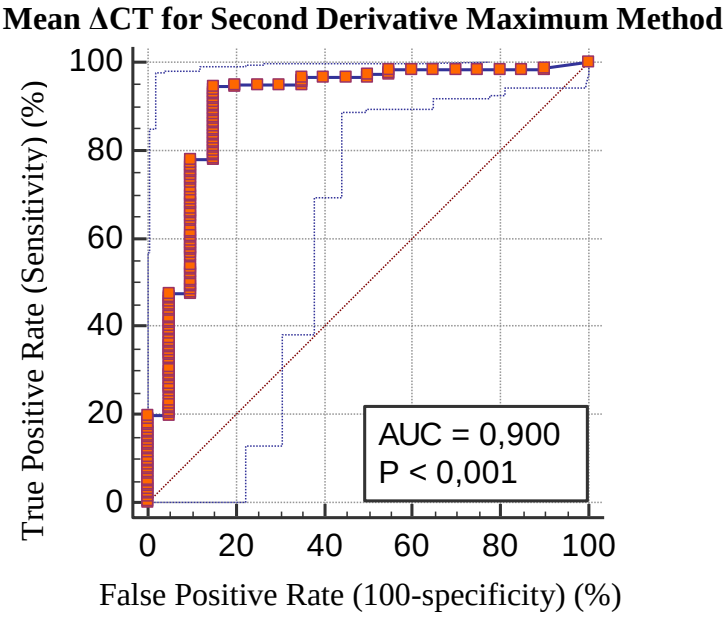

Figure 3.15: Receiver operating characteristic curve for mean TC Ct values analysed using the second derivative maximum method compared to a viral load greater or equal to 200 copies/ml. Receiver operating characteristic curve displaying the change in sensitivity and false positive rate (100-specificity) for mean TC Ct values (orange squares) classified based according to the VL being ≥ 200 copies/ml.

Figure 3.16 summarises the results of the comparison of the RNV assay to standard VL methodologies using a TC Ct cut-off of ≤ 21.78 cycles for determination of a VL ≥ 200 copies/ml. With these thresholds, there were 188 (93.5%) specimens that were concordant and 13 (6.5%) specimens discordant between the RNV assay and standard VL assays.

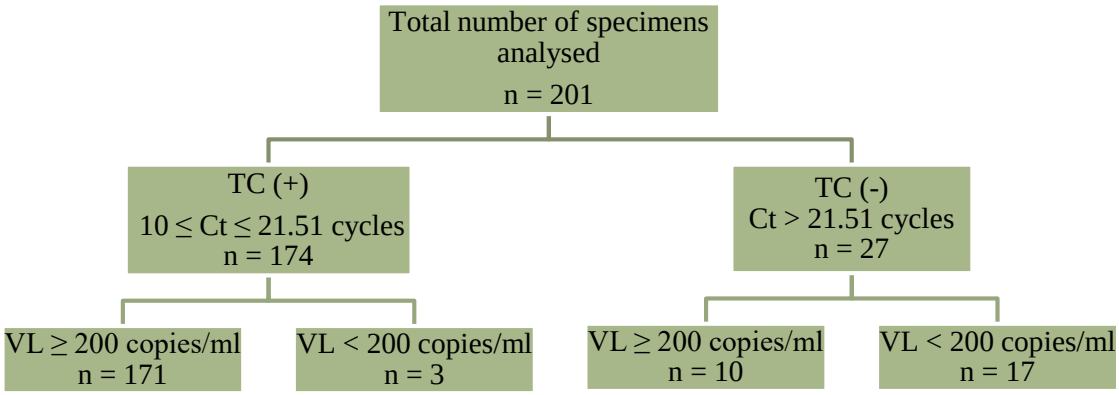

Figure 3.16: Comparison of the results of the RNV assay TC component to standard viral load methodology using the optimised cut-off for the second derivative maximum method of analysis. The results of the mean TC Ct value analysed using the second derivative maximum method for al specimens compared to the VL data available for each specimen.

Based on the above thresholds described for the TC component, the optimal ΔCt cut-off for mutation detection was determined. The 171 that had a positive TC and a VL ≥ 200 copies/ml were compared to standard genotyping methods with the exception of 13 specimens which had no available genotyping data and three specimens that did not amplify on the RNV component of the assay. The comparison performed on the 155 is shown in the ROC curve in Figure 3.17 below.

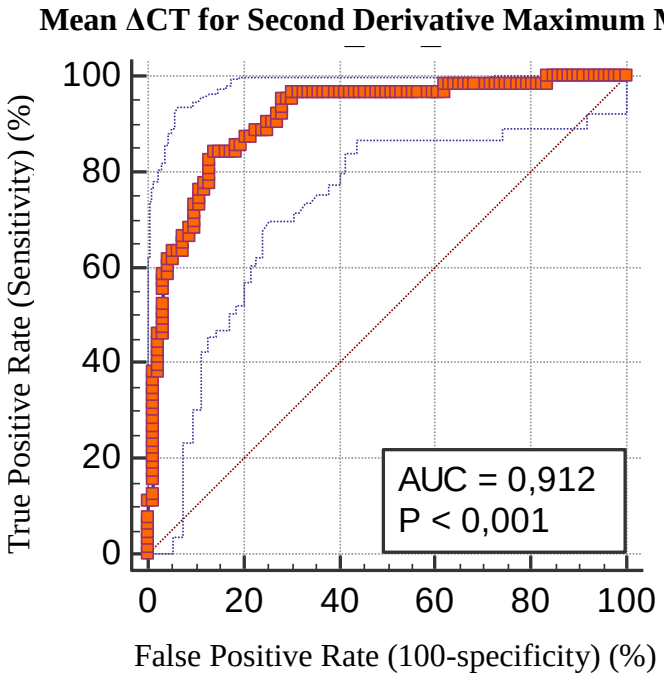

Figure 3.17: Receiver operating characteristic curve for mean ΔCt values analysed using the fit point method compared to standard genotyping. Receiver operating characteristic curve displaying the change in sensitivity and false positive rate (100-specificity) for mean ΔCt values (red squares) classified based according to the Sanger sequencing genotype. The diagonal line represents where the sensitivity equals 100-specificity.

The Youden J index of 0.7000 was associated with a ΔCt value of ≤ 8.26 cycles. The sensitivity, specificity and area under the ROC curve compared to standard genotyping methods were 84.13%%, 85.87%% and 0.912. Figure 3.18 summarises the comparison of the results of the RNV assay mutation detection component to standard genotyping methodologies.

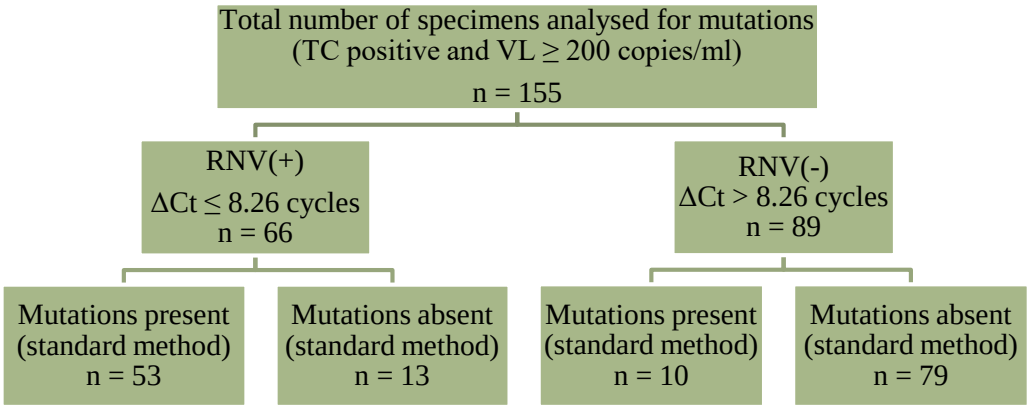

Figure 3.18**: Comparison of the results of the RNV assay RNV component using the second derivative maximum method of analysis to standard genotyping methodology using the optimised cut-off.** The results of the mean ΔCt value analysed using the second derivative method for all specimens with a positive TC and VL greater than 200 copies/ml compared to the genotype data available for each specimen.

CHAPTER 4:

DISCUSSION

The HIV Drug Resistance RNV Multiplex Assay was developed by the Centers for Disease Control and Prevention for the purpose of screening plasma specimens for three key drug resistance mutations associated with resistance to reverse transcriptase inhibitors, namely K65R, K103N and M184V. This multiplex multi-subtype allele-specific assay uses a real-time platform with a fluorescent dye for qualitative detection of these three key mutations, and has a lower limit of sensitivity equivalent to a VL of 600 copies/ml, which can simultaneously be used as a signal of virological failure. The assay is cost-effective when compared to the Sanger sequencing-based resistance testing technologies that are routinely used for detection of HIV-1 drug resistance mutations. This RNV assay is a relatively simple assay to set up and can be used on any real-time platforms, making it feasible to implement in most laboratories. The detection of these mutations uses a ΔCt value to classify specimens as mutant (RNV positive, or having one or more mutations present) and thus is dependent on accurate detection of HIV above the assay limit of detection.

This study set out to validate and optimise the RNV multiplex assay in a South African setting, by comparing the results of the assay to previously determined VL and genotype data. Specimens that had discrepant genotypic results between the RNV assay and Sanger sequencing results were re-sequenced using NGS technologies to establish if the RNV assay is more sensitive at detecting the mutations. We further optimised the assay by recommending alternative thresholds.

The validation was performed on the LightCycler 480 Real-time PCR instrument, based on the availability of this instrument in the HIV Drug resistance laboratory at NICD. The instrument software has the capacity to interpret raw data amplification curves using the fit point method or the second derivative maximum method. When using the fit point analysis method, the operator can manually select a noise band, beneath which variations in fluorescent signal are considered as background noise. The cycle threshold (Ct) is then determined as the point at which each specimen amplification curve passes this noise band. Using the second derivative maximum method, this noise band is calculated internally by the software. The second derivative maximum ideally is a preferred method

for analysis, as it minimises operator variability. However, threshold methods, including the fit point method, are the more commonly used analysis methods for real-time PCR amplification curves due to them being the first method implemented in real-time PCR machine software and widespread availability. Literature reviews of preferred methods for analysis of real-time PCR amplification curves indicate that while threshold methods are highly susceptible to errors in baselining and signal anomalies, there is value in these methods due to their consistency (Clemens and Shain, 2008; Spiess *et al.*, 2016). This method of analysis is the most commonly used, making it an ideal option for universal analyses, particularly due to the lack of other quantification analysis tools in some software packages (Spiess *et al.*, 2016).

A total of 225 remnant plasma specimens were selected for this study, with known VL and drug resistance genotype. Of these, 47 specimens had a VL < 600 copies/ml, and 178 specimens had a VL ≥ 600 copies/ml. Of 171 specimens with known genotype, 105 specimens had a WT genotype and 66 specimens had one or more mutation present. The initial validation of the assay and the instrument were successful, with all controls passing validation criteria when analysed using the fit point method. The in-run controls did not pass validation criteria when using the second derivative maximum method; therefore, we did not pursue this method further for validation purposes. This method was explored further using new thresholds later in the discussion.

The validation of the RNV assay was successful for detection of virological failure (VL ≥ 600 copies/ml). The results of the total copy (TC) component of the RNV assay produced 180 (84.0%) results were concordant with the VL results, whilst 45 (16.0%) had discrepant results, of which 19 (8.4%) could be considered false positive and 17 (7.5%) could be considered false negative. The sensitivity of the TC component of the RNV assay was high (90.5%), however, the specificity was lower (59.6%). Despite this, however, the overall accuracy reflected by the area under the ROC curve statistic was fair (0.750).

The 161 specimens that had a positive TC and a VL > 600 copies/ml were compared to standard genotyping performed previously. Of these, 130 (93.2%) had concordant results with Sanger sequencing, and 28 (17.4%) were discordant. An additional three specimens were characterised as having no amplification. Of the discordant specimens, 24 (14.9%) were positive for mutations on the RNV assay but did not have mutations present in the

Sanger sequence, and 4 (2.5%) were RNV negative yet mutations were detected using Sanger sequencing. Considering the limit of detection of Sanger sequencing being approximately 20% while AS-PCRs can have a limit of < 1%, the high number of false positives may be explained by this. This would be reflected by a high sensitivity when compared to a less sensitive assay, as was seen with the RNV assay when compared to Sanger sequencing. However, minority variants were detected in five of the 24 false positive specimens using NGS. The mutation analysis component had improved statistics over the TC component: greater accuracy was signalled by a higher area under the ROC curve statistic (0.841), and the sensitivity and specificity were determined to be 93.7% and 74.5%, respectively. The two specimens that had no mutations in the RNV assay but had mutations in the Sanger sequence genotype revealed that these mutations are true RNV discrepant specimens as the same mutations were present in the NGS sequence.

Comparison of the results of the agarose gel electrophoresis to the NGS revealed that all 14 of the specimens had additional mutations in the agarose gel that were not confirmed by NGS. The agarose gel analysis of the RNV amplification product is time-consuming (four to six hours), this combined with potential to falsely detect mutations that may not be present make this component of the analysis particularly infeasible.

An RNV assay ΔCt positive indicates one or more of the K65R, K103N or M184V mutations are present, however, the assay is unable to differentiate between these mutations. This is due to the assay using an intercalating dye in the RNV multiplex primer mixture with only one detection wavelength. Due to this, an alternative method will need to be employed in order to determine the mutations present. As the agarose gel electrophoresis of the RNV PCR product is not feasible, this would be done by Sanger sequencing or NGS. Due to the cost of these assays, such an approach is not recommended for low-middle income countries.

The additional 270 bp amplification product present in the agarose gel electrophoresis has had an undetermined impact on the performance of the RNV assay. Due to the assay using an intercalating dye, however, amplification not due to the presence of the K65R, K103N or M184V mutations in the RNV PCR reaction may result in a false positive result. This is an issue that will need to be addressed prior to implementation of this assay.

The statistical tests presented here indicate a need for further optimisation of the assay. The RNV assay was initially validated by using DBS cards and resulted in a limit of

detection of 600 copies/ml. A review published by the WHO to provide a reference for the use of DBS cards for HIV-1 VL quantification and genotyping found that the sensitivity when using DBS cards for VL quantification was 2 log lower than when using plasma (Bertagnolio *et al.*, 2010). Since this study used plasma, a lower VL threshold was explored, with the optimal threshold determined to be ≥ 200 copies/ml. The recommended TC cut-off associated with this lower VL limit of detection was reduced from ≤ 25.0 cycles to ≤ 21.78 cycles. Using these statistics, the sensitivity, specificity and area under the ROC curve of the assay increased to 94.5%, 85.0% and 0.913.

Using the specimens that had a positive TC based on a Ct value ≤ 21.78 cycles and a VL ≥ 200 copies/ml, the mutational analysis component cut-off was analysed. The analysis comparing the ΔCt value to the Sanger sequencing genotype determined the optimal cut-off to be ≤ 10.94, a value that was very similar to that originally proposed. Using these statistics, the sensitivity, specificity and area under the ROC curve of the assay increased to 84.1%, 85.9% and 0.912.

Despite being validated successfully on control plasmids, analysing specimen runs using the second derivative method resulted in only three runs falling within the range specified for the RNCV and WT controls. Alternative thresholds for analysis using the second derivative method were similarly proposed. The second derivative maximum analysis method was also optimised further and new ranges for the RNCV and WT controls recommended. The advantages of using this method over the fit point method to analyse the amplification curves lies in the way in which the Ct values are calculated. This mathematical model requires no user input and thus is simple as there is no separate analysis for the TC and RNV components and there is no variation between users.

One of the drawbacks of the fit point method to analyse the amplification curves is that the threshold generated by the software did not cross the exponential phase of the amplification curves and thus it had to be set for every analysis. In addition, there were many instances where this threshold drawn according to the exponential phase of the RNCV and WT controls were inaccurate for other specimens in the analysis. The second derivative maximum method of amplification curve analysis does not suffer from this limitation, as it bases the concentration of amplified DNA on the shape of the amplification curve and rejects the idea that specimens with the same fluorescence have the same DNA concentration (Rasmussen, 2001).

Even with the optimised thresholds and cut-offs proposed using the second derivative maximum method, there were a number of false positive and false negative mutations detected by the RNV assay (13[8.4%] and 10[6.5%], respectively). Should the RNV assay be implemented in low-middle income countries, the impact of these would be substantial. The false positive mutation results could potentially result in changes from first-line to second-line ART at significant cost implications in patients who are non-adherent as opposed to failing ART due to mutations. The impact of this would be that those patients are at risk of failing second-line ART due to non-adherence as well. The recommendation in this case would be that adherence counselling be performed prior to performing the RNV assay, however, for a shorter period that currently performed to limit the time patients harbouring major drug resistance mutations remain on a failing regimen.

The implications of RNV false negative specimens is that a patient harbouring drug resistance mutations would remain on a failing regimen, possibly without the potential for viral re-suppression. It would therefore be feasible to suggest that the current guideline regarding virological failure, enhanced adherence counselling and an eventual regimen change should these be ineffective still be in place for such cases.

Using the RNV assay as a screening tool for HIV-1 infected patients failing first-line ART allows for the identification of patients harbouring key drug resistance mutations and require a change in regimen. South Africa, like many other low-middle income countries, does not provide resistance testing at ART regimen initiation or at first-line failure. Instead, patients are switched to second line following two successive VL results that are > 1,000 copies/ml (World Health Organization, 2016b). However, a screening assay could assist in identifying patients that harbour resistance, as opposed to those who are non-adherent.

The relevance of a screening assay that detects the NNRTI mutation K103N could be questioned as many countries transition to a dolutegravir-based regime for first-line treatment for HIV infection (Vitoria *et al.*, 2019). However, many countries are exploring retaining efavirenz-based regimens for women of child bearing age; therefore, the assay may retain its value in the future.

Future work into the RNV assay includes the performance of the assay in other countries where different HIV-1 subtypes dominate and its performance in a large study where the

dynamics involved around implementation of this assay can be analysed. Assessing the molecular aspects of the assay to improve the sensitivity and specificity should also be performed. This includes analysing primer binding to assess the impact of non-specific amplification products on the possible generation of false positive results. As the assay is designed with two separate enzyme mixtures, additional mutational enzyme mixtures could also be developed to identify additional mutations present either in combination with or independently from the RNV enzyme mixture.

To conclude, the RNV assay was successfully validated with the controls as well as the HIV-1 Subtype C specimens with a high sensitivity and accuracy as reflected by the area under the ROC curve value. Optimisation of the RNV assay resulted in higher sensitivity, specificity and area under the ROC curve value. With these improved statistics, the RNV assay is a viable option for implementation in a clinical setting as a screening tool for HIV-infected patients failing first-line ART due to the development of major drug resistance mutations.

APPENDIX A:

RNV Assay Results

The results of the RNV assay using the fit point method are summarised in Table A.1 below. The amplification column describes whether on not amplification was observed in at least two runs. The mean TC, RNV and ΔCt values were calculated using the results of the runs performed in triplicate. The agarose gel results column describes the consensus of the bands observed after performing agarose gel electrophoresis on the RNV amplification product of specimens with a TC < 25 cycles and a ΔCt < 11 cycles.

Table A.1: Specimen information and RNV assay results using the fit point method.

Specimen ID	Viral Load (copies/ml)	Sanger Sequencing Results			RNV Assay Results							Agarose Gel Results
		65	103	184	Dilution Factor	TC Amplification	Mean TC	RNV Amplification	Mean RNV	Mean ΔCt	Mean ΔCt Interpretation	
AMP001	8905	K	N	M	20	Yes	12,43	Yes	22,60	10,16	Mutant	RNV
AMP002	640	No Amplification			1	No		No				
AMP003	3260	No Amplification			1	Yes	17,54	Yes	28,44	10,91	Mutant	RNV
AMP004	1257	K	K	M	20	Yes	13,28	Yes	25,24	11,96	Wild-type	V
AMP005	12004	K	K	M	400	Yes	24,03	Yes	32,04	8,77	Mutant	V
AMP006	26000	R	N	V	1	Yes	17,54	Yes	21,72	4,18	Mutant	RNV
AMP008	2180	K	K	M	20	Yes	12,89	Yes	27,65	14,76	Wild-type	RV
,AMP010	1184	K	K	M	1	No		No				
AMP012	<40	K	K	M	1	Yes	15,19	Yes	24,33	9,14	Mutant	RNV
AMP013	362	K	N	M	1	Yes	16,85	Yes	26,08	9,23	Mutant	RN
AMP015	334	No Amplification			1	No		No				

Table A.1: Continued

Specimen ID	Viral Load (copies/ml)	Sanger Sequencing Results			RNV Assay Results							Agarose Gel Results
		65	103	184	Dilution Factor	TC Amplification	Mean TC	RNV Amplification	Mean RNV	Mean ΔCt	Mean ΔCt Interpretation	
AMP016	29760	K	K	M	20	Yes	12,47	Yes	24,43	11,96	Wild-type	
AMP017	398	No Amplification			1	Yes	14,37	Yes	27,09	12,71	Wild-type	
AMP020	120975	K	K	M	400	Yes	13,73	Yes	26,56	12,83	Wild-type	
AMP021	285	No Amplification			1	Yes	27,59	No				
AMP023	596	K	K	M	1	Yes	13,49	Yes	22,53	9,04	Mutant	RNV
AMP025	2076	K	K	M	1	Yes	27,73	No				
AMP026	55720	K	K	M	400	Yes	13,32	Yes	28,37	15,05	Wild-type	
AMP027	302605	K	K	M	400	Yes	10,37	Yes	20,30	9,93	Mutant	R
AMP028	42	No Amplification			1	No		No				
AMP029	674	K	K	M	20	Yes	14,62	Yes	26,63	12,02	Wild-type	
AMP031	36846	K	S	V	20	Yes	11,27	Yes	20,22	8,95	Mutant	V
AMP033	224	K	N	M	1	Yes	16,19	Yes	22,45	6,26	Mutant	RNV
AMP034	22013	R	N	V	1	Yes	12,42	Yes	17,11	4,69	Mutant	NV
AMP035	58000	K	K	M	20	Yes	11,89	Yes	23,22	11,33	Wild-type	RV
AMP036	906828	K	N	V	20	Yes	16,55	Yes	23,51	6,97	Mutant	NV
AMP039	<40	No Amplification			1	No		No				
AMP040	96	No Amplification			1	No		No				
AMP041	5295	K	K	M	20	Yes	12,88	Yes	28,15	15,28	Wild-type	
AMP042	316880	K	K	M	8000	Yes	16,98	Yes	29,84	12,86	Wild-type	
AMP043	6025	K	K	M	20	Yes	12,02	Yes	19,70	7,68	Mutant	RV

Table A.1: Continued

Specimen ID	Viral Load (copies/ml)	Sanger Sequencing Results			RNV Assay Results							Agarose Gel Results
		65	103	184	Dilution Factor	TC Amplification	Mean TC	RNV Amplification	Mean RNV	Mean ΔCt	Mean ΔCt Interpretation	
AMP046	375	K	K	M	1	Yes	10,71	Yes	19,28	8,57	Mutant	R
AMP047	1590	K	K	M	1	Yes	16,42	Yes	24,64	8,21	Mutant	RNV
AMP048	233375	K	K	M	400	Yes	12,57	Yes	27,36	14,79	Wild-type	
AMP049	1815	K	N	M	400	Yes	15,07	Yes	23,42	8,35	Mutant	N
AMP050	29005	K	K	M	20	Yes	10,87	Yes	22,80	11,93	Wild-type	
AMP051	12930	K	N	M	400	Yes	12,1	Yes	18,54	6,44	Mutant	NV
AMP055	47082	K	S	V	400	Yes	15,09	Yes	20,05	4,96	Mutant	V
AMP056	88332	No Amplification			1	No		No				
AMP059	49	No Amplification			1	Yes	29,44	Yes	31,21			
AMP060	952	K	K	M	20	Yes	15,47	Yes	28,25	12,77	Wild-type	
AMP061	3922	K	K	M	1	Yes	12,14	Yes	17,65	5,51	Mutant	V
AMP064	1946	K	N	V	1	Yes	12,38	Yes	15,06	2,68	Mutant	NV
AMP065	107475	K	K	M	400	Yes	10,66	Yes	24,27	13,62	Wild-type	
AMP068	222230	K	K	M	400	Yes	12,95	Yes	25,73	12,79	Wild-type	
AMP069	199690	K	K	M	400	Yes	12,28	Yes	25,09	12,82	Wild-type	
AMP070	20744	K	K	M	400	Yes	14,71	Yes	26,73	12,02	Wild-type	
AMP074	< LDL	No Amplification			1	Yes	29,61	No				
AMP075	309690	K	K	M	400	Yes	11,76	Yes	29,56	17,80	Wild-type	
AMP076	69705	K	K	M	20	Yes	11,73	Yes	22,95	11,22	Wild-type	RNV
AMP077	1038270	K	K	M	8000	Yes	21,17	No				

Table A.1: Continued

Specimen ID	Viral Load (copies/ml)	Sanger Sequencing Results			RNV Assay Results							Agarose Gel Results
		65	103	184	Dilution Factor	TC Amplification	Mean TC	RNV Amplification	Mean RNV	Mean ΔCt	Mean ΔCt Interpretation	
AMP078	1950	K	K	M	20	Yes	11,29	Yes	25,95	14,66	Wild-type	
AMP079	4759	K	N	V	20	Yes	12,19	Yes	17,65	5,45	Mutant	N
AMP081	<40	No Amplification			1	Yes	25,71	No				
AMP082	1178	K	K	M	1	Yes	16,43	Yes	26,03	9,60	Mutant	RN(V)
AMP083	34223	R	N	V	20	Yes	14,43	Yes	19,97	5,54	Mutant	RV
AMP085	98770	R	K	M	20	Yes	10,74	Yes	20,54	9,80	Mutant	R
AMP086	7840	K	K	M	20	Yes	15,56	Yes	27,68	12,12	Wild-type	
AMP088	10550	K	K	M	1	Yes	15	Yes	24,09	9,09	Mutant	RNV
AMP089	806	K	K	M	1	Yes	12,03	Yes	19,57	7,54	Mutant	NV
AMP090	1238	K	N	M	1	Yes	12,92	Yes	19,01	6,08	Mutant	N
AMP091	53640	K	K	M	20	Yes	11,99	Yes	23,11	11,12	Wild-type	RN
AMP093	2106	No Amplification			1	No		No				
AMP094	62	No Amplification			1	No		No				
AMP095	160180	K	K	M	20	Yes	12,22	Yes	25,06	12,84	Wild-type	
AMP097	78075	K	K	M	20	Yes	11,5	Yes	23,05	11,55	Wild-type	
AMP098	31235	K	K	M	1	Yes	10,42	Yes	13,53	6,59	Mutant	
AMP099	< DL	No Amplification			1	Yes	30,06	No				
AMP100	1692	K	N	M	1	Yes	12,41	Yes	21,34	8,93	Mutant	NV
AMP101	1772	K	K	M	1	Yes	11,84	Yes	26,17	6,61	Mutant	R(N)V
AMP102	380	No Amplification			1	Yes	28,62	No				

Table A.1: Continued

Specimen ID	Viral Load (copies/ml)	Sanger Sequencing Results			RNV Assay Results							Agarose Gel Results
		65	103	184	Dilution Factor	TC Amplification	Mean TC	RNV Amplification	Mean RNV	Mean ΔCt	Mean ΔCt Interpretation	
AMP103	195910	K	K	M	20	Yes	13,81	Yes	23,05	9,24	Mutant	V
AMP104	191500	K	KN	M	1	Yes	11,99	Yes	20,81	8,16	Mutant	NV
AMP106	1330	K	K	M	1	Yes	14,39	Yes	26,60	12,21	Wild-type	RNV
AMP110	1130	K	K	M	1	Yes	18,54	Yes	27,16	7,61	Mutant	RNV
AMP111	7816	R	N	V	1	Yes	21,78	Yes	28,05	6,28	Mutant	RNV
AMP112	1644050	K	K	M	20	Yes	11,09	Yes	23,55	12,45	Wild-type	
AMP113	9035	K	K	M	400	Yes	13,67	Yes	25,43	11,76	Wild-type	N(V)
AMP114	3098	K	NK	V	1	Yes	27,19	No				
AMP115	31100	K	K	M	400	Yes	12,95	Yes	26,35	13,40	Wild-type	
AMP117	72665	K	K	M	400	Yes	13,48	Yes	26,13	12,64	Wild-type	
AMP118	165	No Amplification			1	Yes	27,7	Yes	31,53	3,84	Mutant	
AMP120	10665	K	K	M	20	Yes	13,45	Yes	27,15	13,70	Wild-type	
AMP121	1650	K	K	M	20	Yes	14,22	Yes	29,07	14,86	Wild-type	
AMP122	12784	No Amplification			20	Yes	13,31	Yes	24,99	11,68		
AMP123	13966	KR	KR	V	400	Yes	14,14	Yes	20,07	5,93	Mutant	RV
AMP124	208	No Amplification			1	Yes	19,9	Yes	28,78	8,88	Mutant	R(N)
AMP125	45091	K	N	V	400	Yes	11,77	Yes	21,62	9,85	Mutant	RNV
AMP126	608	K	K	M	1	Yes	11,34	Yes	22,85	11,51	Wild-type	
AMP127	1623	K	K	M	20	Yes	11,96	Yes	21,79	9,83	Mutant	RV
AMP128	102070	K	K	M	400	Yes	12,38	Yes	25,89	13,51	Wild-type	

Table A.1: Continued

Specimen ID	Viral Load (copies/ml)	Sanger Sequencing Results			RNV Assay Results							Agarose Gel Results
		65	103	184	Dilution Factor	TC Amplification	Mean TC	RNV Amplification	Mean RNV	Mean ΔCt	Mean ΔCt Interpretation	
AMP129	1462	K	N	M	1	Yes	14,93	Yes	21,95	8,32	Mutant	N
AMP130	3593	K	K	M	20	Yes	10,85	Yes	23,34	12,49	Wild-type	
AMP132	945	K	S	V	20	Yes	14,47	Yes	24,26	9,79	Mutant	RNV
AMP133	808	K	K	M	20	Yes	11,27	Yes	25,37	14,11	Wild-type	
AMP136	10803	K	K	M	400	Yes	20,62	No				
AMP138	1650000	R	K	M	20	Yes	14,73	Yes	20,86	6,13	Mutant	R
AMP139	4695	K	K	M	1	No		No				
AMP140	104	No Amplification			1	No		No				
AMP142	835	K	K	M	1	Yes	30,72	No				
AMP143	20910	K	N	M	400	Yes	13,36	Yes	21,43	8,07	Mutant	N
AMP145	17430	K	K	M	20	Yes	14,06	Yes	28,77	14,71	Wild-type	
AMP146	152	No Amplification			1	Yes	29,37	No				
AMP147	30920	K	K	M	1	Yes	13,13	Yes	23,68	10,55	Mutant	RNV
AMP148	1580	K	N	V	1	Yes	19,18	Yes	25,12	5,94	Mutant	NV
AMP149	26079	R	N	M	1	Yes	14,67	Yes	22,12	7,45	Mutant	N
AMP150	11121	K	K	V	1	Yes	15,16	Yes	25,91	10,75	Mutant	RNV
AMP151	176505	K	K	M	1	Yes	12,81	Yes	26,89	14,08	Wild-type	
AMP152	40245	K	K	M	1	Yes	13,26	Yes	18,07	4,82	Mutant	V
AMP155	54770	K	K	M	1	Yes	11,27	Yes	20,85	9,59	Mutant	RNV
AMP158	255230	K	K	M	400	Yes	16,28	Yes	27,27	10,99	Mutant	RV

Table A.1: Continued

Specimen ID	Viral Load (copies/ml)	Sanger Sequencing Results			RNV Assay Results							Agarose Gel Results
		65	103	184	Dilution Factor	TC Amplification	Mean TC	RNV Amplification	Mean RNV	Mean ΔCt	Mean ΔCt Interpretation	
AMP159	114925	K	K	M	20	Yes	14,84	Yes	27,32	12,48	Wild-type	
AMP160	66620	K	K	M	20	Yes	13,24	Yes	26,74	13,50	Wild-type	
AMP161	59	No Amplification			1	Yes	24,97	No				
AMP162	112	No Amplification			1	Yes	28,06	No				
AMP164	58285	K	K	M	8000	Yes	12,64	Yes	28,82	16,18	Wild-type	
AMP166	102735	R	N	M	8000	Yes	14,36	Yes	22,44	8,08	Mutant	RN
AMP167	4620	K	K	M	400	Yes	15,82	Yes	23,49	7,67	Mutant	V
AMP168	1525	K	N	V	20	Yes	14,28	Yes	20,82	6,55	Mutant	NV
AMP169	363	No Amplification			1	Yes	14,35	Yes	28,04	13,69	Wild-type	
AMP170	780	K	K	M	20	Yes	13,07	Yes	28,01	14,95	Wild-type	
AMP171	471	K	K	M	1	Yes	16,07	Yes	27,14	11,07	Wild-type	RNV
AMP172	54	No Amplification			1	Yes	26,32	No				
AMP173	106	No Amplification			1	Yes	30,66	No				
AMP175	30865	K	K	M	400	Yes	12,39	Yes	26,96	14,57	Wild-type	
AMP176	56622	K	K	M	160000	Yes	15,5	Yes	29,08	13,58	Wild-type	
AMP177	11745	K	KN	M	400	Yes	11,73	Yes	19,11	7,38	Mutant	NV
AMP178	25865	K	K	M	8000	Yes	14,62	Yes	27,98	13,36	Wild-type	
AMP181	44	No Amplification			1	Yes	24,63	No				
AMP182	8605	K	K	M	400	Yes	18,23	Yes	29,88	11,65	Wild-type	
AMP183	90865	K	K	M	8000	Yes	15,77	No				

Table A.1: Continued

Specimen ID	Viral Load (copies/ml)	Sanger Sequencing Results			RNV Assay Results							Agarose Gel Results
		65	103	184	Dilution Factor	TC Amplification	Mean TC	RNV Amplification	Mean RNV	Mean ΔCt	Mean ΔCt Interpretation	
AMP184	147065	K	K	M	8000	Yes	16,41	Yes	28,65	12,25	Wild-type	
AMP188	12650	K	K	M	8000	Yes	15,07	Yes	29,99	14,93	Wild-type	
AMP189	<40	No Amplification			1	Yes	24,97	No				
AMP190	90	No Amplification			1	No		No				
AMP191	3308	No Amplification			1	Yes	25,62	No				
AMP192	3425	K	K	M	400	Yes	15,14	Yes	31,81	16,36	Wild-type	
AMP193	219525	K	K	M	400	Yes	20,89	Yes	32,58	11,69	Wild-type	V
AMP194	11846	R	N	V	400	Yes	18,39	Yes	27,32	8,93	Mutant	RN
AMP196	8015	K	KN	M	400	Yes	16,49	Yes	27,92	11,43	Wild-type	N
AMP197	17250	No Amplification			1	Yes	10,89	Yes	24,01	13,12	Wild-type	
AMP199	6828	No Amplification			1	Yes	26,23	No				R
AMP200	145388	K	K	M	8000	Yes	17,09	Yes	31,12	14,03	Wild-type	
AMP201	140	No Amplification			1	Yes	22,4	Yes	23,77	1,37	Mutant	RNV
AMP204	58	K	N	M	1	Yes	15,36	Yes	21,38	6,02	Mutant	N
AMP205	1394	K	K	M	1	No		No				
AMP206	404	No Amplification			1	Yes	24,92	No				
AMP207	19162	K	N	M	20	Yes	15,62	Yes	22,97	7,35	Mutant	N
AMP208	1011	R	N	V	20	Yes	14,08	Yes	19,37	5,29	Mutant	RNV
AMP210	20715	K	K	M	20	Yes	14,09	Yes	24,02	9,94	Mutant	(R)V
AMP212	<40	No Amplification			1	Yes	28,4	No				

Table A.1: Continued

Specimen ID	Viral Load (copies/ml)	Sanger Sequencing Results			RNV Assay Results							Agarose Gel Results
		65	103	184	Dilution Factor	TC Amplification	Mean TC	RNV Amplification	Mean RNV	Mean ΔCt	Mean ΔCt Interpretation	
AMP214	3130	K	K	V	20	Yes	14,94	Yes	21,31	6,38	Mutant	V
AMP215	< DL	No Amplification			1	Yes	28,33	No				
AMP217	344375	K	S	V	400	Yes	17,29	Yes	26,34	9,05	Mutant	NV
AMP218	107255	K	K	M	400	Yes	13	Yes	26,17	13,17	Wild-type	
AMP221	82300	K	K	M	400	Yes	15,78	Yes	30,15	14,37	Wild-type	N
AMP223	24225	K	K	M	20	Yes	15,23	Yes	28,11	12,88	Wild-type	
AMP224	459	No Amplification			1	Yes	27,42	No				
AMP226	8287	K	N	M	400	Yes	13,88	Yes	22,69	8,81	Mutant	N
AMP227	6985	K	K	M	20	Yes	13,84	Yes	27,22	13,38	Wild-type	
AMP228	4853	K	N	V	20	Yes	14,61	Yes	24,13	9,52	Mutant	NV
AMP229	548	No Amplification			1	Yes	16,1	Yes	26,53	10,43	Mutant	RV
AMP230	145318	R	SN	V	20	Yes	16,14	Yes	19,98	3,84	Mutant	RNV
AMP231	1569	K	K	M	20	Yes	12,2	Yes	26,46	14,26	Wild-type	
AMP232	254	No Amplification			1	No		No				
AMP233	24674	K	N	M	400	Yes	15,57	Yes	24,07	8,51	Mutant	N
AMP236	202777	K	S	V	400	Yes	12,47	Yes	23,41	10,94	Mutant	RV
AMP237	132	No Amplification			1	Yes	30,6	No				
AMP238	22674	No Amplification			20	Yes	12,58	Yes	26,11	13,53	Wild-type	
AMP240	13128	No Amplification			1	Yes	10,72	Yes	22,67	11,94	Wild-type	
AMP241	83	No Amplification			1	No		No				

Table A.1: Continued

Specimen ID	Viral Load (copies/ml)	Sanger Sequencing Results			RNV Assay Results							Agarose Gel Results
		65	103	184	Dilution Factor	TC Amplification	Mean TC	RNV Amplification	Mean RNV	Mean ΔCt	Mean ΔCt Interpretation	
AMP242	2875	K	K	M	1	Yes	11,33	Yes	24,05	12,72	Wild-type	
AMP243	828	No Amplification			1	No		No				
AMP244	5770	K	K	M	400	Yes	14,77	Yes	29,12	14,35	Wild-type	
AMP245	5852	K	N	M	400	Yes	16,28	Yes	24,38	8,10	Mutant	RN
AMP246	986	K	K	M	1	Yes	13	Yes	25,95	12,94	Wild-type	
AMP249	148000	R	N	V	1	No		No				
AMP251	104	No Amplification			1	Yes	30,17	No				
AMP252	1310	K	N	M	1	Yes	12,38	Yes	25,71	13,33	Wild-type	
AMP253	310	No Amplification			1	Yes	13,91	Yes	28,60	14,69	Wild-type	
AMP254	2830	R	N	M	20	Yes	11,77	Yes	20,05	8,28	Mutant	R
AMP255	203	No Amplification			1	No		No				
AMP260	384	No Amplification			1	Yes	13,52	Yes	25,89	12,37	Wild-type	
AMP261	216250	K	K	M	400	Yes	11,74	Yes	20,57	8,83	Mutant	V
AMP263	7545	K	K	M	400	Yes	13,52	Yes	28,15	14,64	Wild-type	
AMP265	1676	No Amplification			1	No		No				
AMP267	119385	K	N	V	400	Yes	15,5	Yes	23,49	7,98	Mutant	NV
AMP268	766	No Amplification			1	Yes	12,99	Yes	24,98	11,99	Wild-type	
AMP271	1536	No Amplification			1	No		No				
AMP272	16015	K	K	V	1	Yes	13,55	Yes	27,81	14,26	Wild-type	
AMP273	1076255	K	K	M	8000	Yes	12,5	Yes	19,35	6,85	Mutant	V

Table A.1: Continued

Specimen ID	Viral Load (copies/ml)	Sanger Sequencing Results			RNV Assay Results							Agarose Gel Results
		65	103	184	Dilution Factor	TC Amplification	Mean TC	RNV Amplification	Mean RNV	Mean ΔCt	Mean ΔCt Interpretation	
AMP275	98	No Amplification			1	Yes	11,88	Yes	24,16	12,28	Wild-type	
AMP276	1300	K	K	M	400	Yes	16,35	Yes	29,68	13,33	Wild-type	
AMP278	2738	K	K	M	1	No		No				
AMP279	69530	R	KR	MV	400	Yes	12,99	Yes	21,68	8,68	Mutant	RV
AMP280	7000	K	K	M	20	Yes	14,85	Yes	27,28	12,44	Wild-type	NV
AMP282	12630	K	K	M	20	Yes	13,81	Yes	28,27	14,47	Wild-type	
AMP283	2129	K	K	M	20	Yes	13,31	Yes	27,15	13,85	Wild-type	
AMP284	1268	No Amplification			1	Yes	13,2	Yes	24,13	10,93	Mutant	RV
AMP285	6115	K	K	M	1	Yes	11,63	Yes	25,49	13,86	Wild-type	
AMP287	47950	R	N	V	400	Yes	12,43	Yes	18,00	5,57	Mutant	RV
AMP288	67665	K	K	M	400	Yes	14,3	Yes	25,83	11,53	Wild-type	
AMP289	112445	K	KN	M	400	Yes	11,7	Yes	19,53	7,84	Mutant	N
AMP290	334	No Amplification			1	No		No				
AMP291	287522	K	NS	M	400	Yes	11,62	Yes	23,32	11,70	Wild-type	
AMP292	232465	K	K	M	8000	Yes	14,99	Yes	26,11	11,12	Wild-type	
AMP293	66655	K	N	M	400	Yes	10,88	Yes	15,91	5,04	Mutant	NV
AMP294	3761180	K	K	M	160000	Yes	14,49	Yes	27,92	13,43	Wild-type	
AMP296	63910	R	K	V	400	Yes	12,32	Yes	21,83	9,51	Mutant	RV
AMP297	471495	K	K	V	20	Yes	12,89	Yes	22,34	9,45	Mutant	
AMP298	1314	K	K	M	1	No		No				

Table A.1: Continued

Specimen ID	Viral Load (copies/ml)	Sanger Sequencing Results			RNV Assay Results							Agarose Gel Results
		65	103	184	Dilution Factor	TC Amplification	Mean TC	RNV Amplification	Mean RNV	Mean ΔCt	Mean ΔCt Interpretation	
AMP299	6396	R	N	V	20	Yes	15,86	Yes	19,58	3,72	Mutant	RNV
AMP301	241580	K	K	M	400	Yes	10,71	Yes	24,10	13,38	Wild-type	
AMP302	207764	R	R	V	8000	Yes	14,1	Yes	19,70	5,59	Mutant	RV
AMP303	125	No Amplification			1	No		No				
AMP304	776	R	N	V	1	Yes	13,55	Yes	19,92	6,37	Mutant	RNV
AMP305	800	K	N	M	20	Yes	15,7	Yes	24,15	8,44	Mutant	N
AMP306	19488	K	KN	M	400	Yes	13,75	Yes	21,76	8,01	Mutant	N
AMP307	191100	K	K	M	400	Yes	13,7	Yes	27,20	13,50	Wild-type	
AMP308	2202	K	K	V	20	Yes	15,57	Yes	22,25	6,68	Mutant	V
AMP309	10665	K	K	M	20	Yes	11,67	Yes	26,15	14,48	Wild-type	
AMP310	9109	K	N	V	1	Yes	11,17	Yes	16,69	5,51	Mutant	NV
AMP313	1196	K	N	V	20	Yes	15,66	Yes	22,55	6,89	Mutant	NV
AMP314	1605	R	K	M	400	Yes	14,95	Yes	22,09	7,14	Mutant	R
AMP315	141925	K	N	V	400	Yes	10,4	Yes	18,52	8,13	Mutant	RV

* Results in brackets indicate bands that were faint on the agarose gel.

REFERENCES

Adamson, C. S. (2012) 'Protease-Mediated Maturation of HIV: Inhibitors of Protease and the Maturation Process', *Molecular biology international*, 2012, p. 604261. doi: 10.1155/2012/604261.

Badowski, M. E., Pérez, S. E., Biagi, M. and Littler, J. A. (2016) 'New Antiretroviral Treatment for HIV', *Infectious Diseases and Therapy*, 5(3), pp. 329–352. doi: 10.1007/s40121-016-0126-x.

Barré-Sinoussi, F., Cherman, J.-C., Rey, F., Nugeyre, M. T., Chamaret, S., Gruest, J., Dauget, C., Axler-Blin, C., Vézinet-Brun, F., Rouzioux, C., Rozenbaum, W. and Montagnier, L. (1983) 'Isolation of a T-lymphotropic retrovirus from a patient at risk for aquired immune deficiency syndrome (AIDS)', *Science*, 220(4599), pp. 868–871.

Beilhartz, G. L. and Götte, M. (2010) 'HIV-1 Ribonuclease H: Structure, Catalytic Mechanism and Inhibitors', *Viruses*. Molecular Diversity Preservation International (MDPI), 2(4), pp. 900–926. doi: 10.3390/v2040900.

Bertagnolio, S., Parkin, N. T., Jordan, M., Brooks, J. and García-Lerma, J. G. (2010) 'Dried blood spots for HIV-1 drug resistance and viral load testing: A review of current knowledge and WHO efforts for global HIV drug resistance surveillance', *AIDS reviews*. World Health Organization, Geneva, Switzerland. bertagnolios@who.int, 12(4), pp. 195–208. Available at: http://europepmc.org/abstract/MED/21179184.

de Béthune, M.-P. (2010) 'Non-nucleoside reverse transcriptase inhibitors (NNRTIs), their discovery, development, and use in the treatment of HIV-1 infection: A review of the last 20 years (1989–2009)', *Antiviral Research*, 85(1), pp. 75–90. doi: https://doi.org/10.1016/j.antiviral.2009.09.008.

Boerma, R. S., Sigaloff, K. C. E., Akanmu, A. S., Boele van Hensbroek, M., Rinke de Wit, T. F. and Calis, J. C. (2016) 'Alarming increase in pretreatment HIV drug resistance in children living in sub-Saharan Africa: a systematic review and meta-analysis', *Journal of Antimicrobial Chemotherapy*, 72(2), pp. 365–371. doi: 10.1093/jac/dkw463.

Brenner, B. G., Oliveira, M., Doualla-Bell, F., Moisi, D. D., Ntemgwa, M., Frankel, F., Essex, M. and Wainberg, M. A. (2006) 'HIV-1 subtype C viruses rapidly develop K65R resistance to tenofovir in cell culture', *AIDS*, 20(9), pp. F9–F13. doi: 10.1097/01.aids.0000232228.88511.0b.

Broder, S. (2010) 'The development of antiretroviral therapy and its impact on the HIV-1/AIDS pandemic', *Antiviral Research*, 85(1), pp. 1–18. doi: https://doi.org/10.1016/j.antiviral.2009.10.002.

Bustin, S. A. and Nolan, T. (2004) 'Pitfalls of quantitative real-time reverse-transcription polymerase chain reaction', *Journal of biomolecular techniques : JBT*. The Association of Biomolecular Resource Facilities, 15(3), pp. 155–166. Available at: https://www.ncbi.nlm.nih.gov/pubmed/15331581.

Checkley, M. A., Luttge, B. G. and Freed, E. O. (2011) 'HIV-1 Envelope Glycoprotein Biosynthesis, Trafficking, and Incorporation', *Journal of Molecular Biology*, 410(4), pp. 582–608. doi: 10.1016/j.jmb.2011.04.042.

Cihlar, T. and Fordyce, M. (2016) 'Current status and prospects of HIV treatment', *Current Opinion in Virology*, 18, pp. 50–56. doi: 10.1016/j.coviro.2016.03.004.

Cihlar, T. and Ray, A. S. (2010) 'Nucleoside and nucleotide HIV reverse transcriptase inhibitors: 25 years after zidovudine', *Antiviral Research*, 85(1), pp. 39–58. doi: 10.1016/j.antiviral.2009.09.014.

Clemens, J. M. and Shain, E. B. (2008) 'A new method for robust quantitative and qualitative analysis of real-time PCR', *Nucleic Acids Research*, 36(14), pp. e91–e91. doi: 10.1093/nar/gkn408.

Clutter, D. S., Jordan, M. R., Bertagnolio, S. and Shafer, R. W. (2016) 'HIV-1 drug resistance and resistance testing', *Infection, Genetics and Evolution*, 46, pp. 292–307. doi: 10.1016/j.meegid.2016.08.031.

Coffin, J. M. (1995) 'HIV Population Dynamics in vivo: Implications for genetic variation, pathogenesis, and therapy' *Science* 267(5197) pp. 483-487.

Cohen, C. J., Hunt, S., Sension, M., Farthing, C., Conant, M., Jacobson, S., Nadler, J., Verbiest, W., Hertogs, K., Ames, M., Rinehart, A. R., Graham, N. M. and Team, and the V. S. (2002) 'A randomized trial assessing the impact of phenotypic resistance testing on antiretroviral therapy', *AIDS*, 16(4), pp. 579–588. Available at: http://journals.lww.com/aidsonline/Fulltext/2002/03080/A_randomized_trial_assessing_the_impact_of.9.aspx.

Cohen, M. S., Chen, Y. Q., McCauley, M., Gamble, T., Hosseinipour, M. C., Kumarasamy, N., Hakim, J. G., Kumwenda, J., Grinsztejn, B., Pilotto, J. H. S., Godbole, S. V, Chariyalertsak, S., Santos, B. R., Mayer, K. H., Hoffman, I. F., Eshleman, S. H., Piwowar-Manning, E., Cottle, L., Zhang, X. C., Makhema, J., Mills, L. A., Panchia, R., Faesen, S., Eron, J., Gallant, J., Havlir, D., Swindells, S., Elharrar, V., Burns, D., Taha, T. E., Nielsen-Saines, K., Celentano, D. D., Essex, M., Hudelson, S. E., Redd, A. D. and Fleming, T. R. (2016) 'Antiretroviral Therapy for the Prevention of HIV-1 Transmission', *New England Journal of Medicine*. Massachusetts Medical Society, 375(9), pp. 830–839. doi: 10.1056/NEJMoa1600693.

Coovadia, A., Hunt, G., Abrams, E. J., Sherman, G., Meyers, T., Barry, G., Malan, E., Marais, B., Stehlau, R., Ledwaba, J., Hammer, S. M., Morris, L. and Kuhn, L. (2009) 'Persistent Minority K103N Mutations among Women Exposed to Single-Dose Nevirapine and Virologic Response to Nonnucleoside Reverse-Transcriptase Inhibitor–Based Therapy', *Clinical Infectious Diseases*, 48(4), pp. 462–472. doi: 10.1086/596486.

Daar, E. S. and Richman, D. D. (2005) 'Confronting the Emergence of Drug-Resistant HIV Type 1: Impact of Antiretroviral Therapy on Individual and Population Resistance', *AIDS Research and Human Retroviruses*. Mary Ann Liebert, Inc., publishers, 21(5), pp. 343–357. doi: 10.1089/aid.2005.21.343.

Das, K., Bandwar, R. P., White, K. L., Feng, J. Y., Sarafianos, S. G., Tuske, S., Tu, X., Clark, A. D., Boyer, P. L., Hou, X., Gaffney, B. L., Jones, R. A., Miller, M. D., Hughes, S. H. and Arnold, E. (2009) 'Structural basis for the role of the K65R mutation in HIV-1 reverse transcriptase polymerization, excision antagonism, and tenofovir resistance', *Journal of Biological Chemistry*. doi: 10.1074/jbc.M109.022525.

Daskalakis, D. (2016) 'HIV diagnostic testing: evolving technology and testing strategies', *Topics in antiviral medicine*. IAS-USA, 19(1), pp. 18–22. Available at: https://www.ncbi.nlm.nih.gov/pubmed/21852712.

Debaisieux, S., Rayne, F., Yezid, H. and Beaumelle, B. (2012) 'The Ins and Outs of HIV-1 Tat', *Traffic*, 13(3), pp. 355–363. doi: 10.1111/j.1600-0854.2011.01286.x.

Deeks, E. D. (2018) 'Doravirine: First Global Approval', *Drugs*, 78(15), pp. 1643–1650. doi: 10.1007/s40265-018-0993-4.

Delelis, O., Carayon, K., Saïb, A., Deprez, E. and Mouscadet, J.-F. (2008) 'Integrase and integration: biochemical activities of HIV-1 integrase', *Retrovirology*, 5, p. 114. doi: 10.1186/1742-4690-5-114.

DeLong, E., DeLong, D. and Clarke-Pearson, D. (1988) 'Comparing the areas under two or more correlated reciever operating characteristic curves: a nonparametric approach', *Biometrics*, 44, pp. 837–845.

Dow, D. E. and Bartlett, J. A. (2014) 'Dolutegravir, the Second-Generation of Integrase Strand Transfer Inhibitors (INSTIs) for the Treatment of HIV', *Infectious Diseases and Therapy*, 3(2), pp. 83–102. doi: 10.1007/s40121-014-0029-7.

El-Khatib, Z., Ekstrom, A. M., Ledwaba, J., Mohapi, L., Laher, F., Karstaedt, A., Charalambous, S., Petzold, M., Katzenstein, D. and Morris, L. (2010) 'Viremia and drug resistance among HIV-1 patients on antiretroviral treatment: a cross-sectional study in Soweto, South Africa', *AIDS*, 24(11), pp. 1679–1687. doi: 10.1097/QAD.0b013e32833a097b.

Faria, N. R., Rambaut, A., Suchard, M. A., Baele, G., Bedford, T., Ward, M. J., Tatem, A. J., Sousa, J. D., Arinaminpathy, N., Pépin, J., Posada, D., Peeters, M., Pybus, O. G. and Lemey, P. (2014) 'HIV epidemiology. The early spread and epidemic ignition of HIV-1 in human populations', *Science (New York, N.Y.)*. 2014/10/02, 346(6205), pp. 56–61. doi: 10.1126/science.1256739.

Fearon, M. (2005) 'The laboratory diagnosis of HIV infections', *The Canadian journal of infectious diseases & medical microbiology*. Medical Microbiology, Canadian Blood Services, Toronto, Ontario., 16(1), pp. 26–30. doi: 10.1155/2005/515063.

Fiebig, E. W., Wright, D. J., Rawal, B. D., Garrett, P. E., Schumacher, R. T., Peddada, L., Heldebrant, C., Smith, R., Conrad, A., Kleinman, S. H. and Busch, M. P. (2003) 'Dynamics of HIV viremia and antibody seroconversion in plasma donors: implications for diagnosis and staging of primary HIV infection', *AIDS*, 17(13). Available at: https://journals.lww.com/aidsonline/Fulltext/2003/09050/Dynamics_of_HIV_viremia_and_antibody.5.aspx.

Frahm, N. and Brander, C. (2007) 'HIV viral diversity and escape from cellular immunity', *Current Infectious Disease Reports*, 9(2), pp. 161–166. doi: 10.1007/s11908-007-0012-5.

Freed, E. O. and Martin, M. A. (2013) 'Human Immunodeficiency Viruses: Replication', in Knipe, D. M. and Howley, P. M. (eds) *Fields Virology*. 6th edn. Philadelphia: Lippincott Williams & Wilkins, pp. 1502–1560.

Fujii, K., Munshi, U. M., Ablan, S. D., Demirov, D. G., Soheilian, F., Nagashima, K., Stephen, A. G., Fisher, R. J. and Freed, E. O. (2009) 'Functional role of Alix in HIV-1 replication', *Virology*, 391(2), pp. 284–292. doi: 10.1016/j.virol.2009.06.016.

Gao, H.-Q., Boyer, P. L., Sarafianos, S. G., Arnold, E. and Hughes, S. H. (2000) 'The role of steric hindrance in 3TC resistance of human immunodeficiency virus type-1 reverse transcriptase11Edited by A. R. Fersht', *Journal of Molecular Biology*, 300(2), pp. 403–418. doi: 10.1006/jmbi.2000.3823.

Garforth, S. J., Lwatula, C. and Prasad, V. R. (2014) 'The lysine 65 residue in HIV-1 reverse transcriptase function and in nucleoside analog drug resistance', *Viruses*, 6(10), pp. 4080–4094. doi: 10.3390/v6104080.

Geyer, M., Fackler, O. T. and Peterlin, B. M. (2001) 'Structure–function relationships in HIV-1 Nef', *EMBO Reports*. Oxford, UK: Oxford University Press, 2(7), pp. 580–585. doi: 10.1093/embo-reports/kve141.

Glencross, D. K., Coetzee, L. M., Faal, M., Masango, M., Stevens, W. S., Venter, W. F. and Osih, R. (2012) 'Performance evaluation of the Pima™ point-of-care CD4

analyser using capillary blood sampling in field tests in South Africa', *Journal of the International AIDS Society*. The International AIDS Society, 15(1), p. 3. doi: 10.1186/1758-2652-15-3.

Glencross, D. K., Janossy, G., Coetzee, L. M., Lawrie, D., Aggett, H. M., Scott, L. E., Sanne, I., McIntyre, J. A. and Stevens, W. (2008) 'Large-scale affordable Panleucogated CD4+ testing with proactive internal and external quality assessment: In support of the South African national comprehensive care, treatment and management programme for HIV and AIDS', *Cytometry Part B: Clinical Cytometry*. John Wiley & Sons, Ltd, 74B(S1), pp. S40–S51. doi: 10.1002/cyto.b.20384.

Gray, R. H., Wawer, M. J., Brookmeyer, R., Sewankambo, N. K., Serwadda, D., Wabwire-Mangen, F., Lutalo, T., Li, X., VanCott, T., Quinn, T. C. and and the Rakai Project Team (2001) 'Probaility of HIV-1 transmission per coital act in monogamous, heterosexual, HIV-1-discordant couples in Rakai, Uganda', *The Lancet*, 357, pp. 1149–53.

Greenwald, J. L., Burstein, G. R., Pincus, J. and Branson, B. (2006) 'A rapid review of rapid HIV antibody tests', *Current Infectious Disease Reports*, 8(2), pp. 125–131. doi: 10.1007/s11908-006-0008-6.

Groom, H. C. T., Anderson, E. C. and Lever, A. M. L. (2009) 'Rev: beyond nuclear export', *The Journal of general virology*, 90(Pt 6), p. 1303—1318. doi: 10.1099/vir.0.011460-0.

Gu, S.-X., Lu, H.-H., Liu, G.-Y., Ju, X.-L. and Zhu, Y.-Y. (2018) 'Advances in diarylpyrimidines and related analogues as HIV-1 nonnucleoside reverse transcriptase inhibitors', *European Journal of Medicinal Chemistry*, 158, pp. 371–392. doi: 10.1016/j.ejmech.2018.09.013.

Gulick, R. M., Mellors, J. W., Havlir, D., Eron, J. J., Gonzalez, C., McMahon, D., Richman, D. D., Valentine, F. T., Jonas, L., Meibohm, A., Emini, E. A., Chodakewitz, J. A., Deutsch, P., Holder, D., Schleif, W. A. and Condra, J. H. (1997) 'Treatment with Indinavir, Zidovudine, and Lamivudine in Adults with Human Immunodeficiency Virus Infection and Prior Antiretroviral Therapy', *New England Journal of Medicine*. Massachusetts Medical Society, 337(11), pp. 734–739. doi: 10.1056/NEJM199709113371102.

Hammer, S. M., Kessler, H. A., Saag, M. S. (1994) 'Issues in Combination Antiretroviral Therapy: A Review', *Journal of Acquired Immune Deficiency Syndromes*, 7(Suppl. 2) pp. 524-537.

Hammer, S. M., Squires, K. E., Hughes, M. D., Grimes, J. M., Demeter, L. M., Currier, J. S., Eron, J. J., Feinberg, J. E., Balfour, H. H., Deyton, L. R., Chodakewitz, J. A., Fischl, M. A., Phair, J. P., Pedneault, L., Nguyen, B.-Y. and Cook, J. C. (1997) 'A Controlled Trial of Two Nucleoside Analogues plus Indinavir in Persons with Human Immunodeficiency Virus Infection and CD4 Cell Counts of 200 per Cubic Millimeter or Less', *New England Journal of Medicine*. Massachusetts Medical Society, 337(11), pp. 725–733. doi: 10.1056/NEJM199709113371101.

Hanna, G. J. and D'Aquila, R. T. (2001) 'Clinical Use of Genotypic and Phenotypic Drug Resistance Testing to Monitor Antiretroviral Chemotherapy', *Clinical Infectious Diseases*, 32, pp. 774–782.

Hansen, J., Schulze, T., Mellert, W. and Moelling, K. (1988) 'Identification and characterization of HIV-specific RNase H by monoclonal antibody.', *The EMBO Journal*, 7(1), pp. 239–243. Available at: http://www.ncbi.nlm.nih.gov/pmc/articles/PMC454263/.

Harrigan, P. R., Mo, T., Wynhoven, B., Hirsch, J., Brumme, Z., McKenna, P., Pattery, T., Vingerhoets, J. and Bacheler, L. T. (2005) 'Rare mutations at codon 103 of HIV-

1 reverse transcriptase can confer resistance to non-nucleoside reverse transcriptase inhibitors', *AIDS*, 19(6). Available at: https://journals.lww.com/aidsonline/Fulltext/2005/04080/Rare_mutations_at_codon_103_of_HIV_1_reverse.2.aspx.

Hemelaar, J., Gouws, E., Ghys, P. D., Osmanov, S. and Characterisation, W.-U. N. for H. I. V. I. and (2011) 'Global trends in molecular epidemiology of HIV-1 during 2000-2007', *AIDS (London, England)*, 25(5), pp. 679–689. doi: 10.1097/QAD.0b013e328342ff93.

Herschhorn, A. and Hizi, A. (2010) 'Retroviral reverse transcriptases', *Cellular and molecular life sciences : CMLS*, 67(16), p. 2717—2747. doi: 10.1007/s00018-010-0346-2.

Hoffman, C. J., Ledwaba, J., Li, J., Johnston, V., Hunt, G., Fielding, K. L., Chaisson, R. E., Churchyard, G. J., Grant, A. D., Johnson, J. A., Charalambous, S. and Morris, L. (2013) 'Resistance to tenofovir-based regimens during treatment failure of subtype C HIV-1 in South Africa', *Antiviral Therapy*, 18, pp. 915–920.

Hosseinipour, M. C., Gupta, R. K., Van Zyl, G., Eron, J. J. and Nachega, J. B. (2013) 'Emergence of HIV Drug Resistance During First- and Second-Line Antiretroviral Therapy in Resource-Limited Settings', *The Journal of Infectious Diseases*, 207(suppl_2), pp. S49–S56. doi: 10.1093/infdis/jit107.

Hsiou, Y., Ding, J., Das, K., Clark, A. D., Boyer, P. L., Lewi, P., Janssen, P. A. J., Kleim, J.-P., Rösner, M., Hughes, S. H. and Arnold, E. (2001) 'The Lys103Asn mutation of HIV-1 RT: a novel mechanism of drug resistance11Edited by J. Karn', *Journal of Molecular Biology*, 309(2), pp. 437–445. doi: 10.1006/jmbi.2001.4648.

Human Sciences Research Council (2018) *The Fifth South African National HIV Prevalence, Incidence, Behaviour and COmmunication Survey, 2017 (SABSSM V)*.

Hunt, G. M., Coovadia, A., Abrams, E. J., Sherman, G., Meyers, T., Morris, L. and Kuhn, L. (2011) 'HIV-1 drug resistance at antiretroviral treatment initiation in children previously exposed to single-dose nevirapine', *AIDS*, 25(12), pp. 1461–1469. doi: 10.1097/QAD.0b013e3283492180.

Hunt, G. M., Dokubo, E. K., Takuva, S., De Oliveira, T., Ledwaba, J., Dube, N., Moodley, P., Sabatier, J., Deyde, V., Morris, L. and Raizes, E. (2017) 'Rates of virological suppression and drug resistance in adult HIV-1-positive patients attending primary healthcare facilities in KwaZulu-Natal, South Africa', *Journal of Antimicrobial Chemotherapy*, 72(11), pp. 3141–1348. doi: 10.1093/jac/dkx252.

Hunt, P. W. (2007) 'Role of immune activation in HIV pathogenesis', *Current HIV/AIDS Reports*, 4(1), pp. 42–47. doi: 10.1007/s11904-007-0007-8.

Inzaule, S. C., Ondoa, P., Peter, T., Mugyenyi, P. N., Stevens, W. S., de Wit, T. F. R. and Hamers, R. L. (2016) 'Affordable HIV drug-resistance testing for monitoring of antiretroviral therapy in sub-Saharan Africa', *The Lancet Infectious Diseases*. doi: 10.1016/S1473-3099(16)30118-9.

Iweala, O. I. (2004) 'HIV diagnostic tests: An overview', *Contraception*, 70(2), pp. 141–147. doi: 10.1016/j.contraception.2004.03.012.

Johnson, J. A., Li, J.-F., Wei, X., Lipscomb, J., Irlbeck, D., Craig, C., Smith, A., Bennett, D. E., Monsour, M., Sandstrom, P., Lanier, E. R. and Heneine, W. (2008) 'Minority HIV-1 Drug Resistance Mutations Are Present in Antiretroviral Treatment–Naïve Populations and Associate with Reduced Treatment Efficacy', *PLoS Medicine*. Edited by S. G. Deeks. San Francisco, USA: Public Library of Science, 5(7), p. e158. doi: 10.1371/journal.pmed.0050158.

Joint United Nations Programme on HIV/AIDS (2014) *90-90-90: An ambitious treatment target to help end the AIDS epidemic*. Geneva, Switzerland.

Joint United Nations Programme on HIV/AIDS (2016a) ‘Global AIDS Update 2016’. Edited by UNAIDS. Geneva, Switzerlands.

Joint United Nations Programme on HIV/AIDS (2016b) *Prevention Gap Report*. Geneva, Switzerland.

Joint United Nations Programme on HIV/AIDS (2018a) *Miles to go: Closing gaps, breaking barriers, righting injustices*. Geneva, Switzerland.

Joint United Nations Programme on HIV/AIDS (2018b) *UNAIDS Data 2018*. Geneva, Switzerland. Available at: http://www.unaids.org/en/resources/documents/2018/unaids-data-2018.

Jordan, M. R., Penazzato, M., Cournil, A., Vubil, A., Jani, I., Hunt, G., Carmona, S., Maphalala, G., Mthethwa, N., Watera, C., Kaleebu, P., Musanhu, C. C., Mtapuri-Zinyowera, S., Dzangare, J., Peeters, M., Yang, C., Parkin, N. and Bertagnolio, S. (2017) ‘Human imunodeficiency virus (HIV) drug resistance in African infants and young children newly diagnosed eith HIV: a multicountry analysis’, *Clinical Infectious Diseases*, 65(12), pp. 2018–2025. doi: 10.1093/cid/cix698.

Karmon, S. L. and Markowitz, M. (2013) ‘Next-Generation Integrase Inhibitors’, *Drugs*, 73(3), pp. 213–228. doi: 10.1007/s40265-013-0015-5.

Kaslow, R. A., Erelding, E. J. and Goepfort, P. A. (2014) ‘Human Immunodeficiency Viruses Types 1 and 2’, in Kaslow, R. A., Stanberry, L. R., and Le Duc, J. W. (eds) *Viral Infections of Humans*. 5th edn. New York: Springer, pp. 1001–1062.

Kharsany, A. B. M. and Karim, Q. A. (2016) ‘HIV Infection and AIDS in Sub-Saharan Africa: Current Status, Challenges and Opportunities’, *The open AIDS journal*. Bentham Open, 10, pp. 34–48. doi: 10.2174/1874613601610010034.

Kijak, G. H. and McCutchan, F. E. (2005) ‘HIV diversity, molecular epidemiology, and the role of recombination’, *Current Infectious Disease Reports*, 7(6), pp. 480–488. doi: 10.1007/s11908-005-0051-8.

Kosack, C. S., Page, A.-L., Beelaert, G., Benson, T., Savane, A., Ng’ang’a, A., Andre, B., Zahinda, J.-P. B. N., Shanks, L. and Fransen, K. (2017) ‘Towards more accurate HIV testing in sub-Saharan Africa: a multi-site evaluation of HIV RDTs and risk factors for false positives’, *Journal of the International AIDS Society*. John Wiley & Sons, Ltd, 20(1), p. 21345. doi: 10.7448/IAS.20.1.21345.

Kuhn, L., Hunt, G., Technau, K.-G., Coovadia, A., Ledwaba, J., Pickerill, S., Penazzato, M., Bertagnolio, S., Mellins, C. A., Black, V., Morris, L. and Abrams, E. J. (2014) ‘Drug resistance among newly diagnosed HIV-infected children in the era of more efficacious antiretroviral prophylaxis’, *AIDS (London, England)*, 28(11), pp. 1673–1678. doi: 10.1097/QAD.0000000000000261.

Kuritzkes, D. R. and Koup, R. A. (2013) ‘HIV-1: Pathogenesis, Clinical Manifestations, and Treatment’, in Knipe, D. M. and Howley, P. M. (eds) *Fields Virology*. 6th edn. Philadelphia, PA: Wolters Kluwer/Lippincott Williams & Wilkins Health, pp. 1561–1583.

Larson, K. B., Wang, K., Delille, C., Otofokun, I. and Acosta, E. P. (2014) ‘Pharmacokinetic Enhancers in HIV Therapeutics’, *Clinical Pharmacokinetics*, 53(10), pp. 865–872. doi: 10.1007/s40262-014-0167-9.

Levin, J. G., Mitra, M., Mascarenhas, A. and Musier-Forsyth, K. (2010) ‘Role of HIV-1 nucleocapsid protein in HIV-1 reverse transcription’, *RNA Biology*. Landes Bioscience, 7(6), pp. 754–774. doi: 10.4161/rna.7.6.14115.

Levy, J. A. (2009) ‘HIV pathogenesis: 25 years of progress and persistent challenges’, *AIDS*, 23(2). Available at: https://journals.lww.com/aidsonline/Fulltext/2009/01140/HIV_pathogenesis__25_years_of_progress_and.1.aspx.

Li, J., Lipscomb, J. T., Wei, X., Martinson, N. A., Morris, L., Heneine, W. and Johnson, J. A. (2011) 'Detection of Low-Level K65R Variants in Nucleoside Reverse Transcriptase Inhibitor–Naive Chronic and Acute HIV-1 Subtype C Infections', *The Journal of Infectious Diseases*. Oxford University Press, 203(6), pp. 798–802. doi: 10.1093/infdis/jiq126.

Li, Y., Luo, L., Rasool, N. and Kang, C. Y. (1993) 'Glycosylation Is Necessary for the Correct Folding of Human Immunodeficiency Virus gp120 in CD4 Binding', *Journal of Virology*, 67(1), pp. 584–588.

Liu, J., Henao-mejia, J., Liu, H., Zhao, Y. and He, J. J. (2011) 'Translational Regulation of HIV-1 Replication by HIV-1 Rev Cellular Cofactors Sam68, eIF5A, hRIP, and DDX3', *Journal of Neuroimmune Pharmacology*. The First Affiliated Hospital, Xi'an Jiaotong University College of Medicine, Xi'an, Shaanxi, People's Republic of China; Department of Microbiology and Immunology, Indiana University School of Medicine, Indianapolis, IN, USA ; Department of Microbiology: Springer Science & Business Media, 6(2), pp. 308–321. doi: 10.1007/s11481-011-9265-8.

Lu, K., Heng, X. and Summers, M. F. (2011) 'Structural Determinants and Mechanism of HIV-1 Genome Packaging', *Journal of molecular biology*, 410(4), pp. 609–633. doi: 10.1016/j.jmb.2011.04.029.

Lyseng-Williamson, K. A., Reynolds, N. A. and Plosker, G. L. (2005) 'Tenofovir Disoproxil Fumarate', *Drugs*, 65(3), pp. 413–432. doi: 10.2165/00003495-200565030-00006.

Maartens, G., Celum, C. and Lewin, S. R. (2014) 'HIV infection: epidemiology, pathogenesis, treatment, and prevention', *The Lancet*, 384(9939), pp. 258–271. doi: 10.1016/S0140-6736(14)60164-1.

Mansky, L. M., Temin, H. M. (1995) 'Lower in vivo mutation rate of human immunodeficiency virus type 1 than predicted from the fidelity of purified reverse transcriptase', *Journal of Virology*, 69(8), pp. 5089-5094.

Markham, A. (2018) 'Bictegravir: First Global Approval', *Drugs*, 78(5), pp. 601–606. doi: 10.1007/s40265-018-0896-4.

Martinez-Cajas, J. L. and Wainberg, M. A. (2008) 'Antiretroviral Therapy', *Drugs*, 68(1), pp. 43–72. doi: 10.2165/00003495-200868010-00004.

Massarotti, A. and Coluccia, A. (2016) 'An in-silico approach aimed to clarify the role of Y181C and K103N HIV-1 reverse transcriptase mutations versus Indole Aryl Sulphones', *Journal of Molecular Graphics and Modelling*, 63, pp. 49–56. doi: 10.1016/j.jmgm.2015.11.013.

Matthews, T., Salgo, M., Greenberg, M., Jain, C., DeMasi, R. and Bolognesi, D. (2004) 'Enfuvirtide: the first therapy to inhibit the entry of HIV-1 into host CD4 lymphocytes', *Nature Reviews. Drug Discovery*. London: Nature Publishing Group, 3(3), pp. 215–225. doi: 10.1038/nrd1331.

McColl, D. J. and Chen, X. (2010) 'Strand transfer inhibitors of HIV-1 integrase: Bringing IN a new era of antiretroviral therapy', *Antiviral Research*, 85(1), pp. 101–118. doi: 10.1016/j.antiviral.2009.11.004.

MedCalc Software bvba (2014) 'MedCalc Statistical Software'. Ostend, Belgium.

Meintjes, G., Moorhouse, M. A., Carmona, S., Davies, N., Dlamini, S., van Vuuren, C., Manzini, T., Mathe, M., Moosa, Y., Nash, J., Nel, J., Pakade, Y., Woods, J., Van Zyl, G., Conradie, F. and Venter, F. (2017) 'Adult antiretroviral therapy guidelines 2017', *Southern African journal of HIV medicine*. AOSIS, 18(1), p. 776. doi: 10.4102/sajhivmed.v18i1.776.

Melhuish, A. and Lewthwaite, P. (2018) 'Natural history of HIV and AIDS', *Medicine*, 46(6), pp. 356–361. doi: 10.1016/j.mpmed.2018.03.010.

Menéndez-Arias, L., Sebastián-Martín, A. and Álvarez, M. (2017) 'Viral reverse transcriptases', *Virus Research*, 234, pp. 153–176. doi: 10.1016/j.virusres.2016.12.019.

Mesplède, T. and Wainberg, M. A. (2013) 'Integrase Strand Transfer Inhibitors in HIV Therapy', *Infectious Diseases and Therapy*, 2(2), pp. 83–93. doi: 10.1007/s40121-013-0020-8.

Miller, V., Stark, T., Loeliger, A. E. and Lange, J. M. A. (2002) 'The impact of the M184V substitution in HIV-1 reverse transcriptase on treatment response', *HIV Medicine*. Blackwell Science Ltd, 3(2), pp. 135–145. doi: 10.1046/j.1468-1293.2002.00101.x.

Mossoro-Kpinde, C. D., Ralph-Sydney, M. B., Mohammad-Ali, J., Wolyec, S. T., Leman, R., Matta, M., Longo, J. de D., Grésenguet, G., Andreoletti, L. and Bélec, L. (2016) 'Analytical Performances of Human Immunodeficiency Virus Type 1 RNA-Based Amplix® Real-Time PCR Platform for HIV-1 RNA Quantification', *AIDS Research and Treatment*. New York: Hindawi Limited, 2016. doi: 10.1155/2016/7954810.

Moyle, G. J., Gazzard, B. G., Cooper, D. A. and Gatell, J. (1998) 'Antiretroviral Therapy for HIV Infection', *Drugs*, 55(3), pp. 383–404. doi: 10.2165/00003495-199855030-00005.

Muthumani, K., Choo, A. Y., Zong, W.-X., Madesh, M., Hwang, D. S., Premkumar, A., Thieu, K. P., Emmanuel, J., Kumar, S., Thompson, C. B. and Weiner, D. B. (2006) 'The HIV-1 Vpr and glucocorticoid receptor complex is a gain-of-function interaction that prevents the nuclear localization of PARP-1', *Nature cell biology*, 8(2), pp. 170–179. doi: 10.1038/ncb1352.

National Department of Health (2015) *National Consolidated Guidelines for the prevention of mother to child transmission of HIV and the management of HIV in children, adolescents and adults*.

National Department of Health (2016) *South African Primary Healthcare Essential Medicines List Chapter 11: HIV & AIDS NEMLC Recommendations for Medicine Management (2016-2018)*.

Natoli, M., Rohrman, B., van Zyl, G. and Richards-Kortum, R. (2017) 'Development of a proof-of-concept point-of-care diagnostic for the HIV drug resistance mutation M184V', in *XXVI International Workshop on HIV Drug Resistance and Treatment Strategies*. Johannesburg, South Africa.

Newman, H., Breunig, L., van Zyl, G., Stich, A. and Preiser, W. (2014) 'A qualitative PCR minipool strategy to screen for virologic failure and antiretroviral drug resistance in South African patients on first-line antiretroviral therapy', *Journal of Clinical Virology*, 60(4), pp. 387–391. doi: 10.1016/j.jcv.2014.05.011.

Nikolenko, G. N., Kotelkin, A. T., Oreshkova, S. F. and Ilyichev, A. A. (2011) 'Mechanisms of HIV-1 drug resistance to nucleoside and nonnucleoside reverse transcriptase inhibitors', *Molecular Biology*, 45(1), pp. 93–109. doi: 10.1134/S0026893311010092.

Nomaguchi, M., Fujita, M. and Adachi, A. (2008) 'Role of HIV-1 Vpu protein for virus spread and pathogenesis', *Microbes and Infection*, 10(9), pp. 960–967. doi: 10.1016/j.micinf.2008.07.006.

O'Cofaigh, E. and Lewthwaite, P. (2013) 'Natural history of HIV and AIDS', *Medicine*, 41(8), pp. 411–416. doi: 10.1016/j.mpmed.2013.05.009.

Orman, J. S. and Perry, C. M. (2008) 'Tipranavir', *Drugs*, 68(10), pp. 1435–1463. doi: 10.2165/00003495-200868100-00006.

Panpradist, N., Beck, I., Vrana, J., Higa, N., McIntyre, D., Ruth, P., So, I., Kline, E., Milne, R., Kanthula, R., Wong-on-Wing, A., Lim, J., Ko, D., Rossouw, T., Feucht,

U., Chung, M., Jourdain, G., Ngo-Giang-Huong, N., Laomanit, L., Soria, J., Klavins, E., Frenkel, L. and Lutz, B. (2018) 'OLA Simple: A software guided assay that novices can perform to genotype HIV DNA and RNA subtypes A, B, C, D and E for detection of drug resistance', in *XXVII International Workshop on HIV Drug Resistance and Treatment Strategies*, p. 42.

Panpradist, N., So, I., Beck, I., McIntyre, D., Higa, N., Kline, E., Wong-on-Wing, A., Kanthula, R., Rossouw, T., van Dyk, G., Lim, J., Ko, D., Frenkel, L. and Lutz, B. (2017) 'Evaluation of low-cost "OLA Simple" lab kit for detection of HIV drug resistance in dried blood spot specimens from South African infants', in *XXVI International Workshop on HIV Drug Resistance and Treatment Strategies*. Johannesburg, South Africa.

Parikh, U. M., McCormick, K., van Zyl, G. and Mellors, J. W. (2017) 'Future technologies for monitoring HIV drug resistance and cure', *Current Opinion in HIV and AIDS*, 11. doi: 10.1097/coh.0000000000000344.

Pillay, V., Ledwaba, J., Hunt, G., Rakgotho, M., Singh, B., Makubalo, L., Bennet, D. E., Puren, A. and Morris, L. (2008) 'Antiretroviral drug resistance surveillance among drug-naive HIV-1-infected individuals in Gauteng Province, South Africa in 2002 and 2004', *Antiviral Therapy*, 13(Supplementary 2), pp. 101–107.

Poignard, P., Saphire, E. O., Parren, P. W. H. I. and Burton, D. R. (2001) 'GP120: Biologic aspects of structural features', *Annual Review of Immunology*. Palo Alto: Annual Reviews, Inc., 19, pp. 253–274. Available at: https://search.proquest.com/docview/201637549?accountid=15083.

Rasmussen, R. (2001) 'Rapid Cycle Real-Time PCR: Methods and Applications BT - Rapid Cycle Real-Time PCR: Methods and Applications', in Meuer, S., Wittwer, C., and Nakagawara, K.-I. (eds). Berlin, Heidelberg: Springer Berlin Heidelberg, pp. 21–34. doi: 10.1007/978-3-642-59524-0_1.

Recordon-Pinson, P., Alves, B. M., Tumiotto, C., Bellecave, P., Bonnet, F., Neau, D., Soares, E. A., Soares, M. A. and Fleury, H. (2018) 'A New HIV-1 Circulating Recombinant Form (CRF98_cpx) Between CRF06_cpx and Subtype B Identified in Southwestern France', *AIDS Research and Human Retroviruses*, 34(11), pp. 1005–1009. doi: 10.1089/aid.2018.0122.

Ren, J. and Stammers, D. K. (2008) 'Structural basis for drug resistance mechanisms for non-nucleoside inhibitors of HIV reverse transcriptase', *Virus Research*, 134(1), pp. 157–170. doi: 10.1016/j.virusres.2007.12.018.

Rhee, S.-Y., Blanco, J. L., Jordan, M. R., Taylor, J., Lemey, P., Varghese, V., Hamers, R. L., Bertagnolio, S., de Wit, T. F. R., Aghokeng, A. F., Albert, J., Avi, R., Avila-Rios, S., Bessong, P. O., Brooks, J. I., Boucher, C. A. B., Brumme, Z. L., Busch, M. P., Bussmann, H., Chaix, M.-L., Chin, B. S., D'Aquin, T. T., De Gascun, C. F., Derache, A., Descamps, D., Deshpande, A. K., Djoko, C. F., Eshleman, S. H., Fleury, H., Frange, P., Fujisaki, S., Harrigan, P. R., Hattori, J., Holguin, A., Hunt, G. M., Ichimura, H., Kaleebu, P., Katzenstein, D., Kiertiburanakul, S., Kim, J. H., Kim, S. S., Li, Y., Lutsar, I., Morris, L., Ndembi, N., NG, K. P., Paranjape, R. S., Peeters, M., Poljak, M., Price, M. A., Ragonnet-Cronin, M. L., Reyes-Terán, G., Rolland, M., Sirivichayakul, S., Smith, D. M., Soares, M. A., Soriano, V. V, Ssemwanga, D., Stanojevic, M., Stefani, M. A., Sugiura, W., Sungkanuparph, S., Tanuri, A., Tee, K. K., Truong, H.-H. M., van de Vijver, D. A. M. C., Vidal, N., Yang, C., Yang, R., Yebra, G., Ioannidis, J. P. A., Vandamme, A.-M. and Shafer, R. W. (2015) 'Geographic and Temporal Trends in the Molecular Epidemiology and Genetic Mechanisms of Transmitted HIV-1 Drug Resistance: An Individual-Patient- and Sequence-Level Meta-Analysis', *PLOS Medicine*. Public Library of Science,

12(4), p. e1001810. doi: 10.1371/journal.pmed.1001810.
Roche Diagnostics GmbH (2008) *MagNA Pure LC 2.0 Instrument Operator's Manual*. Penzburg, Germany.
Rong, L., Feng, Z. and Perelson, A. S. (2007) 'Emergence of HIV-1 drug resistance during antiretroviral treatment', *Bulletin of Mathematical Biology*, 69(6), pp. 2027–2060.
Rowley, C. F., Boutwell, C. L., Lee, E. J., MacLeod, I. J., Ribaudo, H. J., Essex, M. and Lockman, S. (2010) 'Ultrasensitive Detection of Minor Drug-Resistant Variants for HIV After Nevirapine Exposure Using Allele-Specific PCR: Clinical Significance', *AIDS Research and Human Retroviruses*. Mary Ann Liebert, Inc., publishers, 26(3), pp. 293–300. doi: 10.1089/aid.2009.0082.
El Safadi, Y., Vivet-Boudou, V. and Marquet, R. (2007) 'HIV-1 reverse transcriptase inhibitors', *Applied Microbiology and Biotechnology*, 75(4), pp. 723–737. doi: 10.1007/s00253-007-0919-7.
Safrin, S. (2015) 'Antiviral Agents', in Katzung, B. G. and Trevor, A. J. (eds) *Basic & Clinical Pharmacology*. 13th edn. San Francisco, USA: McGraw-Hill Education, pp. 842–856.
Samuel, R., Bettiker, R., Byungse, S. (2006) 'Antiretroviral Therapy 2006: Pharmacology, Applications, and Special Situations', *Archives of Pharmacal Research*, 29(6), pp431-458.
Scarlata, S. and Carter, C. (2003) 'Role of HIV-1 Gag domains in viral assembly', *Biochimica et Biophysica Acta (BBA) - Biomembranes*, 1614(1), pp. 62–72. doi: 10.1016/S0005-2736(03)00163-9.
Sharp, P. M. and Hahn, B. H. (2011) 'Origins of HIV and the AIDS pandemic', *Cold Spring Harbor perspectives in medicine*. Cold Spring Harbor Laboratory Press, 1(1), pp. a006841–a006841. doi: 10.1101/cshperspect.a006841.
Shaw, G. M. and Hunter, E. (2012) 'HIV Transmission', *Cold Spring Harbor Perspectives in Medicine*. doi: 10.1101/cshperspect.a006965.
Sherman, E. (2015) 'Antiviral Drugs', in Whalen, K., Finkel, R., and Panavelil, T. A. (eds) *Pharmacology*. 6th edn. Philadelphia, PA: Wolters Kluwer, pp. 574–584.
Sigaloff, K. C. E., Ramatsebe, T., Viana, R., Rinke de Wit, T. F., Wallis, C. L. and Stevens, W. S. (2011) 'Accumulation of HIV Drug Resistance Mutations in Patients Failing First-Line Antiretroviral Treatment in South Africa', *AIDS Research and Human Retroviruses*. Mary Ann Liebert, Inc., publishers, 28(2), pp. 171–175. doi: 10.1089/aid.2011.0136.
Skhosana, L., Steegen, K., Bronze, M., Lukhwareni, A., Letsoalo, E., Papathanasopoulos, M. A., Carmona, S. C. and Stevens, W. S. (2015) 'High prevalence of the K65R mutation in HIV-1 subtype C infected patients failing tenofovir-based first-line regimens in South Africa', *PLOS ONE*, 10(2), p. e0118145. doi: 10.1371/journal.pone.0118145.
Soogoor, M. and Daar, E. S. (2005) 'Primary HIV-1 infection: Diagnosis, pathogenesis, and treatment', *Current Infectious Disease Reports*, 7(2), pp. 147–153. doi: 10.1007/s11908-005-0075-0.
Spiess, A.-N., Rödiger, S., Burdukiewicz, M., Volksdorf, T. and Tellinghuisen, J. (2016) 'System-specific periodicity in quantitative real-time polymerase chain reaction data questions threshold-based quantitation', *Scientific Reports*. The Author(s), 6, p. 38951. doi: 10.0.4.14/srep38951.
Steegen, K., Bronze, M., Papathanasopoulos, M. A., van Zyl, G., Goedhals, D., Variava, E., MacLeod, W., Sanne, I., Stevens, W. S. and Carmona, S. (2017) 'HIV-1 antiretroviral drug resistance patterns in patients failing NNRTI-based treatment:

results form a national survey in South Africa', *Journal of Antimicrobial Chemotherapy*, 72, pp. 210–219. doi: 10.1093/jac/dkw358.

Steegen, K., Carmona, S., Bronze, M., Papathanasopoulos, M. A., van Zyl, G., Goedhals, D., MacLeod, W., Sanne, I. and Stevens, W. S. (2016) 'Moderate Levels of Pre-Treatment HIV-1 Antiretroviral Drug Resistance Detected in the First South African National Survey', *PLOS ONE*, 11(12). doi: 10.1371/journal.pone.0166305.

Steegen, K., Levin, L., Ketseoglou, I., Bronze, M., Papathanasopoulos, M. A., Carmona, S. and Stevens, W. (2014) 'High-level cross-resistance to didanosine observed in South African children failing an abacavir- or stavudine-based 1st-line regimen', *PLOS ONE*, 9(5), p. e97067. doi: 10.1371/journal.pone.0097067.

Tang, M. W. and Shafer, R. W. (2012) 'HIV-1 Antiretroviral Resistance', *Drugs*, 72(9), pp. e1--e25. doi: 10.2165/11633630-000000000-00000.

Taylor, B. S., Sobieszczyk, M. E., McCutchan, F. E. and Hammer, S. M. (2008) 'The challenge of HIV-1 subtype diversity', *The New England journal of medicine*, 358(15), pp. 1590–1602. doi: 10.1056/NEJMra0706737.

TEMPRANO ANRS 12136 Study Group (2015) 'A Trial of Early Antiretrovirals and Isoniazid Preventive Therapy in Africa', *New England Journal of Medicine*. Massachusetts Medical Society, 373(9), pp. 808–822. doi: 10.1056/NEJMoa1507198.

The INSIGHT START Study Group (2015) 'Initiation of antiretroviral therapy in early asymptomatic HIV infection', *New England Journal of Medicine*. Massachusetts Medical Society, 373(9), pp. 795–807. doi: 10.1056/NEJMoa1506816.

The Strategies for Management of Antiretroviral Therapy (SMART) Study Group (2008) 'Major Clinical Outcomes in Antiretroviral Therapy (ART)–Naive Participants and in Those Not Receiving ART at Baseline in the SMART Study', *The Journal of Infectious Diseases*, 197(8), pp. 1133–1144. doi: 10.1086/586713.

Tichopad, A., Dilger, M., Schwarz, G. and Pfaffl, M. W. (2003) 'Standardized determination of real-time PCR efficiency from a single reaction set-up', *Nucleic acids research*. Oxford University Press, 31(20), pp. e122–e122. doi: 10.1093/nar/gng122.

Tilton, J. C. and Doms, R. W. (2010) 'Entry inhibitors in the treatment of HIV-1 infection', *Antiviral Research*, 85(1), pp. 91–100. doi: 10.1016/j.antiviral.2009.07.022.

Valuev-Elliston, V. T. and Kochetkov, S. N. (2017) 'Novel HIV-1 non-nucleoside reverse transcriptase inhibitors: A combinatorial approach', *Biochemistry (Moscow)*, 82(13), pp. 1716–1743. doi: 10.1134/S0006297917130107.

Vandegraaff, N. and Engelman, A. (2007) 'Molecular mechanisms of HIV integration and therapeutic intervention', *Expert Reviews in Molecular Medicine*. Cambridge: Cambridge University Press, 9(6), pp. 1–19. Available at: https://search.proquest.com/docview/207212104?accountid=15083.

Venter, W. D. F. (2017) 'A Complex but Exciting Future: New Options for Second-Line Antiretroviral Therapy', *Current Tropical Medicine Reports*, 4(1), pp. 6–10. doi: 10.1007/s40475-017-0097-3.

Vivet-Boudou, V., Didierjean, J., Isel, C. and Marquet, R. (2006) 'Nucleoside and nucleotide inhibitors of HIV-1 replication', *Cellular and Molecular Life Sciences CMLS*, 63(2), pp. 163–186. doi: 10.1007/s00018-005-5367-x.

Wainberg, M. A. (2004) 'The impact of the M184V substitution on drug resistance and viral fitness', *Expert Review of Anti-Infective Therapy*. London: Informa Healthcare, 2(1), pp. 147–151. doi: 10.1586/14787210.2.1.147.

Wallis, C. L., Mellors, J. W., Venter, W. D., Sanne, I. and Stevens, W. (2010) 'Varied

Patterns of HIV-1 Drug Resistance on Failing First-Line Antiretroviral Therapy in South Africa', *Journal of Acquired Immune Deficiency Syndromes*, 53(4), pp. 480–484. doi: 10.1097/QAI.0b013e3181bc478b.

Watts, J. M., Dang, K. K., Gorelick, R. J., Leonard, C. W., Bess Jr, J. W., Swanstrom, R., Burch, C. L. and Weeks, K. M. (2009) 'Architecture and secondary structure of an entire HIV-1 RNA genome', *Nature*. Macmillan Publishers Limited. All rights reserved, 460(7256), pp. 711–716. doi: 10.1038/nature08237.

Wei, X., Lipscomb, J. T. and Johnson, J. A. (2015) 'HIV RNA Preservation and Resistance Mutation Multiplex PCR for Screening Dried Blood Spots in Resource-limited Setting', *Global Antiviral Journal*, 11(Suppl. 1), p. xvii.

Welman, M., Lemay, G. and Cohen, É. A. (2007) 'Role of envelope processing and gp41 membrane spanning domain in the formation of human immunodeficiency virus type 1 (HIV-1) fusion–competent envelope glycoprotein complex', *Virus Research*, 124(1), pp. 103–112. doi: 10.1016/j.virusres.2006.10.009.

Wensing, A. M. J., van Maarseveen, N. M. and Nijhuis, M. (2010) 'Fifteen years of HIV Protease Inhibitors: raising the barrier to resistance', *Antiviral Research*, 85(1), pp. 59–74. doi: 10.1016/j.antiviral.2009.10.003.

White, K. L., Margot, N. A., Ly, J. K., Chen, J. M., Ray, A. S., Pavelko, M., Wang, R., McDermott, M., Swaminathan, S. and Miller, M. D. (2005) 'A combination of decreased NRTI incorporation and decreased excision determines the resistance profile of HIV-1 K65R RT', *AIDS*, 19(16). Available at: https://journals.lww.com/aidsonline/Fulltext/2005/11040/A_combination_of_decreased_NRTI_incorporation_and.3.aspx.

Wilson, A. G., Cross, S., Nurutdinova, D. and Presti, R. (2015) 'Development of the M184V mutation in HIV-1 infection and sub-sequent treatment outcomes', *HIV/AIDS Research and Treatment*, 2(3), pp. 86–89. doi: 10.17140/HARTOJ-2-144.

World Health Organization (2013) *Consolidated Guidelines on the use of antiretroviral drugs for treating HIV infection: reccomndations for a public health approach*. Geneva, Switzerland. Available at: http://www.who.int/hiv/pub/guidelines/arv2013/download/en.

World Health Organization (2015a) *Consolidated Guidelines on HIV Testing Services*. Geneva, Switzerland.

World Health Organization (2015b) *Guideline on when to start antiretroviral therapy and on pre-exposure prophylaxis for HIV*. Geneva, Switzerland. Available at: http://www.who.int/hiv/pub/guidelines/earlyrelease-arv/en/.

World Health Organization (2016a) *Consolidated Guidelines on HIV Prevention, Diagnosis, Treatment and Care for Key Populations*. Geneva, Switzerland.

World Health Organization (2016b) *Consolidated guidelines on the use of antiretroviral drugs for treating and preventing HIV infection: recommendations for a public health approach*. 2nd edn. Edited by World Health Organization. Geneva, Switzerland: World Health Organization. Available at: http://www.who.int/hiv/pub/arv/arv-2016/en/.

World Health Organization (2017) *HIV Drug Resistance Report 2017*. Geneva, Switzerland.

World Health Organization (2018) *Updated recommendations on first-line antiretroviral regimens and post-exposure prophylaxis and recommendations on early infant diagnosis of HIV: interim guidance*. Geneva, Switzerland. Available at: http://www.who.int/hiv/pub/guidelines/ARV2018update/en/.

Wu, Y. (2004) 'HIV-1 gene expression: lessons from provirus and non-integrated DNA',

Retrovirology, 1(1), p. 13. doi: 10.1186/1742-4690-1-13.

Zhou, Z., Wagar, N., DeVos, J. R., Rottinghaus, E., Diallo, K., Nguyen, D. B., Bassey, O., Ugbena, R., Wadonda-Kabondo, N., McConnell, M. S., Zulu, I., Chilima, B., Nkengasong, J. and Yang, C. (2011) 'Optimization of a Low Cost and Broadly Sensitive Genotyping Assay for HIV-1 Drug Resistance Surveillance and Monitoring in Resource-Limited Settings', *PLOS ONE*. Public Library of Science, 6(11), p. e28184. doi: 10.1371/journal.pone.0028184.

Vitoria, M., Rangaraj, A., Ford, N., Doherty, M. (2019) "Current and future priorities for the development of optimal HIV drugs' *Current Opinion un HIV and AIDS.* 14(2) p. 143-149. doi: 10.1097/COH.0000000000000527.

van Zyl, G. U., van der Merwe, L., Claassen, M., Zeier, M. and Preiser, W. (2011) 'Antiretroviral resistance patterns and factors associated with resistance in adult patients failing NNRTI-based regimens in the western cape, South Africa', Journal of Medical Virology. Wiley Subscription Services, Inc., A Wiley Company, 83(10), pp. 1764–1769. doi: 10.1002/jmv.22189.